

**ENDOTHELIAL HEPARANASE REGULATION OF
CARDIAC METABOLISM**

by
Fang Wang

M.D., Wuhan University, China 2004

M.Sc., Wuhan University, China 2006

A THESIS SUBMITTED IN PARTIAL FULFILLMENT OF
THE REQUIREMENTS FOR THE DEGREE OF

DOCTOR OF PHILOSOPHY

in

THE FACULTY OF GRADUATE STUDIES

(Pharmaceutical Sciences)

THE UNIVERSITY OF BRITISH COLUMBIA

(Vancouver)

August 2011

© Fang Wang, 2011

Abstract

Following diabetes, the heart increases its lipoprotein lipase (LPL) at the coronary lumen by transferring LPL from the cardiomyocyte to the endothelial lumen. Heparanase is an endoglycosidase that specifically cleaves carbohydrate chains of heparan sulfate (HS). We examined the mechanisms behind endothelial heparanase control of cardiac LPL translocation. Using diazoxide (DZ) to decrease serum insulin, we observed that within 30 min of DZ, interstitial heparanase increased, an effect that closely mirrored an augmentation in interstitial LPL. In bovine coronary artery endothelial cells incubated with glucose or palmitic acid (PA), glucose dose-dependently increased heparanase secretion, a process that required ATP release, purinergic receptor activation, cortical actin disassembly and stress actin formation. Phosphorylation of filamin likely contributed towards the cortical actin disassembly, whereas Ca^{2+} /calmodulin-dependent protein kinase II and p38 mitogen activated protein kinase/heat shock protein 25 phosphorylation mediated stress actin formation. The endothelial-secreted heparanase in response to HG demonstrated endoglycosidase activity, cleaved HS, and released attached proteins like lipoprotein lipase and basic fibroblast growth factor. Unlike glucose, PA increased intracellular heparanase and induced rapid nuclear accumulation of heparanase that was dependent on Bax activation and lysosome permeabilization. Heat shock protein 90 was an important mediator of PA-induced shuttling of heparanase to the nucleus. Nuclear heparanase promoted cleavage of HS, a potent inhibitor of histone acetyltransferase activity and gene transcription. A TaqMan gene expression assay revealed an increase in genes related to glucose metabolism and inflammation. In addition, glycolysis was uncoupled from glucose oxidation, resulting in accumulation of lactate. Our data suggest that following hyperglycemia, translocation of

LPL from the cardiomyocyte cell surface to the apical side of endothelial cells is influenced by the ability of fatty acid to increase endothelial intracellular heparanase followed by rapid secretion of this enzyme by glucose. Given that both LPL and heparanase have been implicated in the progression of diabetes, our data may serve to reduce the associated cardiovascular complications by limiting the utilization of fatty acid after diabetes.

Preface

Chapter 2, 3 and 4 is based on work that I have published during my Ph.D. study. For each publication, I have indicated the contributions of my co-authors.

1. **Wang F**, Kim MS, Puthanveetil P, Kewalramani G, Deppe S, Ghosh S, Abrahani A, and Rodrigues B. *Endothelial heparanase secretion after acute hypoinsulinemia is regulated by glucose and fatty acid*. **Am. J. Physiol.** 296(4):H1108-16, 2009. (DOI: 10.1152/ajpheart.01312.2008)

I was the first author, and together with my supervisor, was the principal source of the idea and writing the manuscript. I was also mainly responsible for acquiring and analyzing the data, and designing and conducting most of the experiments. Minsuk Kim and Prasanth Puthanveetil helped with the immunohistochemistry. Girish Kewalramani and Sylvia Deppe were involved in acquiring part of the Western blot data, and Sanjoy Ghosh measured heparanase activity. Ashraf Abrahani assisted in setting up the modified Langendorff model, and Brian Rodrigues is the corresponding author.

2. **Wang F**, Wang Y, Kim MS, Puthanveetil P, Ghosh S, Dan S Luciani, Johnson JD, Abrahani A, and Rodrigues B. *Glucose-induced endothelial heparanase secretion requires cortical and stress actin reorganization*. **Cardiovasc. Res.** 87(1):127-36, 2010. (DOI: 10.1093/cvr/cvq051)

I conceived and designed the research, acquired most of the data, analyzed and interpreted the results, performed statistical analysis and wrote the manuscript. Ying Wang was involved in acquiring some of the Western blot data. Minsuk Kim and Prasanth Puthanveetil

helped with the Immunofluorescence, and Sanjoy Ghosh measured heparanase activity. Dan S Luciani and James Johnson made contributions to calcium measurements. Ashraf Abrahani helped with the isolation of actin cytoskeleton. Brian Rodrigues is the corresponding author.

The investigation conforms to the guide for the care and use of laboratory animals published by the US National Institutes of Health and the University of British Columbia, and was approved by the Animal Care Committee in the University of British Columbia (Certificate No. A08-0627).

Table of Contents

Abstract.....	ii
Preface.....	iv
Table of Contents	vi
List of Figures.....	x
List of Abbreviations	xiii
Acknowledgements	xiv
Dedication	xv
Chapter 1: Introduction	1
1.1 Diabetes mellitus.....	1
1.2 Heart metabolism.....	2
1.2.1 Cardiomyocytes	2
1.2.2 Endothelial cells.....	3
1.3 Lipoprotein lipase	5
1.4 Heparan sulfate proteoglycans	7
1.4.1 Synthesis and structure	7
1.4.2 Functions.....	8
1.5 Heparanase	9
1.5.1 Synthesis and processing	9
1.5.2 Mechanism of catalysis.....	10
1.5.3 Regulation of gene transcription.....	11
1.5.4 Pathological functions.....	13
1.5.4.1 Tumor metastasis.....	13

1.5.4.2 Diabetes.....	15
1.6 Hypothesis and research objectives	17
Chapter 2: Methods.....	22
2.1 Materials	22
2.2 Animal model	22
2.3 Plasma measurements.....	23
2.4 Isolated heart perfusions	23
2.5 Immunohistochemistry	24
2.6 Cell culture	25
2.7 Treatments	25
2.8 Isolation of membrane, cytosolic, nuclear, lysosome and mitochondrial fractions .	26
2.9 Western blotting and immunoprecipitation	28
2.10 Immunofluorescence	29
2.11 Filamentous (F) and globular (G) actin	29
2.12 Heparanase activity	30
2.13 Extracellular ATP determination	30
2.14 Determination of heparan sulfate-bound proteins	30
2.15 Estimation of endothelial intracellular free Ca ²⁺	30
2.16 Small interfering RNA (siRNA) transfection	31
2.17 Lactate assay	31
2.18 Reverse transcription-quantitative polymerase chain reaction	31
2.19 Statistical analysis	32
Chapter 3: Results.....	33

3.1	Endothelial heparanase secretion in diabetes is regulated by glucose and FA	33
3.1.1	Coronary lumen LPL increases after acute diazoxide injection	33
3.1.2	Rapid release of heparanase is associated with changes in interstitial LPL	33
3.1.3	Fatty acids facilitate endothelial intracellular heparanase accumulation.....	34
3.1.4	Dose-dependent secretion of endothelial heparanase by glucose	34
3.1.5	Simulating DZ-induced increase in substrates in vitro augments endothelial heparanase secretion	35
3.1.6	Endothelial cytoskeleton mediates both FA and high glucose induced changes in heparanase.....	36
3.2	Glucose-induced endothelial heparanase secretion requires cortical and stress actin reorganization	36
3.2.1	High glucose induces endothelial lysosomal heparanase secretion.....	36
3.2.2	Extracellular ATP mediates the effect of high glucose to induce heparanas secretion	37
3.2.3	Glucose-induced endothelial heparanase secretion is dependent on cytoskeleton reorganization	38
3.2.4	Ca ²⁺ /CaMKII and p38 MAPK/Hsp25 phosphorylation are augmented in endothelial cells exposed to high glucose.....	38
3.2.5	Inhibiting CaMKII or p38 MAPK regulated stress actin formation prevents glucose-induced endothelial heparanase secretion	39
3.2.6	Colocalization of filamin with the P2Y ₂ receptor is disrupted by high glucose bringing about filamin redistribution.....	39

3.2.7	Endothelial secreted heparanase cleaves cardiomyocyte heparan sulfate to release attached proteins	40
3.3	Fatty acid-induced nuclear translocation of heparanase uncouples glucose metabolism in endothelial cells.....	41
3.3.1	Fatty acid stimulates rapid nuclear accumulation of heparanase.....	41
3.3.2	Nuclear translocation of heparanase is dependent on Bax-induced lysosome permeabilization.....	42
3.3.3	Hsp90 accompanies the nuclear translocation of heparanase	43
3.3.4	Nuclear heparanase is associated with cleavage of HS.....	43
3.3.5	Heparanase regulates HAT activity and genes related to glycolysis	44
3.3.6	PDK2 expression and extracellular lactate accumulation are regulated by nuclear heparanase.....	44
Chapter 4: Discussion.....		89
4.1	Endothelial heparanase secretion in diabetes is regulated by glucose and FA	89
4.2	Glucose-induced endothelial heparanase secretion requires cortical and stress actin reorganization	94
4.3	Fatty acid-induced nuclear translocation of heparanase uncouples glucose metabolism in endothelial cells.....	98
Chapter 5: Conclusions and Future Directions.....		105
5.1	Conclusions.....	105
5.2	Future directions	107
References.....		110

List of Figures

Figure 1	LPL synthesis and translocation in the heart	19
Figure 2	A schematic representation of heparanase structure and processing	20
Figure 3	Schematic model of cellular trafficking of heparanase.....	21
Figure 4	Effect of DZ on blood glucose and fatty acids and coronary LPL activity	46
Figure 5	Acute changes in cardiac heparanase and LPL following diazoxide.....	48
Figure 6	Dose-dependent effect of palmitic acid on endothelial heparanase.....	50
Figure 7	Dose-dependent effect of glucose on endothelial heparanase	52
Figure 8	Dual effect of palmitic acid and glucose on endothelial heparanase	54
Figure 9	Endothelial cytoskeleton regulates the effects of palmitic acid and glucose on endothelial cells	56
Figure 10	High glucose induces endothelial lysosomal heparanase secretion.....	58
Figure 11	High glucose and TNF- α induces endothelial heparanase secretion shown in multiple cells	60
Figure 12	Extracellular ATP mediates the effect of high glucose to induce heparanase secretion	61
Figure 13	MeSAMP duplicates the effect of high glucose to induce endothelial heparanase secretion	63
Figure 14	Glucose-induced endothelial heparanase secretion is dependent on cytoskeleton reorganization	64
Figure 15	Glucose-induced endothelial heparanase secretion is dependent on cytoskeleton reorganization	65

Figure 16 High glucose stimulates Ca^{2+} /calmodulin-dependent protein kinase II (CaMKII) and p38/MAPK/Hsp25 phosphorylation.....	66
Figure 17 Inhibiting CaMKII or p38 MAPK regulated stress actin formation prevents glucose-induced endothelial heparanase secretion	68
Figure 18 Colocalization of filamin with the P2Y ₂ receptor is disrupted by high glucose bringing about filamin redistribution	70
Figure 19 Endothelial secreted heparanase cleaves cardiomyocyte heparan sulfate to release attached proteins	72
Figure 20 Cellular distribution of endothelial heparanase	74
Figure 21 Fatty acid induces a rapid nuclear accumulation of heparanase in EC	75
Figure 22 Nuclear translocation of heparanase following PA is dependent on Bax-induced permeabilization of lysosomes.....	77
Figure 23 PA for up to 24 hr is unable to induce caspase 3 cleavage	79
Figure 24 Hsp90 directs the nuclear translocation of heparanase	80
Figure 25 Heparanase cleaves nuclear heparan sulfate (HS)	82
Figure 26 Nuclear heparanase regulates HAT activity and genes involved with glucose metabolism	84
Figure 27 Genes related to inflammation are influenced by PA induced nuclear entry of heparanase	85
Figure 28 Nuclear heparanase increases PDK2 expression and extracellular lactate accumulation	86
Figure 29 PA has no influence on the expression of endothelial PPAR α	88

Figure 30 A summary diagram describe the mechanism of endothelial heparanase regulation of cardiac LPL	102
Figure 31 Schematic mechanism of how high glucose stimulates endothelial heparanase secretion	103
Figure 32 Scheme of probable mechanisms of how high FA stimulates nuclear translocation of endothelial heparanase.....	104

List of Abbreviations and Acronyms

AMPK	AMP-activated protein kinase
bCAECs	Bovine coronary artery endothelial cells
bFGF	Basic fibroblast growth factor
BPA	2-bromohexadecanoic acid
CaMKII	Ca ²⁺ /calmodulin-dependent protein kinase II
Ctsb	Cathepsin B
DAPI	4',6-Diamidino-2-phenylindole
DZ	Diazoxide
ECs	Endothelial cells
ECM	Extracellular matrix
FA	Fatty acid
GA	Geldanamycin
GBM	Glomerular basement membrane
HAT	Histone acetyltransferase
Hsp	Heat shock protein
HSPG	Heparan sulfate proteoglycans
LAMP-1	Lysosomal-associated membrane protein 1
LDHA	Lactate dehydrogenase A
LPL	Lipoprotein lipase
MAPK	Mitogen-activated protein kinase
Mnt	Mannitol
NEFA	Non-esterified fatty acid
PA	Palmitic acid
PDH	Private dehydrogenase
PDK	Private dehydrogenase kinase
PPAR α	Peroxisome proliferator-activated receptor α
SLC2A1	Solute carrier family 2, facilitated glucose transporter member 1
TG	Triglyceride
TNF α	Tumor necrosis factor α
T1D	Type 1 diabetes
T2D	Type 2 diabetes
VCAM1	Vascular cell adhesion molecule 1
VEGF	Vascular endothelial growth factor

Acknowledgements

It is a great opportunity to offer my sincerest gratitude to so many people who made this thesis possible.

I first give my deepest appreciation to my Ph.D. supervisor, Dr. Brian Rodrigues. Thanks for your encouragement, your support and your time spending with us. It has been an honor to work with you for four years.

I sincerely thank all the members of my Ph.D. supervisory committee: Dr. Helen Burt, Dr. Ismail Laher, and Dr. Roger Brownsey, who raised good questions and wise advices on my project, and more importantly, trained me to question and think more deeply. Special thanks to Dr. Adam Frankle for willing to be my temporary committee chair.

My research project was funded by Canadian Institutes of Health Research, and Canadian Diabetes Association provided me with Doctoral Student Research Award. Thank you very much for your generous support.

I have worked with a group of friendly and fascinating lab mates: Ashraf, Prasanth, MinSuk, Girish, Sanjoy, and Dahai, who gave inspiration and support. Dr. Zhengyuan Xia and his family give me so much help and care through these years. I am so fortunate to meet all of you here.

Lastly and most importantly, sincere thanks are owed to my parents and brother who give me continuous support all the time. To them I dedicate this thesis.

Dedication

To the three most important people in my life: my parents and my brother. Without your support, my life will go nowhere.

Chapter 1: Introduction

1.1 Diabetes mellitus

Diabetes mellitus is a chronic disease, which is characterized by inappropriate elevation in blood glucose due to insulin deficiency or insulin resistance. It is becoming a worldwide health problem. In the present, more than 220 million people were diagnosed with diabetes, and WHO projects that diabetes death will double between year of 2005 and 2030 (<http://www.who.int/mediacentre/factsheets/fs312/en/index.html>). There are two kinds of diabetes: Type 1 and Type 2 diabetes. Type 1 diabetes (T1D) has an absolute deficiency of insulin production from pancreatic β -cells, which are destroyed by autoreactive T cells.¹ People are usually diagnosed as T1D before the age of 30, and mostly during childhood. Type 2 diabetes (T2D) mainly results from peripheral insulin resistance and relative insulin deficiency. The hallmark of T2D is the hyperglycemia-induced overstimulation of β -cell secretion of insulin, which results primarily in hyperinsulinemia and over time, hypoinsulinemia due to failure of β -cell function. T2D is the most common form of diabetes, accounting for 90 to 95% of patients with diabetes in North America.² Compared to T1D, T2D are often diagnosed in adults over the age 40. Patients can be unnoticed for many years and some serious complications can result from improper control of this disease. Cardiovascular complications, such as coronary artery disease and hypertension are responsible for about 80% of the mortality observed in patients with diabetes.³ In addition to vascular defects, increasing evidence from clinical and experimental studies have established the existence of metabolic, functional and structural alterations specifically in the heart muscle of diabetic patients, which can occur in the absence of coronary vessel disease.^{4, 5} For example, in the heart, increased stiffness of the left ventricular wall and deposition of

connective tissue together with insoluble collagen have been observed.^{6, 7} Diabetic cardiomyopathy has been used to describe this specific cardiac injury, characterized by decreased diastolic function (with or without systolic function) of the left ventricle. Although the underlying mechanisms that predispose the diabetic heart to these abnormalities remains unclear, accumulating lines of evidence suggest that early metabolic alterations play a crucial role in the development of diabetic cardiomyopathy.^{8, 5, 9}

1.2 Heart metabolism

1.2.1 Cardiomyocytes

As uninterrupted contraction is a unique feature of the heart, cardiac muscle has a high demand for provision of energy.¹⁰ Under normal physiological conditions, hearts can utilize multiple substrates, including fatty acid (FA), carbohydrates, amino acids and ketone bodies. Among these substrates, carbohydrate and FAs are the dominant substrates from which the heart derives most of its energy. About 70% of ATP is generated through FA β -oxidation, whereas glucose and lactate provide 30% of energy to the cardiac muscle.¹¹ Cardiac FAs originate from different resources: i) release from adipose tissue and transport to the heart after complexing with albumin,¹² ii) provision through the breakdown of endogenous cardiac triglyceride stores,¹³ iii) internalization of whole lipoproteins,¹⁴ and iv) hydrolysis of circulating TG-rich lipoproteins (very low density lipoproteins and chylomicrons) to FA by lipoprotein lipase (LPL) positioned at the endothelial surface of the coronary lumen.¹⁵ It should be noted that this LPL-mediated hydrolysis of TG-rich lipoproteins to FA is suggested to be the major supply of free FA for cardiac utilization, as the molar concentration of FA in TG-rich lipoproteins is 10 times higher than albumin-bound FA (the small amount of non-esterified plasma FA are incapable of competing with the substantial amounts of FA

generated through lipoprotein-TG breakdown).¹⁶ FA delivery and utilization by the cardiomyocytes involves transport through endothelial cells, diffusion across the interstitial space with albumin, and uptake by cardiomyocytes. Once inside the myocytes, FAs are transported across the mitochondrial membranes by carnitine palmitoyl transferase I and II, and undergo β -oxidation.

During diabetes, with insulin deficiency or resistance, glucose utilization is prevented in cardiomyocytes because of impaired glucose uptake, glycolysis and glucose oxidation. In addition, insulin dysfunction increases lipolysis in adipose tissue and results in elevated plasma FA. In this condition, the heart rapidly switches to use FA exclusively for ATP generation.^{17, 18} Although this change in substrate choice is critical to guarantee continuous energy supply to maintain cardiac function, elevated FA utilization is associated with a number of deleterious consequences. For example, augmented FA metabolism inhibits glycolysis and glucose oxidation, which occurred even before the onset of impaired insulin signaling in the heart of *ob/ob* and *db/db* mice.¹⁹ High rate of FA oxidation also decreases efficiency of cardiac oxygen consumption and increases reactive oxygen species production, leading to lipotoxicity and mitochondrial dysfunction.^{20, 21} These effects eventually contribute towards the development of diabetic cardiomyopathy.

1.2.2 Endothelial cells

Endothelial cells (ECs) are a thin layer of flat nucleated cells that cover the innermost portion of blood vessels. They not only function as a selective barrier for oxygen and nutrient exchange, but also provide paracrine signaling to regulate inflammation, coagulation and vascular tone.²² In the heart, coronary artery ECs are placed at a strategic position between blood and cardiomyocytes, which make them the first line to confront pathologic

conditions such as hyperglycemia and dyslipidemia. ECs have traditionally been considered as quiescent with low energy demand and different metabolic properties compared to cardiomyocytes. As ECs have a small number of mitochondria compared to metabolically active cells,²³ the oxidative metabolism of different fuel substrates, such as glucose and FA, seems less important for them than for cardiomyocytes. Krutzfeldt *et al* examined the metabolism of coronary ECs and reported that glucose instead of FA is the preferential fuel source to generate ATP for normal EC function.²⁴ They reported that 99% of glucose is metabolized to lactate by aerobic glycolysis, with only 0.04% oxidized in the Krebs cycle at 5 mM glucose. However, glucose oxidation was elevated at a lower glucose concentration (1 mM).²⁴ Thus, oxidative metabolism in mitochondria is suppressed at physiologic concentrations of glucose in these cells, a phenomenon called the Crabtree effect.^{24, 25} In the heart, glucose uptake by ECs is mainly regulated by glucose transporter 1, which facilitates constant glucose uptake at physiologic concentrations, and is not responsive to insulin.²⁶ Glucose transporter 1 expression is down-regulated in bovine aortic EC exposed to hyperglycemia for 48 hr,²⁷ an adaptive response that may protect EC against glucose toxicity.

There is limited knowledge describing FA metabolism in ECs. Earlier studies on long-chain FA transport through non-fenestrated endothelium suggested that interaction of albumin-bound FA complex with albumin-binding proteins facilitate the dissociation of FA from albumin.²⁸ Fatty acid translocase (CD36), fatty acid transport protein and fatty acid binding proteins subsequently assist the free FA transport from the apical to the basolateral side of ECs.²⁹ Compared with cardiomyocytes, a very low β -oxidation rate of palmitate was reported in ECs from rat heart, which was inhibited by more than 80% in the presence of 5 mM glucose.³⁰ However, other studies have suggested that ECs have the potential to use FA

as an energy source. ECs demonstrate high carnitine acyl-CoA transferase activity, which indicate a high capacity for β -oxidation.³¹ In human umbilical vein endothelial cells, FA oxidation contributes ~25% of total ATP generated in cells incubated in 5 mM glucose. In the presence of 2 mM 5-aminoimidazole-4-carboxamide riboside, a stimulator of AMP-activated protein kinase, increased palmitate oxidation elevated total ATP by ~35%, with a decrease in glucose uptake and glycolysis.³²

1.3 Lipoprotein lipase

LPL, which is largely expressed in adipose tissue, heart and skeletal muscle, is a major enzyme which hydrolyzes circulating TG-rich lipoproteins to release free FA.³³ This hydrolysis occurs at the vascular endothelium, where LPL is present bound to heparan sulfate proteoglycans (HSPGs).³⁴ Although LPL function at the capillary endothelium surface, ECs do not express LPL mRNA.³⁵ In the heart, this enzyme is synthesized by cardiomyocytes and subsequently secreted onto HSPG binding sites on the myocyte cell surface.³⁶ From here, LPL is transferred to the luminal surface of EC where it actively metabolizes the TG core of lipoproteins to FA,³⁷ these released FA are then transported into the heart for numerous metabolic and structural functions (Figure 1). Electron microscopy using immunogold-labeling established that, in the heart, 78% of total LPL is present in cardiac myocytes, 3-6% in the interstitial space, and 18% at the coronary endothelium.^{15, 37} Even though the majority of enzyme is located in myocytes, vascular endothelial-bound LPL likely determines the rate of plasma lipoprotein-clearance, and hence is termed “functional” LPL.³⁸ In addition to its lipolytic role, LPL also mediates a non-catalytic bridging function that allows it to bind simultaneously to both lipoproteins and specific cell surface proteins, facilitating cellular uptake of lipoproteins.^{39, 40}

LPL synthesis and activity is altered in a tissue specific manner by various physiological conditions such as cold exposure,⁴¹ lactation,⁴² or feeding and fasting.^{43, 44} During fasting, with ensuing hypoinsulinemia, LPL activity decreases in adipose tissue but increases in the heart,⁴⁵ as a result, FA from circulating TG are diverted away from storage to meet the metabolic demands of the heart. Hence, LPL fulfills a "gate-keeping" function by regulating the supply of FA to meet the metabolic demands of different tissues. Through such a role, LPL activity directly affects the level of circulating lipoprotein-TG. For example, in transgenic rabbits that have global overexpression of LPL, attenuation of hypertriglyceridemia was observed.⁴⁶ Contrary to systemic overexpression, cardiac-specific deletion or overexpression of LPL is associated with heart dysfunction.^{47, 48} Accordingly, although loss of cardiomyocyte LPL in adult mice increased glucose metabolism, this effect, nor albumin bound FA could replace the action of LPL, and cardiac ejection fraction decreased.⁴⁹ Cardiac-specific overexpression of LPL causes a severe myopathy, characterized by both muscle fiber degeneration and extensive proliferation of mitochondria and peroxisomes.^{47, 48} In genetically engineered mice that specifically overexpressed an anchored form of cardiomyocyte surface-bound LPL, lipid oversupply and deposition was observed, together with excessive dilatation and impaired left ventricular systolic function.⁵⁰ The latter experiments demonstrate that in the absence of any vascular defects, selective overexpression of LPL in the heart is sufficient to cause cardiac failure.

Regulation of cardiac LPL is intricate and several control mechanisms have been recognized, both within the cardiomyocyte (e.g., trans-Golgi processing, lysosomal degradation, secretory vesicular transport) and at the vascular lumen (e.g., competitive inhibition or displacement of by lipolytic end products, endothelial recycling).^{51, 52} Less well

studied is the arrangement by which LPL is translocated from the cardiomyocyte surface HSPG, across the interstitial space, onto comparable HSPG binding sites on the apical side of vascular endothelial cells. For this to occur, detachment of LPL from the myocyte cell surface is a prerequisite, and is likely mediated by enzymatic cleavage of cardiomyocyte HSPG. At present, the mechanisms that regulate LPL translocation from the parenchyma cells to ECs, particularly from myocytes to endothelial lumen is not completely understood.

1.4 Heparan sulfate proteoglycans

1.4.1 Synthesis and structure

HSPG are ubiquitous macromolecules presented on cell surface, extracellular matrix (ECM) and basement membrane. The basic structure consists of a core protein to which several linear HS side chains are covalently linked.^{53, 54} In the Golgi, HS chains are synthesized as an unbranched polysaccharide of repeating glucosamine and uronic (glucuronic or iduronic) acid disaccharide units, which are extensively modified by various degrees of *N*-sulfation/*N*-acetylation on glucosamine residues, C-5 epimerization on glucuronic acid and *O*-sulfation at various sites.^{53, 55} Due to the great variation in the degree and sequence of these reactions, HS chains present extensive structural heterogeneity, which provide specific sites for protein binding and HS cleavage. For example, HS association with antithrombin III is restricted to the relatively rare modified pentasaccharide units, which contain a central 3-*O*-sulfated glucosamine residue.⁵⁶ Its interaction with basic fibroblast growth factor (bFGF) depends on the arrangement of disaccharides in a sequence-specific manner, in which short *N*-sulfation domains are intersected by *N*-acetylated disaccharide.^{57, 58} As a result, HS serve not only as structural proteins, but also as receptors; HS can bind a wide variety of bioactive molecules (growth factors, chemokines, cytokines, coagulation

factors, and enzymes like LPL).^{59, 60} This binding function protects molecules from proteolytic degradation and inactivation, and provides the cell with a rapidly accessible reservoir, precluding the need for *de novo* synthesis when the requirement for a protein is increased. Thereby, HSPG play a critical role in both physiological and pathological processes ranging from morphogenesis, tissue repair and inflammation to cancer metastasis.

HSPG are divided into several groups based on the core proteins, which include the membrane-spanning syndecan, glycosylphosphatidylinositol-anchored glypican⁵³ and perlecan.⁶¹ Syndecan and glypican are the main types of cell surface HSPG⁵³ and could interact with other ECM component such as fibronectin,⁶² or function as a coreceptor with other molecules such as integrin,⁶³ which facilitate transduction of extracellular signals and control cell adhesion, migration and proliferation. Perlecan is the major HSPG presented in subendothelial matrix,⁶⁴ and is critical for maintaining vascular structure. In addition, it can function as a sequestration store for growth factors, and is also a key target for regulation of atherogenic lipoproteins.⁶¹

1.4.2 Functions

As a key component of ECM and basement membrane, HSPG have diverse effects in regulation of basement membrane permeability, controlling of growth factor activity and mediation of cellular adhesion.^{61, 65} Uncontrolled HSPG degradation is therefore expected to profoundly affect various cell and tissue functions. For example, decreased vascular HSPG have been detected in conditions of atherosclerosis and diabetes and tumor metastasis.⁶⁶⁻⁶⁸ HSPG presented on vascular endothelium interact with a number of cytokines and chemokines, such as IL-8, interferon- γ and antithrombin.^{65, 69} Degradation of HSPG liberated these molecules, which then triggered the process of inflammation and thrombosis.

Moreover, HSPG in the subendothelial matrix form a physical barrier to prevent the entrance of cells and large molecules into tissues.⁷⁰ Additionally, they provide a storage depot for a number of bioactive proteins as mentioned above. Previous data indicated that endothelial cell-derived HSPG are potent inhibitor of vascular smooth muscle cell proliferation and mitogenesis.⁷¹ Atherogenic lipoproteins, such as low density lipoprotein and oxidized-low density lipoprotein reduced HSPG content in the vascular ECM by inhibition of the core protein synthesis as well as stimulation of HS degradation.^{70, 72} Therefore, HSPG participated in a series of events related to atherogenesis, from monocyte recruitment and smooth muscle cell proliferation to thrombosis. In the kidney, anionic polysaccharide HS covalently attached to proteoglycans in glomerular basement membrane (GBM), which were considered as the major determinants for the charge-dependent filtration.^{73, 74} Spiro and colleagues first reported decreased HSPG level in the GBM of patients with diabetic nephropathy,⁷⁵ and an inverse correlation between HS presented in GBM and proteinuria has been consistently reported in different types of glomerular diseases.⁷⁶ Another major effect of HSPG is its contribution to the progress of tumor metastasis and angiogenesis.⁷⁷ Loss of HSPG is the essential process by which malignant cells invade through BM and ECM during tumor metastasis. In blood vessel wall, degradation of HSPG by proliferating ECs is presumed to assist the invasion and migration of ECs toward the angiogenic stimulus, which is the important early event in vascular sprouting and angiogenesis.⁷⁸

1.5 Heparanase

1.5.1 Synthesis and processing

Heparanase is an endoglycosidase that specifically cleaves carbohydrate chains of HS into oligosaccharides.⁷⁹ It is highly expressed in placental trophoblasts, hematopoietic cells

such as platelets, neutrophils and tumor cells.⁸⁰ Human heparanase gene, which was first cloned in 1999, is located on chromosome 4q21.3 and encodes a polypeptide of 543 amino acids.⁸¹ It is first synthesized as a 68 kDa pre-proheparanase that contains a N-terminal signal peptide (Met¹-Ala³⁵), a C-terminal hydrophobic peptide, five cysteine residues and six N-glycosylation sites.^{76, 82} The pre-proheparanase is directed into endoplasmic reticulum where it is glycosylated, and the signal peptide is cleaved to form 65 kDa inactive proheparanase (Figure 2). Following transport into Golgi and packaging into vesicles, the 65 kDa inactive proheparanase is secreted from the cell.⁷⁶ This is followed by reuptake into cells, a process which is suggested to be mediated by HSPG, low density lipoprotein receptor-related protein or mannose 6-phosphate receptors.⁸³ After transport into late endosomes and lysosomes, it undergoes proteolytic cleavage (removal of a 6 kDa linker peptide Ser¹¹⁰-Gln¹⁵⁷) by cathepsin L in lysosomes.⁸⁴ Interestingly, the function of this 6 kDa peptide is suggested to impede HS chain binding or obstruction to the active site of heparanase.⁸⁵ Removal of this peptide produces an active heterodimer, consisting of a 8 kDa (Gln³⁶-Glu¹⁰⁹) peptide non-covalently associated with a 50 kDa (Lys¹⁵⁸-Ile⁵⁴³) peptide, which is ~100-fold more active than the 65 kDa inactive proheparanase.^{86, 87} Within the acidic compartment of the late endosome or lysosome, active heparanase is stored in a stable form (half-life ~30 h).⁸⁸ Mobilization by demand can occur, where the enzyme is either translocated to the nucleus to affect gene transcription, or secreted to degrade cell surface HS chains (Figure 3).⁸⁹

1.5.2 Mechanism of catalysis

Heparanase catalyzes the hydrolysis of glycosidic bonds within the polysaccharide HS chains, using a general acid catalysis mechanism similar to clan A glycosyl hydrolase

enzymes.⁸² Apparently, it is separated from bacterial heparitinase which cleaves HS extensively through a β -eliminase mechanism.⁹⁰ First, the critical active-site catalytic proton donor and nucleophile residues are likely conserved at Glu²²⁵ and Glu³⁴³ within the 50 kDa active form of human heparanase (Figure 2).⁹¹ Depending on the spatial position of the catalytic residues, hydrolysis of glycosidic bonds occurs by inversion or retention of the anomeric configuration.⁹² Site-direct mutation on these two residues on heparanase resulted in abolishment of this HS-cleaving capacity.⁹¹ In addition, secondary structural studies revealed that heparanase is likely to contain an $(\alpha/\beta)_8$ TIM-barrel fold, which is also homologous to family 10, 39 and 51 of clan A glycosyl hydrolase.⁹¹ Interestingly, the α/β units 1 and 2 of many other glycosyl hydrolases are known to participate in substrate binding. On the basis of sequence alignments, the region Lys¹⁵⁸-Asp¹⁷¹ (in α -helix 2) on heparanase has been proved to be the interaction site with HS. Using a KKDC peptide corresponding to this region, and antibody generated against this peptide dose-dependently inhibits HS-cleaving activity of heparanase.⁹³ Heparanase cleaves HS chains at specific sites, which generates HS fragments that are 5-7 kDa in size (10-20 sugar units).⁸²

1.5.3 Regulation of gene transcription

Increased heparanase gene expression has been reported in many different types of cancer cells, and is closely correlated to the metastasis potential and worsening of prognosis. A clinical study revealed that 86% of the patients with myeloma exhibited elevated gene expression of heparanase.⁹⁴ Heparanase promoter is a 0.3 kb region located upstream of the ATG initiation site, containing two GC box but no TATA or CCAAT boxes.⁹⁵ It can be positively or negatively regulated by a variety of transcription factors. Truncation and mutational analysis revealed that Sp1 and Ets are capable of binding with the heparanase

promoter and are responsible for basal heparanase promoter activity.⁹⁶ Compared to Sp1 and Ets, the early growth response 1 appears to be a key regulator of the inducible heparanase transcription in cells exposed to growth factors, cytokines, vascular injury and hypoxia.^{97, 98} In phorbol 12-myristate 13-acetate activated T cells, early growth response 1 expression was rapidly induced, followed by increased heparanase transcription, a process that was dependent on the mitogen-activated protein kinase (MAPK) pathway.⁹⁹ Apart from malignant cells, transcription factor also participates in the regulation of heparanase transcription in normal cells, such as ECs. It has been reported that both high glucose and FA have the ability to induce heparanase gene expression in ECs.^{100, 101} Sp1 has been identified as the mediator for FA,¹⁰¹ whereas the regulatory target of glucose is still controversial. In delayed-type hypersensitivity mouse model, tumor necrosis factor α (TNF α) and interferon- γ increased heparanase gene expression and enzymatic activity in ECs. Analysis on the promoter region demonstrated the presence of two interferon-stimulated response elements, which binds to transcription factors activated by interferon- γ .¹⁰² Recently, it has been shown that heparanase promoter is also under transcriptional repression in normal conditions. p53, a wild-type tumor suppressor, directly binds to heparanase promoter and inhibits transcription.¹⁰³ Mutated p53 lost the ability to bind heparanase promoter and thus enhanced gene transcription. In addition to transcription factors, the methylation status of the promoter region is also an important contributor to heparanase transcriptional regulation. Several lines of evidence have revealed that the methylation prevalence of promoter is inversely correlated with heparanase expression.^{97, 98, 104} In normal bladder and bladder cancer samples, heparanase expression was lowest in methylation-positive samples and highest in methylation-negative samples. Treating with

demethylating agent 5-azacytidine restored heparanase activity in C6 glioma cells that exhibit no heparanase activity.¹⁰⁴

1.5.4 Pathological functions

Heparanase is uniquely capable of cleaving HS chains and participates in degradation and remodelling of ECM and BM. In physiological condition, it is implicated in the regulation of embryonic morphogenesis, wound healing and inflammation.^{80, 82} However, this function has been effectively hijacked or aggravated in several conditions, and its contribution towards pathological diseases is also well documented.

1.5.4.1 Tumor metastasis

Heparanase has been traditionally correlated with cell invasion, angiogenesis and tumor metastasis for many years. Increased expression and activity of heparanase has been detected in an increasing number of primary solid and haematological cancers, and implicated with worsening prognosis of pancreatic, bladder, multiple myeloma and acute myeloid leukemia.^{94, 104-106} Its contribution towards tumor metastasis has been explained in detail by several mechanisms. The endoglycosidase nature of heparanase facilitates degradation of ECM and BM and clearance of the physical barrier for cell invasion, which is a critical step required for tumor metastasis and angiogenesis.⁷⁷ It was shown that non-metastatic T-lymphoma and melanoma were converted into highly metastatic cells following heparanase transfection.⁸⁷ Similarly, enhanced metastasis was reported in pancreatic cancer, myeloma and breast carcinoma cells after overexpression with heparanase.^{105, 107, 108} In fact, augmented heparanase activity was detected from bone marrow plasma in 86% of the patients with myeloma.⁹⁴ Such effects may not only be utilized by tumor cells. Increased heparanase is intimately involved in enhanced microvessel density in tumor tissue, an

angiogenic feature that provides tumor cells with sufficient nutrition and the potential for distant metastasis.⁹⁴ A high heparanase expression was detected in ECs of sprouting capillaries in colon and pancreatic carcinoma tissue, but not in mature, quiescent vessels.⁷⁸ Microvessel density was effectively decreased in tumor developing from cells transfected by anti-heparanase ribozyme.¹⁰⁹ Moreover, PI-88, a heparanase inhibitor in phase II clinical trial, effectively suppressed tumor growth by 50% and neovascularization by 30%.¹¹⁰

Another proposed mechanism is the suggestion that degradation of HS by heparanase liberates HS-bound angiogenic growth factors (VEGF and bFGF) and cytokines, thus enhancing tumor development through their effects on angiogenesis and tumor growth.^{78, 111} Vascular endothelial growth factor (VEGF) and bFGF signaling network plays a ubiquitous role in tumor cell growth, proliferation and angiogenesis. In cell-culture dishes coated with ECM from human umbilical vein endothelial cells, 100 ng/ml of recombinant heparanase spontaneously released bFGF into culture media, which significantly enhanced proliferation and migration of ECs and microvessel outgrowth. These effects were dose-dependently inhibited by the heparanase inhibitor, JG3.¹¹²

Finally, heparanase triggers intracellular signalling cascades, and stimulates protein kinase phosphorylation and gene transcription that are involved in tumor metastasis.⁹⁰ Interestingly, this mechanism appears to be independent of its catalytic activity, and is induced by the inactive form of heparanase. In several tumor-derived cells, heparanase stimulated tumor cell adhesion and spreading in the presence of its enzymatic inhibitory peptide KKDC.^{113, 114} It is possible that inactive heparanase binding to HS forms a bridge between cells and the adhesion surface. However, more convincing evidence suggested that binding of KKDC with HS induced clustering of cell surface syndecans and activated

intracellular signalling including protein kinase C, Src and Rac, which were known to regulate cell adhesion.¹¹⁵ Similarly, inactive heparanase has also been shown to activate ECs and elicit angiogenic response.¹¹⁶ For example, addition of exogenous inactive heparanase to ECs resulted in phosphorylation of Akt/PI3K signalling and stimulated *in vitro* ECs migration and invasion.¹¹⁶ Consistently, a significant elevation of angiogenesis-promoting factor VEGF expression was reported as an Src-dependent, but heparanase enzymatic-independent manner in ECs.^{117, 118} Moreover, inactive heparanase stimulated expression of endothelial tissue factor through p38 MAPK pathway,¹¹⁹ which could explain activation of the coagulation system commonly seen in cancer patients. Cell surface receptor binding of inactive heparanase has also been implicated in initiating signal cascades and gene transcription.¹²⁰ However, existence of these receptor(s) has yet to be elucidated.

1.5.4.2 Diabetes

In addition to its well-known function in tumor metastasis, heparanase also plays pivotal role in diabetes-associated complications, such as diabetic nephropathy and atherosclerosis.^{100, 101} As mentioned above, HSPG were considered as the major determinants for the charge-dependent permeability of GBM. Diabetic nephropathy is characterized by loss of HSPG content in the GBM and proteinuria at a later stage.⁷⁶ Although the exact molecular mechanism for the HSPG decrease remains controversial, clinical and experimental studies have pointed out the critical role of heparanase in the pathogenesis of proteinuria. Elevated heparanase activity has been detected from urinary sample, and heparanase expression was upregulated in the renal epithelial cells in patients with diabetic nephropathy.¹⁰⁰ Immunohistochemical images showed an increased heparanase staining in tubular epithelial cells in the kidney of these patients.¹⁰⁰ *In vitro* mechanistic

studies revealed that heparanase mRNA and protein were increased in glomerular epithelial cells exposed to 25 mM glucose, together with the induction of HS degradation and augmented membrane permeability to albumin. In another study, the above phenomenon was effectively reversed by heparanase inhibitor PI-88 and heparin.¹²¹ These observations provide strong evidence that heparanase dysregulation is at least partly responsible for the reduction of HS content in GBM under diabetic conditions. It is possible that elevated enzymatic heparanase-induced HS degradation disrupted the integrity and increased the permeability of GBM, leading to elevated albumin excretion and proteinuria seen in diabetic nephropathy. In addition, HS cleavage may release HS-bound bioactive molecules, which could modulate cellular processes and enhance glomerular damage.⁷⁶ In addition to the above, inactive heparanase has also been postulated to be involved in the initiation of proteinuria through undefined mechanisms; inactive heparanase appeared at day 5 of acute puromycin aminonucleoside nephrosis, whereas active heparanase was detected at day 14.¹²²

Such effects may not be restricted to diabetic nephropathy. Emerging evidence indicates that heparanase also participated in the pathogenesis of atherosclerosis, which increases morbidity and mortality in diabetic patients. Recently, it has been reported that heparanase was prominently expressed in ECs of the atherosclerosis-prone regions of aortic root from apoE-null mice, but not in nonatherosclerotic mice.¹⁰¹ It was also detected in macrophages of neointima, but only at a later stage. In normal conditions, heparanase expression was undetectable in vascular endothelium.^{59, 70} When ECs are exposed to high fatty acids or oxidized-low density lipoprotein, heparanase expression was stimulated in a time- and dose-dependent manner.^{59, 100} In bovine aortic ECs, 0.6 mM oleic acid notably induced heparanase expression as early as 6 hr. In human microvascular ECs, advanced glycation end-products

induced heparanase expression through activation of FOXO4.¹²³ Furthermore, the early atherogenesis is characterized by leukocyte recruitment and expression of pro-inflammatory cytokines, such as TNF- α and IL-1 β , which can also stimulate heparanase expression and secretion from ECs and blood-born cells.¹⁰¹ At the same time, HSPG cleavage coincided with increased endothelium heparanase, and a negative correlation between HSPG and atherosclerosis was also reported.⁶⁶ The proposed mechanism is that heparanase promotes degradation of the vascular ECM and basement membrane, thereby permitting penetration of monocytes and low density lipoprotein particles into vascular wall. Additionally, the inhibitory effect of HS towards smooth muscle cell migration and proliferation was also lost after HSPG cleavage by heparanase.⁷¹ This notion was supported by recent studies indicating that the inhibitory effect of ECs on smooth muscle cell proliferation was markedly enhanced with reduced endothelial heparanase, and lost with overexpression of heparanase.¹²⁴ Interestingly, Goldberg's study reported that endothelial-secreted heparanase promoted LPL transfer from adipocytes to the luminal endothelial surface in a coculture system.⁵⁹ As LPL is the rate-limiting enzyme in hydrolysis of circulating TG-rich lipoproteins to release free FA, another mechanism of how heparanase affect atherosclerosis may be related to its regulation of lipoprotein metabolism through LPL.

1.6 Hypothesis and research objectives

In the heart, the mechanisms that regulate LPL translocation from the cardiomyocyte surface to the endothelial lumen are poorly understood. My hypothesis is that *endothelial heparanase is a central modulator of the amount of LPL located at the coronary vascular lumen*. This distinctive function of heparanase could be an important means by which the

heart increases its utilization of FA in response to diabetes, and could be potentially relevant in the attempt to lower heart disease during this condition.

The objectives of my research proposal were to:

1. Determine changes in cardiac heparanase during diabetes, and its relation to LPL.
2. Examine the mechanisms by which hyperglycemia induce endothelial heparanase secretion.
3. Investigate the impact of high FA on endothelial heparanase, especially related to substrate utilization.

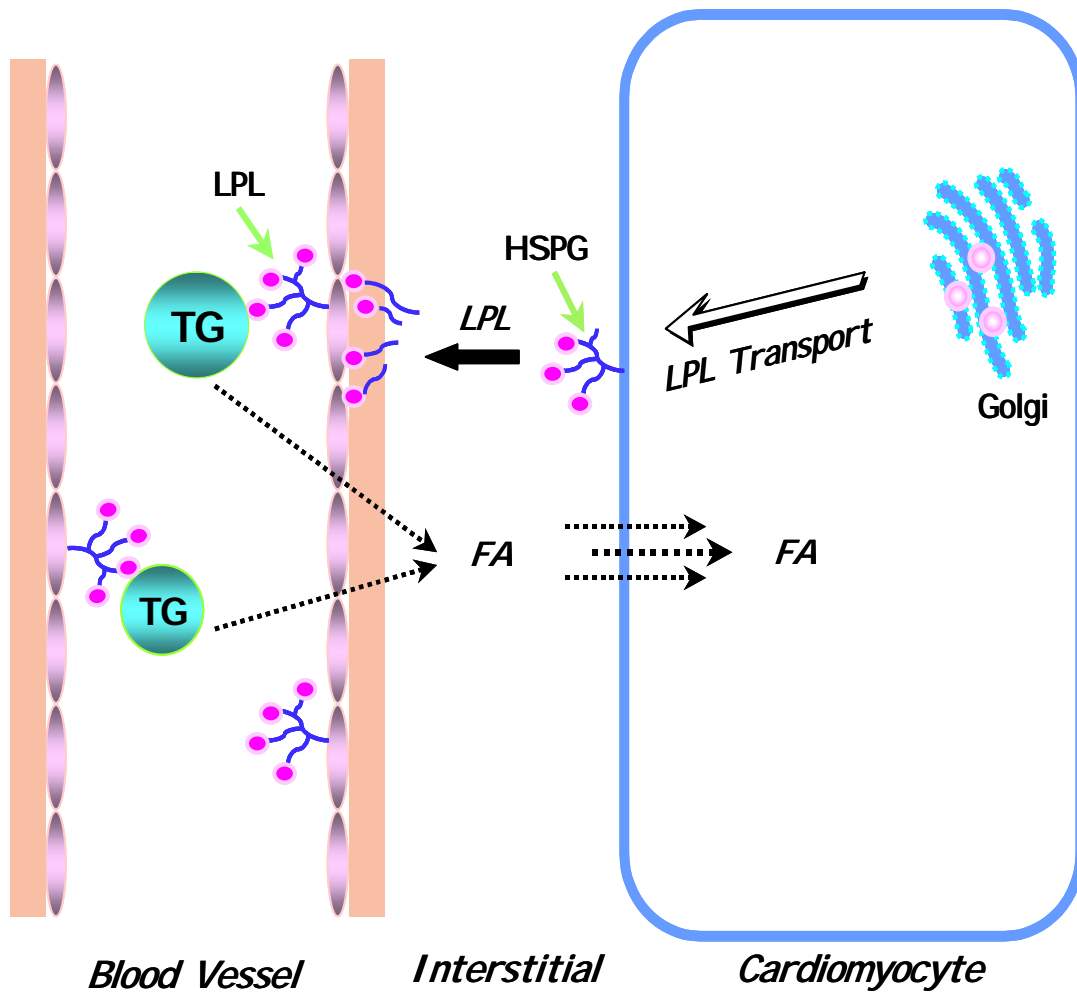


Figure 1 LPL synthesis and translocation in the heart. Following synthesis in the cardiomyocyte, LPL is exported to the myocyte cell surface HSPG, and from here to the luminal side of the endothelial cell. At this location, the enzyme facilitates TG-rich lipoprotein hydrolysis and release FA.

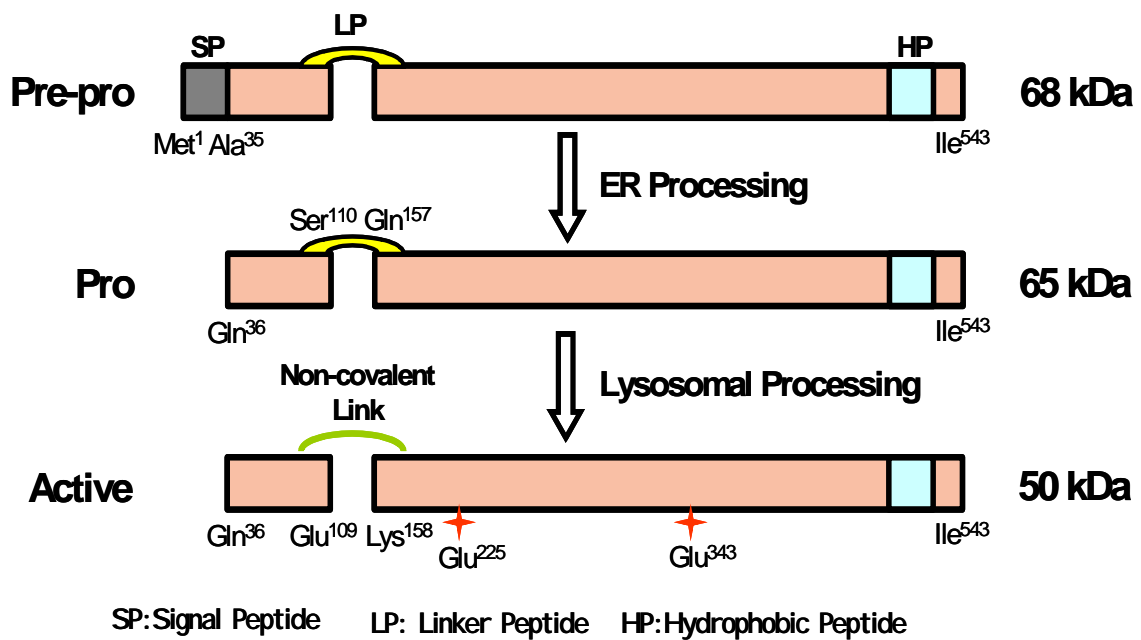


Figure 2 A schematic representation of heparanase structure and processing. Heparanase is first synthesized as a 68 kDa Pre-pro form that contains a N-terminal signal peptide (SP, Met¹-Ala³⁵) and a C-terminal hydrophobic peptide (HP). In the ER, SP is removed and produces a 65 kDa inactive Pro heparanase, which can undergo lysosomal translocation. Inside lysosomes, a 6 kDa linker peptide (LP, Ser¹¹⁰-Gln¹⁵⁷) is cleaved and forms a 50 kDa active heparanase, which contains two non-covalently bound polypeptides (Gln³⁶-Glu¹⁰⁹ and Lys¹⁵⁸-Ile⁵⁴³). Two active-site catalytic proton donor (Glu²²⁵) and nucleophile (Glu³⁴³) residues are marked as red stars.

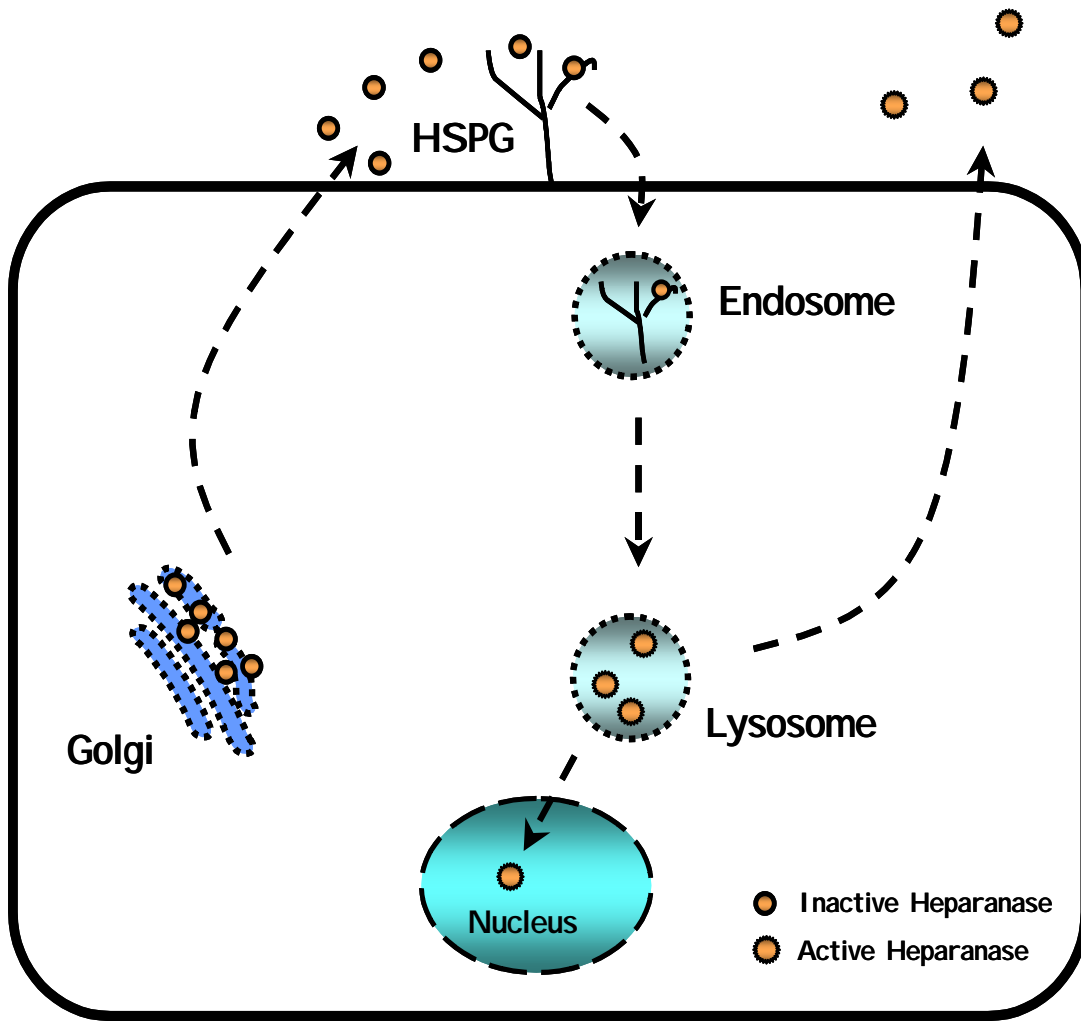


Figure 3 Proposed cellular trafficking model of heparanase. In the Golgi apparatus, inactive heparanase is packaged into vesicles and secreted from the cell. This is followed by reuptake into cells through HSPG, and relocation into endosome and lysosomes. In the lysosomes, active heparanase is formed and stored in a stable form, which can be either translocated to the nucleus or secreted out in response to different stimulus.

Chapter 2: Methods

2.1 Materials

[³H]triolein and the ECL[®] detection kit were purchased from Amersham Canada. Heparin sodium injection (Hapalean, 1000 USP U/ml) was obtained from Organon Teknika. Heparanase mAb 130, which can recognize both the 50 and 65 kDa forms, was obtained from InSight Ltd (Rehovot, Israel). The monoclonal anti-bovine LPL (5D2) was kindly supplied by Dr. JD Brunzell (University of Washington). Anti-phospho Hsp25 (Ser⁸⁶) antibody was from GeneTex, Inc. Anti-heparan sulfate 10E4 and 3G10 antibody was from Seikagaku Corporation (Tokyo, Japan). Hsp90 and caspase 3 antibody were from Cell signaling. Prohibitin antibody was from Abcam Cambridge, MA. Phospho-pyruvate dehydrogenase E1 α (PDHE1 α) antibody was from Novus Biologicals. All other antibodies were from Santa Cruz. The F-actin/G-actin *in vivo* assay kit was obtained from Cytoskeleton Inc. (Denver, CO). Heparanase assay kit was obtained from Cisbio, USA. A diagnostic kit was used to measure non-esterified fatty acid (NEFA, Wako). FGF basic ELISA kit was from R&D systems, Inc. LysoTracker DND-26, Alex633 or Alex488-conjugated goat anti-mouse or anti-rabbit antibodies were from Invitrogen. MeSATP, suramin, anti-Bax mAb 6A7 and Bax channel blocker CN196810 were from Calbiochem. Jasplakinolide was from Alexis Biochemicals. Histone acetyltransferase (HAT) and lactate kits were obtained from BioVision. Lysosome isolation kit and all other chemicals were obtained from Sigma.

2.2 Animal model

The investigation conforms to the guide for the care and use of laboratory animals published by the US National Institutes of Health and the University of British Columbia, and was approved by the Animal Care and Use Committee (Certificate No. A08-0627).

Adult male Wistar rats (260-300 g) were obtained from the UBC Animal Care Unit. Previously, we have reported that an acute reduction in insulin is associated with an increase in LPL at the coronary lumen.¹²⁵ To examine LPL under conditions where insulin levels are rapidly manipulated, we used diazoxide (DZ), a selective K^+_{ATP} channel opener. In the pancreas, opening of the K^+_{ATP} channel hyperpolarizes the β -cell membrane, decreases intracellular calcium, and insulin secretion is rapidly inhibited (within 1 hr). After an intraperitoneal injection of DZ, stable hyperglycemia develops within 1 hr, persists for 4 hr and blood glucose remains 2-3 times higher than normal. Changes in plasma parameters with DZ also included significant and rapid increases in FA and TG, alterations that are reversed by treatment with insulin.^{126, 127} Overall, we have repeatedly demonstrated that DZ is a useful model for the inadequately controlled T1D patient.^{128, 129} DZ (100 mg/kg) was administered i.p., animals euthanized after 1-4 hr, and their hearts removed for measurement of LPL activity and Western blotting.

2.3 Plasma measurements

Rats were injected with DZ at 10 AM (fed state). Following DZ, blood samples from the tail vein were collected over a period of 4 hr, and blood glucose determined using a glucometer (AccuSoft). At varying intervals, blood was also acquired in heparinized glass capillary tubes. Blood samples were immediately centrifuged and plasma was collected and assayed for fatty acid (FA) using a diagnostic kit (NEFA, Wako).

2.4 Isolated heart perfusions

A) Langendorff perfusion: Rats were anesthetized with 65 mg/kg sodium pentobarbital i.p., the thoracic cavity opened, and the heart carefully excised. After the aorta was cannulated and tied below the innominate artery, hearts were perfused retrogradely by the

nonrecirculating Langendorff technique with Krebs-Ringer HEPES buffer as described previously.¹³⁰ To measure endothelium-bound LPL, perfusion solution was changed to buffer containing 1% fatty acid free bovine serum albumin and heparin (5 U/ml). The coronary effluent was collected in timed fractions over 10 min and assayed for LPL activity by measuring the hydrolysis of [³H] triolein. B) Modified Langendorff perfusion: To separate the coronary from the interstitial effluent, a modified Langendorff retrograde perfusion technique was used.^{125, 131, 132} Rats were anesthetized, the thoracic cavity opened, and the left anterior vena cava ligated below the azygous vein followed by ligation of the right anterior vena cava. The hearts were then carefully excised with the aorta, inferior vena cava, and lungs still attached. After the aorta was cannulated and tied below the innominate artery, the hearts were perfused retrogradely by the noncirculating Langendorff technique. The right and left branches of the pulmonary artery were cut before they entered the lungs, and the two branches were then trimmed off at their junction. Subsequently, the inferior vena cava and branches of the right and left pulmonary veins were ligated, the lungs were removed, and the pulmonary artery was cannulated and tied. At this time, most of the perfusate (~98% to 99%) starts flowing through the pulmonary cannula (coronary perfusate), whereas a small amount of fluid (~1% to 2%) drips down to the apex of the heart (interstitial transudate). The coronary and interstitial effluents were collected separately in timed fractions and frozen until assayed for heparanase and LPL using Western blot.

2.5 Immunohistochemistry

Immediately on excision, control and DZ rat hearts were stored in 10% formalin for 48 hr, and processed for immunolocalization of heparanase as described previously.¹³³ Briefly, sections were incubated with the heparanase mAb130 (1:30 dilution) overnight at room

temperature in a humid chamber, and further incubated for 1 hr with the secondary HRP-conjugated goat anti-mouse antibody (1:200 dilution). Color was developed by an AEC kit, followed by counter staining with Mayer's hematoxylin. Slides were mounted and visualized using a Leica fluorescent microscope (Wetzlar, Postfach, Germany). Absence of staining was observed when the primary antibody was omitted and replaced by 1% goat serum.

2.6 Cell culture

Bovine coronary artery endothelial cells (bCAEC, Clonetics) were cultured in endothelial growth medium supplemented with BulletKit (Lonza) at 37°C in a 5% CO₂ humidified incubator. Cells from 5-8th passage were used for the experiment. 0.5×10⁶ cells were placed in 6-well plates and grown to confluence. For co-culturing of endothelial cells with cardiomyocytes, cell culture insert with polyethylene terephthalate track-etched membrane was used for this purpose. The upper insert is separated from the lower compartment by the transwell membrane. bCAECs were cultured on the inserts and then placed in the laminin coated wells containing cardiomyocytes isolated by a previously described method. These cardiomyocytes had been suspended at a final cell density of 125,000 cells/ml and incubated at 37°C.

2.7 Treatments

bCAECs were incubated with albumin bound palmitic (PA, 0.25-1 mM) or oleic (1 mM) acid (molar ratio 1:6), or glucose (15-25 mM) was added for the indicated times. Bovine serum albumin-FA solutions were prepared by first dissolving the FA in ethanol (500 µl) and then adding appropriate amounts to media to obtain the required molar ratio of albumin to FA. Mannitol [Mnt (20 mM) in 5 mM glucose] or 5 ng/ml TNF-α were also added to the culture medium, and served as osmolarity or positive controls respectively. To simulate

hyperglycemia induced by DZ, bCAECs were also incubated for 30 min with 1 mM PA prior to exposure to 25 mM glucose (HG) for another 30 min. Following separation of medium from the cells, heparanase was determined in both cell lysates (using Western blot) and medium (using an activity assay kit). Cells were also used for immunofluorescent detection of heparanase. Finally, intracellular heparanase was measured after pre-incubations with cytochalasin D (an actin polymerization inhibitor) or nocodazole (a microtubule disrupting agent) for 10 min followed by 1 mM PA or HG for 30 min. In some experiments, various antagonists like suramin (100 μ M, P2 receptor antagonist), jasplakinolide (1 μ M, stabilizes actin filaments), cytochalasin D (0.5 μ M, actin-depolymerizing agent), KN93 (10 μ M, CaMKII inhibitor), and SB202190 (20 μ M, p38 MAPK inhibitor) were used where indicated. 2-Methylthio ATP (MeSATP) was used as an ATP analog that acts as a P2Y receptor agonist. A non-metabolizable albumin bound palmitate analog, 2-bromohexadecanoic acid (BPA, 1 mM), 20 μ M CN (Bax inhibitor) and 2 μ M geldanamycin (GA, Hsp90 inhibitor) were used where indicated.

2.8 Isolation of membrane, cytosolic, nuclear, lysosome and mitochondrial fractions

Membrane and cytosolic, nuclear, lysosome and mitochondrial fractions were prepared as previously described.¹³⁴ Briefly, cells were lysed in ice-cold buffer A (containing 20 mM Tris-HCl, 2 mM EDTA, 5 mM EGTA, 50 mM 2-mercaptoethanol, 25 μ g leupeptin, and 4 μ g aprotinin, pH 7.5), and centrifuged for 1h at 35,000 rpm; the supernatant was used as the cytosolic fraction. The pellet was resuspended in buffer B (containing 1% NP-40, 0.1% SDS, 0.5% deoxycholic acid and 5 mM EGTA, pH 7.5), sonicated for 30 s, and centrifuged at 35,000 rpm for 1h; the supernatant was used as the membrane fraction.

In isolation of nuclear fractions, cells were washed twice with ice-cold PBS, and subsequently lysed in ice-cold buffer A [10 mM HEPES (pH 7.9), 10 mM KCl, 1.5 mM MgCl₂, 0.5 mM DTT, 0.5 mM PMSF and 0.05 % NP40] for 10 min. After centrifugation (1,500 g, 10 min, 4°C), the supernatant (cytosolic fraction) was separated, and the pellet was sonicated with buffer B [20 mM HEPES (pH 7.9), 0.42 M NaCl, 1 mM EDTA, 1 mM DTT, 1 mM PMSF and 10% glycerol] for 5 s. Following centrifugation (15,000 g, 5 min, 4°C), the supernatant (nuclear fraction) was quantified using a Bradford protein assay, and used for Western blot to determine the nuclear content of heparanase. Using an antibody against histone 3 as a nuclear marker, and β -actin as a cytoplasmic marker, we confirmed the purity of nuclear fractions. In addition, antibodies against LAMP-1 and prohibitin excluded the contamination of nuclear fractions by lysosomes and mitochondria.

Lysosomal fractions were isolated by differential centrifugation followed by density gradient centrifugation. Briefly, cells were trypsinized and collected by centrifugation (600 g, 5 min, 4°C). After washing twice with ice cold phosphate buffered saline (PBS), cells were sonicated in extraction buffer for 10 sec. Following centrifugation (1,000 g, 10 min, 4°C), the supernatant was collected and further centrifuged at 20,000 g for 20 min. The pellet was resuspended in extraction buffer and loaded on the sucrose gradient. Subsequent to centrifugation (150,000 g, 4 hr, 4°C), 500 μ l fractions were collected, starting from the top of the gradient and further purified using 250 mM CaCl₂. The purification of lysosomes was confirmed using lysosome-associated membrane protein 1 (LAMP1) antibody. To exclude mitochondrial contamination, cytochrome c oxidase was measured.

For mitochondrial isolation, bCAECs were scraped and suspended in a homogenization buffer [10 mM Tris-HCl (pH 7.5), 10 mM KCl, 0.15 mM MgCl₂, 0.5 mM EDTA, 1 mM

phenylmethylsulfonyl fluoride (PMSF), 1 mM dithiothreitol (DTT), and a 1% mixture of protease and phosphatase inhibitors], centrifuged at 4000 g for 15 min, and subjected to further lysis and sucrose gradient [10 mM Tris-HCl (pH 7.5), 0.15 mM MgCl₂, 250 mM sucrose, 0.5 mM EDTA, 1 mM PMSF, and 1 mM DTT] separation at high speed (20,000 g) for 15 min. The isolated pellet was resuspended using a lysis buffer [10 mM Tris-HCl (pH 7.5), 5 mM MgCl₂, 0.5 mM EDTA, 10% glycerol, 0.2 mM PMSF, 1% Triton X-100, and a 1% mixture of protease and phosphatase inhibitors] as described previously. Prohibitin antibody, a mitochondrial marker was used to confirm the purity of mitochondrial fractions.

2.9 Western blotting and immunoprecipitation

Western blot was carried out as described previously.¹²⁹ Briefly, ventricles or bCAECs were homogenized in ice-cold lysis buffer (20 mM Tris-HCl, 50 mM 2-mercaptoethanol, 2 mM EDTA, 5 mM EGTA, 25 µg leupeptin, 4 µg aprotinin, 0.1% NP40, pH 7.5) and kept for 30 min on ice. Samples were quantified, boiled with sample loading dye, and 50 µg used in SDS-polyacrylamide gel electrophoresis. Membranes were blocked in 5% skim milk in Tris-buffered saline containing 0.1% Tween-20 and incubated with respective antibodies, including anti-heparanase mAb130 (that recognizes both 50 and 65 kDa heparanase forms; only the active 50 kDa heparanase data is presented) or anti-LPL antibodies, anti-phospho CaMKII (Thr²⁸⁶), anti-phospho p38 MAPK (Thr¹⁸⁰/Tyr¹⁸²), anti-phospho Hsp25 (Ser⁸⁶), anti-phospho filamin 1 (Ser²¹⁵¹) and anti-filamin 1 antibodies, anti-Bax, anti-Bax mAb 6A7 (conformation dependent; only recognizes activated Bax), anti-cathepsin B (Ctsb), anti-LAMP-1, anti-histone 3, anti-Hsp90, anti-HS 3G10 epitope (recognizes digested heparan sulfate), anti-Ac-histone 3, anti-pyruvate dehydrogenase kinase 2 (PDK2), anti-PPAR α , anti-phospho PDH and anti-prohibitin antibodies, and subsequently treated with secondary

antibodies. Endothelial cells were fractionated and immunoprecipitated using anti-P2Y₂ antibody or anti-Hsp90 for 3 hr at 4°C. The immunocomplex was pulled down with protein A/G-sepharose overnight, and then heated for 5 min with sample loading dye at 95°C. The immunocomplex was immunoblotted for filamin or heparanase and reaction products were visualized using an ECL[®] detection kit, and quantified by densitometry.

2.10 Immunofluorescence

Following various treatments, cells were fixed for 10 min with 4% paraformaldehyde in PBS, permeabilized with 0.1% Triton X-100 in phosphate buffered saline (PBS) for 3 min, treated with PBS containing 1% goat serum for 1 hr, and finally rinsed with PBS. Cells were incubated with indicated antibodies, including anti-heparanase mAb130, rabbit polyclonal P2Y₂, mouse monoclonal filamin 1, anti-Bax mAb 6A7, mouse monoclonal Ctsb and anti-heparan sulphate 10E4 and 3G10 epitopes. Following washes with PBS (3x), cells were incubated with secondary Texas Red-conjugated donkey anti-mouse, Alex633 (red) conjugated goat anti-mouse and Alex488 (green) goat anti-rabbit antibodies. 4',6-Diamidino-2-phenylindole (DAPI) was used to stain nuclei. Where indicated, Rhodamine488 Phalloidin was used to stain actin filaments, and LysoTracker to identify lysosomes. Slides were visualized using a fluorescent microscope, or Zeiss Pascal confocal microscope.

2.11 Filamentous (F) and globular (G) actin

F-actin/G-actin ratio was determined using an assay kit. Briefly, bCAECs were lysed, homogenized and centrifuged at 2,000 rpm for 5 min. Total actin content of the supernatant was centrifuged at 100,000 g for 1 hr at 37°C to isolate F-actin (pellet) and G-actin (supernatant). The pellets were re-suspended to the same volume as the G-actin fraction

using ice-cold Milli-Q water plus 10 μM cytochalasin D, and left on ice for 1 hr to dissociate F-actin. The ratio of F-actin/G-actin was determined using Western blot and densitometry.

2.12 Heparanase activity

To determine heparanase activity, 20 μl of sample medium was added to microtubes, followed by addition of 10 μl of 0.7 $\mu\text{g/ml}$ Biot-HS-K. Incubation was carried out for 30 min at 37 $^{\circ}\text{C}$. To stop the reaction, 25 μl of 1.0 $\mu\text{g/ml}$ SA-XLent was added, and the incubation continued for an additional 15 min at room temperature. The signal was measured by a Victor microplate reader at excitation 337 nm and emissions 620 and 665 nm.

2.13 Extracellular ATP determination

ATP released into the extracellular medium was measured using a bioluminescent assay kit (Sigma). Briefly, cells in 100-mm cell culture dishes were incubated in 5 or 25 mM glucose over a period of 10 min. 500 μl medium was collected at the indicated times and centrifuged at 12,000 rpm for 10 min to remove cell debris. 100 μl samples were taken to detect ATP concentration using an illuminometer.

2.14 Determination of heparan sulfate-bound proteins

Lipoprotein lipase (LPL) activity was assayed by measuring the hydrolysis of a [^3H] triolein substrate emulsion. An ELISA kit was used to determine basic fibroblast growth factor (bFGF).

2.15 Estimation of endothelial intracellular free Ca^{2+}

For the measurement of [Ca^{2+}]_i, endothelial cells grown on glass coverslips were loaded with 1 μM of the acetoxymethylester form of the Ca^{2+} fluorescent dye Fura-2 in culture medium for 25 min. The coverslips were then mounted in a chamber and put on a temperature-controlled (37 $^{\circ}\text{C}$) stage of the Zeiss Axiovert 200 M inverted microscope (Carl

Zeiss, Thornwood, NY). Fura-2 was excited at 340 and 380 nm, and results were expressed as the ratio of the fluorescence emission intensity (F_{340}/F_{380}).

2.16 Small interfering RNA (siRNA) transfection

100 nM siRNAs were mixed with LipofectamineTM in Opti-MEM medium for 15 min. bCAECs were cultured with antibiotic-free endothelial growth medium, which contained heparanase siRNA (or scrambled, scr) solution for 48 hr at 37°C in a CO₂ incubator. Following this, cells were treated with 1 mM PA, and nuclear heparanase, cleaved HS, and PDK2 protein or mRNA were determined.

2.17 Lactate assay

500 µl medium was collected from 6-well culture plate at the indicated times and centrifuged at 12,000 rpm for 10 min to remove cell debris. Subsequently, 50 µl (10 times diluted) samples were taken to detect lactate concentration at 570 nm in a colorimetric microplate reader.

2.18 Reverse transcription-quantitative polymerase chain reaction

Total RNA was extracted using TRIzol (Invitrogen). After spectrophotometric quantification, reverse transcription was carried out using oligo (dT) primer and superscript II RT (Invitrogen). Quantification was performed using the TaqMan gene expression assay on a StepOnePlus system (Applied Biosystems) according to manufacturer's instructions. The result of PDK2 gene expression assay was also validated on a Roche Applied Science LightCycler with a commercial SYBR Green kit (Qiagen). The primer of PDK2: 5'-CTGGACCGCTTCTACCTCAG-3' (left) and 5'-GATGCGTTGATCTCCTGGAT-3' (right). The amplification program included initial activation at 95°C for 5 min, and 40

cycles of steps (95°C for 5 sec, 75°C for 10 sec, and 62°C for 10 sec). The values were normalized with β -actin as the internal standard.

2.19 Statistical analysis

Values are means \pm SEM. Wherever appropriate, one-way ANOVA followed by the Tukey test was used to determine differences between groups mean values. The level of statistical significance was set at $P < 0.05$.

Chapter 3: Results

3.1 Endothelial heparanase secretion in diabetes is regulated by glucose and FA

3.1.1 Coronary lumen LPL increases after acute diazoxide injection

We have previously reported that 100 mg/kg DZ caused a rapid decline in serum insulin within 1 hr.¹²⁷ In this study, blood glucose levels increased within 30 min, and reached a maximum after 2 hr of DZ administration (Figure 4A). Therefore, all subsequent experiments were carried out using DZ administered for up to 2 hr. Changes in plasma parameters with DZ also included significant and rapid increase in FA (Figure 4B). Notably, the near maximum level of FA was reached earlier than the peak for glucose. In a preliminary experiment, to determine the kinetics of LPL upregulation at the vascular lumen, some DZ treated hearts were isolated at 30-120 min, and LPL activity was measured. The increase in LPL activity at the vascular lumen (as measured by retrograde perfusion of hearts with heparin) became apparent as early as 30 min subsequent to injection of DZ, peaked at 60 min, and was maintained for an additional 120 min (Figure 4C and inset).

3.1.2 Rapid release of heparanase is associated with changes in interstitial LPL

We used the modified Langendorff perfused heart to separate the coronary perfusate from interstitial fluid, and measured coronary and interstitial heparanase (the 50 kDa active form) and LPL. Within 30 min of DZ, interstitial heparanase increased approximately 2-fold (Figure 5A). Unlike the changes observed in interstitial heparanase, we were unable to detect heparanase in the coronary outflow of either control or DZ treated hearts (data not shown). Extending the duration of DZ for 2 hr lowered interstitial heparanase to below control values (Figure 5A). As measurement of whole heart heparanase using Western blot and immunohistochemical evaluation indicated a time-dependent loss of heparanase protein

(Figure 5B) over the duration of DZ for 2 hr [more specifically from within the endothelial cells (Figure 5C)], our data suggests that acute hyperglycemia has a robust influence on secretion (into the interstitial space) and subsequent attenuation of stored heparanase. Previously, endothelial heparanase has been shown to have a significant effect on releasing subendothelial LPL. Interestingly, these effects on interstitial heparanase secretion following hyperglycemia closely mirrored changes in interstitial LPL at 30 min after DZ (Figure 5D).

3.1.3 Fatty acids facilitate endothelial intracellular heparanase accumulation

To examine the mechanism by which DZ increases heparanase secretion, we incubated endothelial cells with increasing concentrations of PA, up to the peak circulating FA concentrations seen with DZ. Unexpectedly, concentrations that varied from 0.75-1 mM increased intracellular heparanase (Figure 6A). This effect was not exclusive to PA as 1 mM oleic acid also had a similar outcome (Figure 6A, lower inset). Immunofluorescent detection of intracellular heparanase revealed a novel observation. In control conditions, intracellular heparanase was located predominately around the nucleus (Figure 6B, top panel). However, high concentrations of PA (that resembled the peak circulating concentrations seen with DZ) increased the nuclear staining of heparanase (Figure 6B, lower panel). Quantification using Western blot validated the increased nuclear content of heparanase following PA (Figure 6B, inset). Conversely, measurement of heparanase activity in the incubation medium demonstrated that PA had no effect in secretion of this enzyme from endothelial cells (Figure 6A, top inset).

3.1.4 Dose-dependent secretion of endothelial heparanase by glucose

Unlike FAs, glucose dose-dependently lowered endothelial intracellular heparanase, with significant changes observed after 20 mM glucose (Figure 7A). This decrease in intracellular

heparanase was strongly associated to increased heparanase activity in the incubation medium as the concentration of glucose was raised (Figure 7B). Confirmation of the effects of high glucose (25 mM) on heparanase secretion was done using immunofluorescence. Compared to control, high glucose caused the intracellular heparanase located predominately around the nucleus (Figure 7C, top panel) to disperse towards the plasma membrane (Figure 7C, middle panel). The osmolarity control mannitol had no effect on intracellular (Figure 7A, inset) or medium (Figure 7B, inset) heparanase, whereas the positive control, TNF- α , had effects similar to high glucose; it lowered intracellular heparanase (Figure 7A, inset), increased medium heparanase activity (Figure 7B, inset) and dispersed heparanase located around the nucleus towards the plasma membrane (Figure 7C, lower panel).

3.1.5 Simulating DZ-induced increase in substrates in vitro augments endothelial heparanase secretion

Given the opposite effects of FA and high glucose on endothelial heparanase, we incubated bCAECs with FA or high glucose independently, and compared the results to endothelial cells first exposed to PA and then high glucose (PA+HG). The latter group was expected to simulate the temporal changes seen with DZ; earlier peak in FA followed by a delayed maximum glucose concentration. Interestingly, in the presence of high glucose, PA failed to increase endothelial intracellular heparanase (Figure 8A). More importantly, this pattern of incubation produced an even greater increase in medium heparanase activity when compared to high glucose alone (Figure 8B). Reversing the order of treatment (high glucose followed by fatty acid) produced a similar heparanase release to that seen with glucose alone (data not shown).

3.1.6 Endothelial cytoskeleton mediates both PA and high glucose induced changes in heparanase

The actin cytoskeleton has been implicated in managing heparanase processing.¹³⁵ To determine whether PA or high glucose elicits F-actin polymerization, we quantitated F-actin and G-actin cellular fractions using Western blot. An increase in F-to-G actin ratio indicates actin polymerization. Both PA and high glucose (and TNF- α) increased the F/G actin ratio, an effect that was absent when using mannitol (Figure 9A and inset). Pre-incubation of bCAECs for 10 min with cytochalasin D prevented the PA-induced accumulation and the HG-induced depletion of intracellular heparanase (Figure 9B). Using nocodazole to disrupt microtubules, the effects of PA and HG on intracellular heparanase were dissimilar. Although pre-treatment with nocodazole prevented the HG-induced depletion of heparanase, it had no influence in effecting the PA-induced accumulation of heparanase (Figure 9C).

3.2 Glucose-induced endothelial heparanase secretion requires cortical and stress actin reorganization

3.2.1 High glucose induces endothelial lysosomal heparanase secretion

To simulate diabetes induced hyperglycemia, endothelial cells were incubated with 25 mM glucose. Heparanase mRNA was not affected by HG, up to 2 hr of treatment (data not shown). Glucose time-dependently lowered endothelial intracellular heparanase, with approximately 60% of the cellular enzyme released after 30 min of incubation (Figure 10A). This time-dependent decrease in intracellular heparanase was strongly associated to increased appearance of heparanase activity and protein in the incubation medium (Figure 10B). The osmolarity control mannitol had no effect on either intracellular (Figure 10A, inset) or medium (Figure 10B, inset) heparanase, whereas the positive control, TNF- α , had effects

similar to HG; it lowered intracellular heparanase (Figure 10A, inset), and increased medium heparanase activity (Figure 10B, inset). Confirmation of the effect of HG and TNF- α on heparanase secretion was done using immunofluorescence in single (Figure 10C) and multiple cells (Figure 11). In endothelial cells, heparanase colocalized with lysosomes. Interestingly, both HG and TNF- α caused the intracellular heparanase located predominately around the nucleus to disperse towards the plasma membrane.

3.2.2 *Extracellular ATP mediates the effect of high glucose to induce heparanase secretion*

In various cell types, intracellular ATP can be released into the extracellular space.¹³⁶ bCAECs exposed to glucose (5-25 mM) released ATP into the medium, an effect that was concentration-dependent (Figure 12A, inset). Comparing 5 to 25 mM glucose, the release with both concentrations was rapid, with a maximum effect observed within 2 min. However, at this time, 25 mM glucose induced a more robust release of ATP compared to 5 mM glucose (Figure 12A). With prolongation of the incubation time, medium ATP decreased, and the difference in medium ATP observed with 5 and 25 mM glucose was lost. In HEK293 cells, extracellular nucleotides have been implicated in inducing heparanase secretion through purinergic receptors (P2Y receptor).¹³⁷ Interestingly, the HG-induced endothelial heparanase secretion was inhibited by suramin (a nonspecific P2 receptor antagonist) (Figure 12B and inset). Another strategy used MeSATP, an ATP analog that can act as a P2Y receptor agonist. As shown in Figure 13, MeSATP stimulated endothelial heparanase secretion in a concentration-dependent manner, with the maximum effect seen at 100 μ M. Using this concentration of MeSATP in a different experiment, a time-dependent lowering of endothelial heparanase (Figure 12C) and an augmentation of medium heparanase activity (Figure 12C, inset) was observed.

3.2.3 Glucose-induced endothelial heparanase secretion is dependent on cytoskeleton reorganization

We have previously shown that endothelial actin cytoskeleton plays an important role in glucose-induced heparanase secretion.¹³⁸ In this study, we more closely examined the time-dependent changes in endothelial actin cytoskeleton in response to HG using immunofluorescence in single (Figure 14A) and multiple cells (Figure 15). In untreated cells, actin filaments presented as continuous fluorescent rings, predominantly in the outer portion of the cells (cortical actin). Interestingly, exposure of cells to 25 mM glucose caused discontinuation of this cortical actin ring within 5 min, and after 30 min in HG, no evidence of continuous cortical actin remained. Instead, cells now demonstrated a robust increase in actin formation stretching across the cell body (stress actin). Using cytochalasin D (actin-depolymerizing agent, Figure 14B) or jasplakinolide (that stabilizes actin filaments, Figure 14C), we were able to prevent the glucose-induced endothelial heparanase secretion.

3.2.4 Ca²⁺/calmodulin-dependent protein kinase II (CaMKII) and p38 MAPK/Hsp25 phosphorylation are augmented in endothelial cells exposed to high glucose

CaMKII-mediated activation of p38 MAPK/Hsp has been suggested to play an important role in H₂O₂-induced stress actin formation in bovine aortic endothelial cells.¹³⁹ Measurement of intracellular calcium revealed that HG was able to provoke a rapid elevation of [Ca²⁺]_i within 5 min; this effect was transient with [Ca²⁺]_i rapidly returning to baseline values (Figure 16A). Pretreatment of endothelial cells with the P2 receptor antagonist suramin for 30 min did not affect [Ca²⁺]_i (data not shown). However, in response to subsequent exposure to 25 mM glucose, suramin completely abolished the calcium response seen with HG (Figure 16A). MeSATP also caused a rapid but transient increase in [Ca²⁺]_i.

However, compared to HG, peak $[Ca^{2+}]_i$ after administration of MeSATP was almost 3-fold higher, and demonstrated a small but sustained rise in $[Ca^{2+}]_i$ after the transient spike (Figure 16A, inset). Associated with the increase in $[Ca^{2+}]_i$, measurement of CaMKII demonstrated an increase in Thr²⁸⁶ phosphorylation at 20 min following glucose incubation, with a subsequent return to baseline at 30 min (Figure 16B). Unlike CaMKII phosphorylation, phosphorylation of p38 MAPK (Figure 16C) and Hsp25 (Figure 16D) were elevated by 20 min of glucose incubation, and remained high for the duration of the exposure to HG.

3.2.5 Inhibiting CaMKII or p38 MAPK regulated stress actin formation prevents glucose-induced endothelial heparanase secretion

To examine the relationship between CaMKII and p38 MAPK activation and stress actin formation, we used the specific inhibitors KN93 and SB202190. As depicted in Figure 17A, HG induced cortical actin disassembly and stress actin formation. Inhibiting CaMKII with KN93 reduced phosphorylation of p38 MAPK/Hsp25 (Figure 17B) and prevented the effect of HG on stress actin formation (Figure 17A). With inhibition of p38 MAPK phosphorylation using SB202190, Hsp25 phosphorylation was reduced (Figure 17B), and the stress actin formation observed with HG appeared discontinuous (Figure 17A). More importantly, the glucose-induced endothelial heparanase secretion was abolished by both KN93 and SB202190 (Figure 17C and inset). Our data suggest that in response to HG, stress actin is an important mediator of endothelial heparanase secretion.

3.2.6 Colocalization of filamin with the P2Y₂ receptor is disrupted by high glucose bringing about filamin redistribution

Filamin attaches actin filaments to the plasma membrane through its binding to a number of plasma membrane proteins (including the P2Y₂ receptor), and its phosphorylation disrupts

cortical actin.^{140, 141} Using immunofluorescence, we confirmed the plasma membrane colocalization of P2Y₂ receptor (green) and filamin (red) in untreated endothelial cells (Figure 18A, merge). In the presence of HG, dissociation between the two proteins was observed at 30 min (Figure 18A). Interestingly, at this time, filamin located at the plasma membrane decreased, and much of the protein was observed in the cytosol (Figure 18A). Using immunoprecipitation, we confirmed a decreased association between filamin and the P2Y₂ receptor after 30 min of HG (Figure 18B). In addition, the membrane to cytosolic transfer of filamin in HG was verified using cell fractionation and Western blot (Figure 18C, inset). Coupled to this translocation, HG also time-dependently increased the phosphorylation of filamin (Figure 18C).

3.2.7 Endothelial secreted heparanase cleaves cardiomyocyte heparan sulfate to release attached proteins

The cardiomyocyte cell surface is rich in heparan sulfate side chains that contain many attached proteins like LPL and bFGF.^{36, 142} To test the endoglucuronidase activity of endothelial heparanase to specifically cleave the carbohydrate chains of heparan sulfate, endothelial cells were co-cultured with cardiomyocytes. Initially, we determined that HG time-dependently lowered endothelial intracellular heparanase in the insert, with maximum release observed after 60 min of incubation (Figure 19A). As heparanase secretion is polarized, with preferential secretion towards the basolateral rather than the apical side of endothelial cells,⁵⁹ we also measured heparanase activity in the medium from the lower chamber. Medium heparanase activity increased at 30 min, and reached a maximum at 60 min of HG incubation (Figure 19A, inset). To allow for maximum ability of heparanase to cleave heparan sulfate, cardiac cells were co-cultured with or without endothelial cells in HG

for 4 hr, and cardiomyocytes then imaged for heparan sulfate staining. The increase in heparanase activity in the lower chamber (in the cardiomyocyte+EC group) was associated with a robust decrease in immunofluorescent staining for heparan sulfate (Figure 19B). Given the ability of heparan sulfate to bind proteins, we predicted that loss of cardiomyocyte heparan sulfate would increase the appearance of heparan sulfate-bound proteins like LPL and bFGF in the culture medium. Indeed, co-culture of endothelial cells with cardiomyocytes in HG increased medium LPL activity (Figure 19C) and bFGF protein in the lower chamber (Figure 19D).

3.3 Fatty acid-induced nuclear translocation of heparanase uncouples glucose metabolism in endothelial cells

3.3.1 Fatty acid stimulates rapid nuclear accumulation of heparanase

In endothelial cells, heparanase is located predominantly in the cytoplasm, with a minor amount (~4%) present in the nucleus (Figure 20, lower inset). To simulate hyperlipidemia, bCAECs were incubated with increasing concentrations of PA. PA concentration-dependently increased endothelial nuclear heparanase (Figure 21A, upper inset). Using the 1 mM concentration, cells were next treated for up to 30 min. PA time-dependently increased nuclear heparanase, with an approximately 2-fold augmentation of enzyme observed after 30 min (Figure 21A). This nuclear increase was not reflected by a significant reduction in the cytoplasmic content of heparanase (Figure 20, lower inset). In addition, this effect was not related to metabolism of PA, as 1 mM 2-bromohexadecanoic acid (BPA, a non-metabolizable palmitate analog) also had a similar effect (Figure 21B). Confirmation of the effect of PA on nuclear accumulation of heparanase was done using immunofluorescence. In endothelial cells, heparanase colocalized with lysosomes that had a predominant perinuclear distribution

(Figure 21C). PA caused lysosomal heparanase escape and relocation into the nucleus (Figure 21C, bottom panel). Overall, these experiments demonstrate that fatty acids possess an intrinsic ability to facilitate nuclear translocation of heparanase.

3.3.2 Nuclear translocation of heparanase is dependent on Bax-induced lysosome permeabilization

A prerequisite for nuclear entry of heparanase is likely lysosomal disruption with heparanase released into the cytoplasm. Bax activation has been suggested to induce lysosome permeabilization.¹⁴³ Incubation with PA or BPA significantly increased Bax activation, without changes in total Bax (Figure 22A). Immunofluorescence images confirmed this observation, in addition to demonstrating colocalization of activated Bax with lysosomes (Figure 22B). Interestingly, the isolated lysosomal fraction from PA-treated cells exhibited lower heparanase and a higher content of activated Bax (Figure 22C). Cathepsin B (Ctsb), a lysosomal resident protease used as an indicator for lysosome integrity, was also decreased following PA in both isolated lysosomes (Figure 22C) and immunofluorescent images (Figure 22D). The PA induced decrease in lysosomal Ctsb coincided with appearance of this lysosomal protease in the cytoplasm (Figure 22D). To further examine the effect of Bax activation on lysosome permeabilization, we used a Bax channel blocker CN196810. CN attenuated lysosomal loss of Ctsb (Figure 22D, bottom panel). More importantly, CN prevented the nuclear translocation of heparanase in response to PA (Figure 22E). It should be noted that PA had no effect on caspase 3 activation (Figure 23), suggesting that the increase in lysosomal permeability is not sufficient to trigger apoptosis up to 24 hr. Collectively, these data suggest that PA-induced nuclear translocation of heparanase is dependent on Bax activation and lysosome permeabilization.

3.3.3 *Hsp90 accompanies the nuclear translocation of heparanase*

In HL-60 leukemic cells, Hsp90 has been suggested to function as a chaperone for nuclear shuttling of heparanase.¹⁴⁴ Immunoprecipitation of cytosolic Hsp90 revealed a robust association between this chaperone and heparanase 15 min following PA, an association which tended to decrease with time (Figure 24A). Interestingly, the nuclear presence of Hsp90 bound heparanase following PA also increased after 15 min, with further amplification at 30 min (Figure 24B). As geldanamycin (GA), a specific Hsp90 inhibitor, effectively blocked the nuclear entry of heparanase (Figure 24C), our data indicate that Hsp90 is an important mediator of PA-induced shuttling of heparanase to the nucleus.

3.3.4 *Nuclear heparanase is associated with cleavage of heparan sulfate (HS)*

Heparanase is an endoglycosidase that can degrade HS into small oligosaccharides.⁸² Using immunostaining with anti-HS mAb 10E4 which targets intact HS chains, and anti-HS mAb 3G10 which detects cleaved HS chains, we examined the effect of PA on nuclear HS. With 10E4 staining, intact HS presented a cellular distribution that included both the cytoplasm and nucleus. Treatment with PA eliminated the presence of intact HS mainly in the nucleus (Figure 25A), an effect that was accompanied by the appearance of cleaved nuclear HS (Figure 25B). Quantification of this effect using Western blot demonstrated that the increase in cleaved nuclear HS was apparent at 30 min after PA, increased further with time, and remained high up to 4 hr (Figure 25C). Blocking the nuclear entry of heparanase with GA, reduced the amount of cleaved nuclear HS observed following PA (Figure 25D). These data suggest that nuclear HS can undergo cleavage following translocation of heparanase into the nucleus.

3.3.5 *Heparanase regulates HAT activity and genes related to glycolysis*

Heparan sulfate is a potent inhibitor of HAT activity.¹⁴⁵ To determine if HAT activity changes following nuclear translocation of heparanase and HS cleavage, HAT activity in addition to acetylation of histone were evaluated. Using Western blot, we observed increased HAT activity and augmented histone acetylation after 60 min of PA (Figure 26A). These effects were attenuated by the Hsp90 inhibitor GA (Figure 26B). An expression assay for genes related to glycolysis revealed an increase in SLC2A1, PDK2 and LDHA in endothelial cell treated with PA (Figure 26C). It should be noted that in addition to genes controlling glucose metabolism, nuclear entry of heparanase was also associated with an increase in genes related to inflammation, like IL-8, VCAM1 and VEGFA (Figure 27).

3.3.6 *PDK2 expression and extracellular lactate accumulation are regulated by nuclear heparanase*

PDK can reduce the oxidative breakdown of glucose through its inactivation of PDH. In response to 1 mM PA, both PDK2 gene and protein increased as early as 6 hr, and remained high until 12 hr (Figure 28A). This effect occurred in the absence of activation Peroxisome proliferator-activated receptor (PPAR α) (Figure 29). This increase in PDK2 was associated with augmented PDH phosphorylation (p-PDH) (Figure 28A, inset). Using siRNA, we were successful in reducing total endothelial heparanase (Figure 28B, left panel). In these cells, PA-induced nuclear entry of heparanase and HS cleavage was reduced (Figure 28B, right panel). More importantly, depletion of heparanase completely prevented the PA-induced increases in PDK2 gene and protein, as well as p-PDH (Figure 28C). Phosphorylation and inactivation of PDH uncouples glycolysis from glucose oxidation, resulting in accumulation of lactate. Measurement of lactate revealed a robust increase in the incubation medium

following PA (Figure 28D, inset), an effect that was effectively prevented by GA or heparanase siRNA (Figure 28D). Our data clearly demonstrate an important role of nuclear heparanase on glucose metabolism through its effect on PDK2.

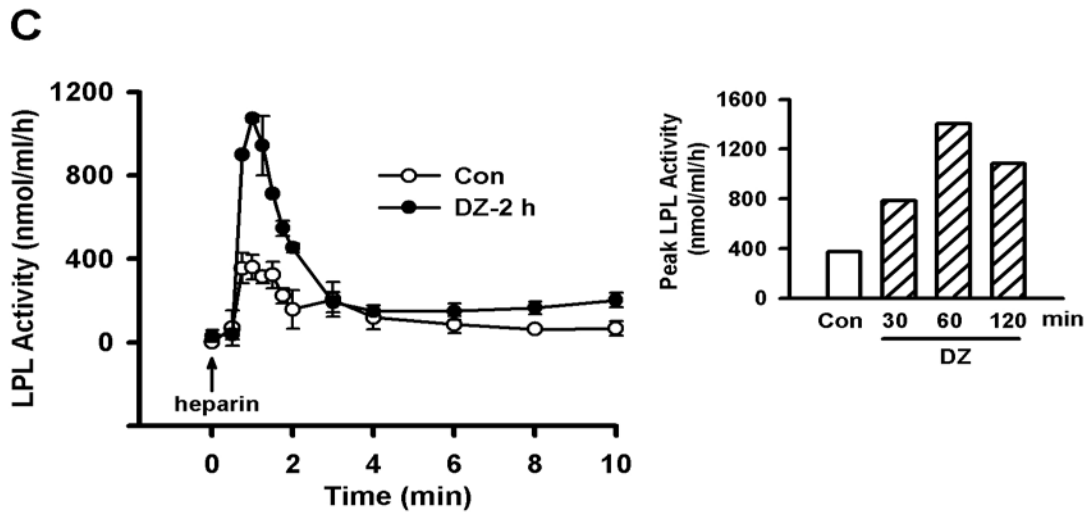
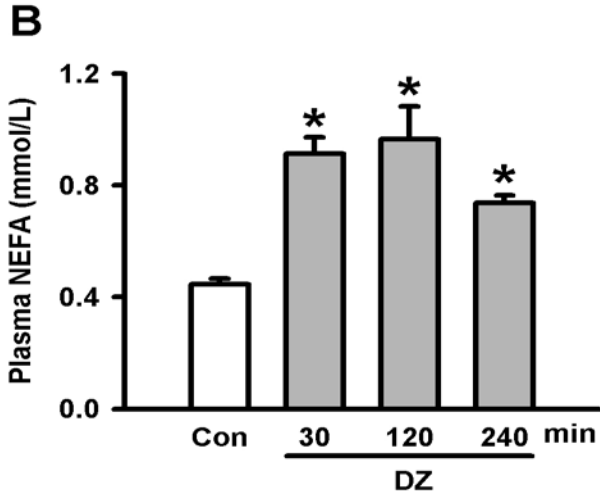
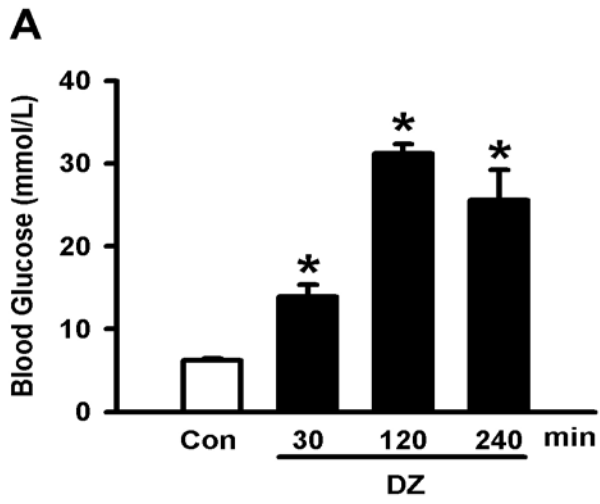


Figure 4 Effect of diazoxide on blood glucose and fatty acids and coronary lumen LPL activity. Animals were treated with DZ (100 mg/kg, i.p.), and blood samples from the tail vein collected over 240 min for determination of glucose (A) and fatty acids (B). Results are the mean±SEM of six rats in each group. (C) Hearts were isolated and perfused in the nonrecirculating retrograde mode, and coronary luminal LPL was released with heparin (5 U/ml). The inset indicates a single experiment measuring peak heparin-releasable LPL activity released after varying durations of DZ (30-120 min). Following determination of the optimal time required for DZ to augment cardiac LPL, six animals were treated with DZ and LPL activity was measured at 120 min. LPL activity was assayed using radiolabeled triolein. *Significantly different from control, $P<0.05$. (Reprinted with permission of The Am Physiol Soc.)

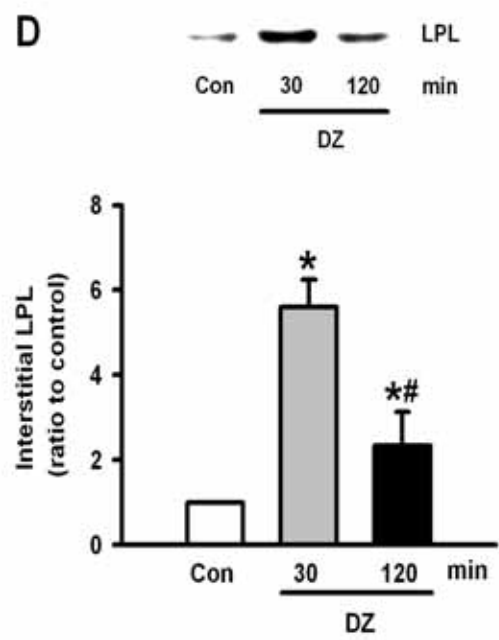
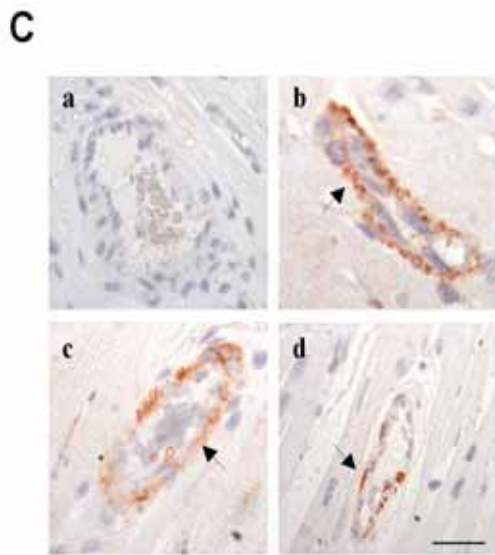
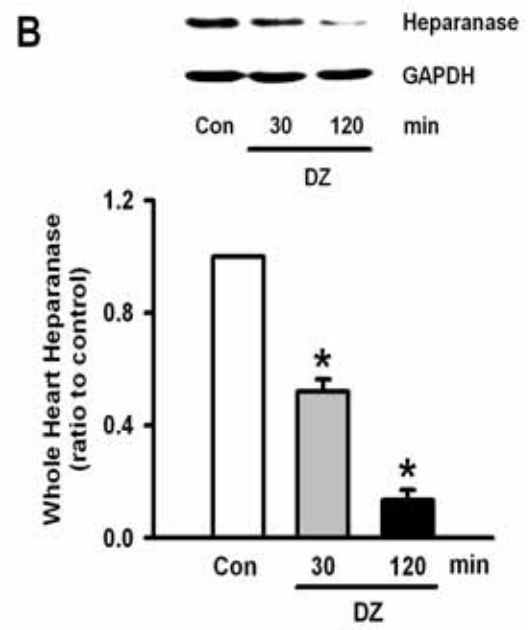
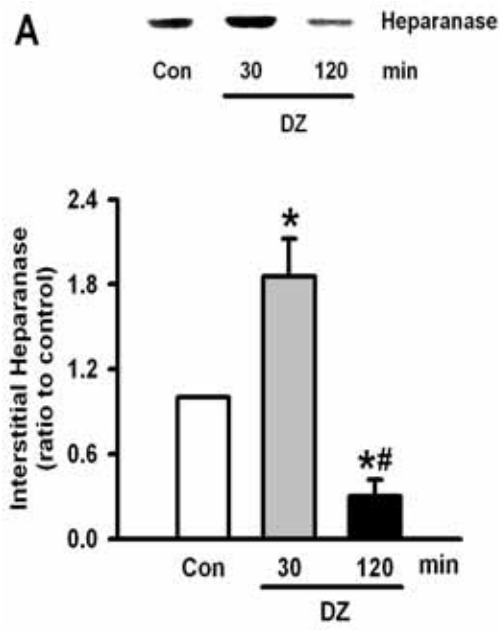


Figure 5 Acute changes in cardiac heparanase and LPL following diazoxide. Hearts were perfused using a modified Langendorff retrograde perfusion technique that separates the coronary perfusate from interstitial fluid. Interstitial heparanase (A) and LPL (D) were assayed using Western blot. Following DZ for different intervals, heparanase was also determined immediately upon removal of the heart using Western blotting (B). Results are mean±SEM for 6 rats in each group and are expressed as ratio to control. Low-magnification image (x400) showing immunohistochemical localization of heparanase after DZ is depicted in C. Cross sections of control (a, negative control; b, control) and DZ (c, after 30 min; d, after 120 min) ventricles were fixed and then immunolabeled using an antibody specific for heparanase. Bar = 25 μm. *Significantly different from control, #Significantly different from DZ 30 min, $P<0.05$. (Reprinted with permission of The Am Physiol Soc.)

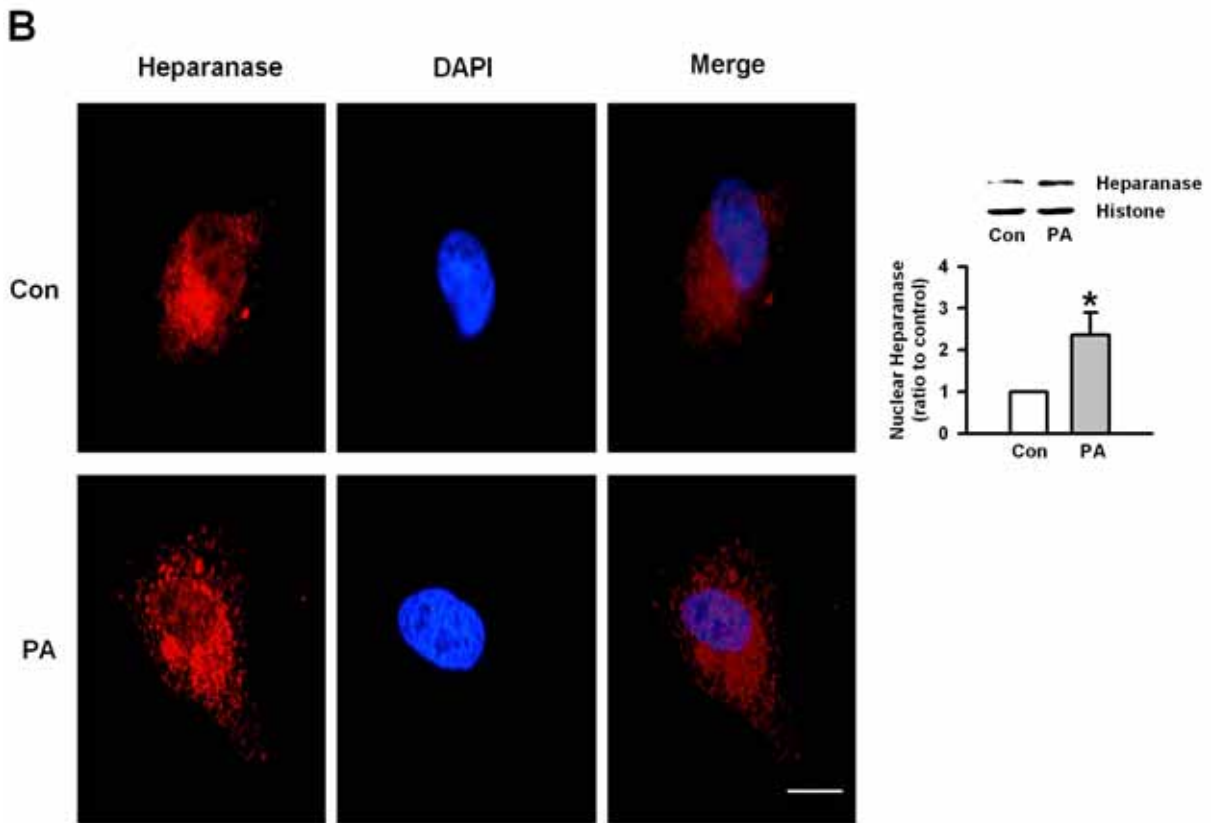
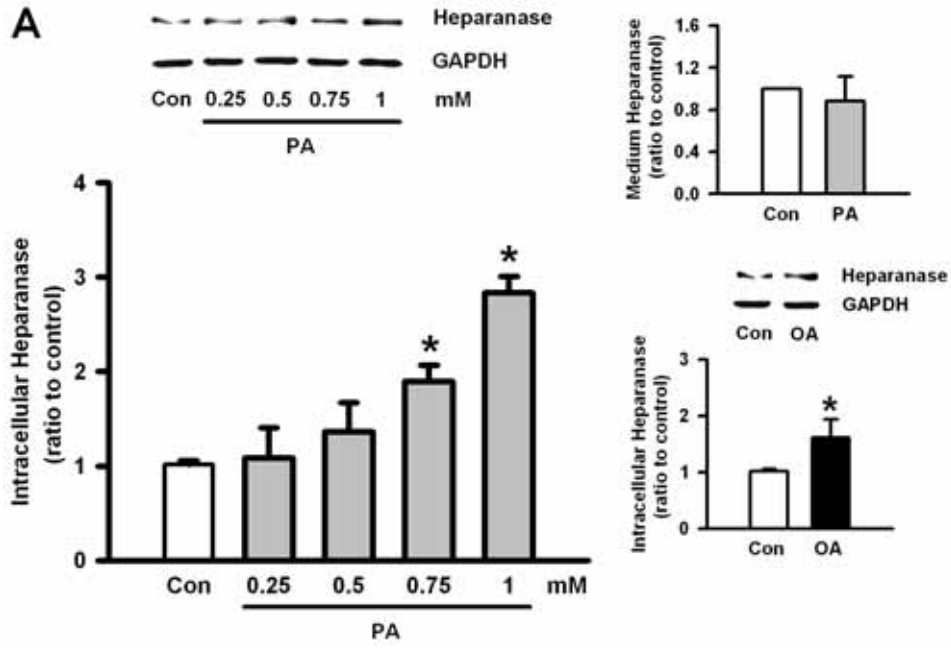


Figure 6 Dose-dependent effect of palmitic acid on endothelial heparanase. bCAECs were incubated, either in the absence or presence of 0.25-1.0 mM albumin bound palmitic acid (PA) (1:6) for 30 min. Following separation of medium from the cells, heparanase was determined in cell lysates (A) and incubation medium (upper inset). The lower inset (A) demonstrates the influence of oleic acid (OA, 1 mM for 30 min) on heparanase in cell lysates. Results are mean±SEM for 6 rats in each group and are expressed as ratio to control. Control and PA-treated bCAECs were fixed, permeabilized, and double stained with anti-heparanase mAb 130 (red) and DAPI (blue) (B). The merged image of heparanase and nucleus is described in the third panel. Bar = 25 μm. Data is from a representative experiment done twice. The inset in B illustrates nuclear heparanase after bCAECs were treated with 1 mM PA for 30 min. *Significantly different from control, $P<0.05$. (Reprinted with permission of The Am Physiol Soc.)

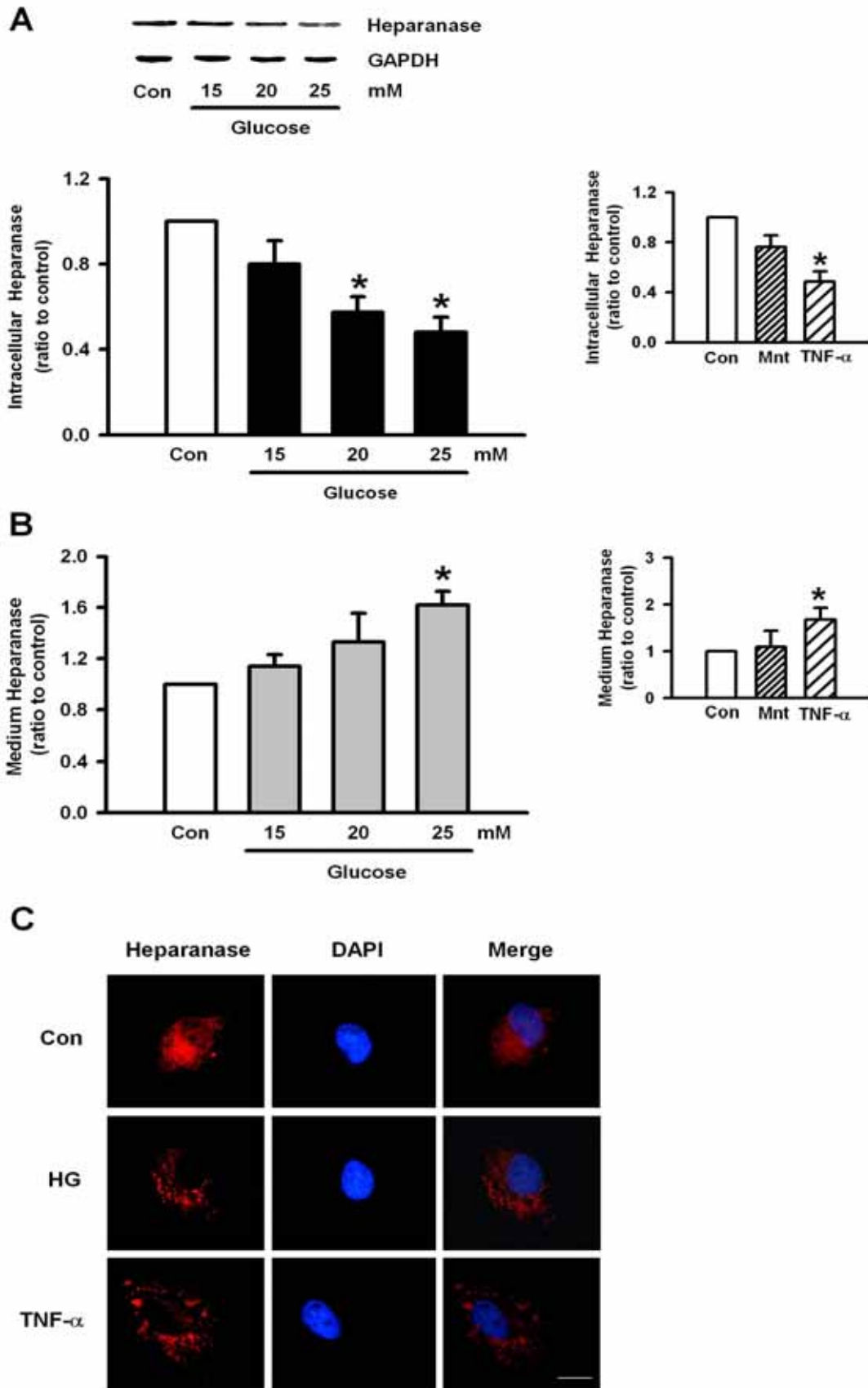


Figure 7 Dose-dependent effect of glucose on endothelial heparanase. bCAECs were incubated, either in the absence or presence of glucose (15-25 mM) for 30 min. Following separation of medium from the cells, heparanase was determined in both cell lysates (A) and medium (B). The insets depict the influence of mannitol (Mnt, 20 mM) and TNF- α (5 ng/ml) on heparanase in cell lysates (A) and medium (B). Results are mean \pm SEM of three separate experiments, and are expressed as ratio to control. bCAECs were fixed, permeabilized, and double stained with anti-heparanase mAb 130 (red) and DAPI (blue). The merged image of heparanase and nucleus is described in the third panel (C). Bar = 25 μ m. Data is from a representative experiment done twice. *Significantly different from control, $P < 0.05$. HG, high glucose (25 mM). (Reprinted with permission of The Am Physiol Soc.)

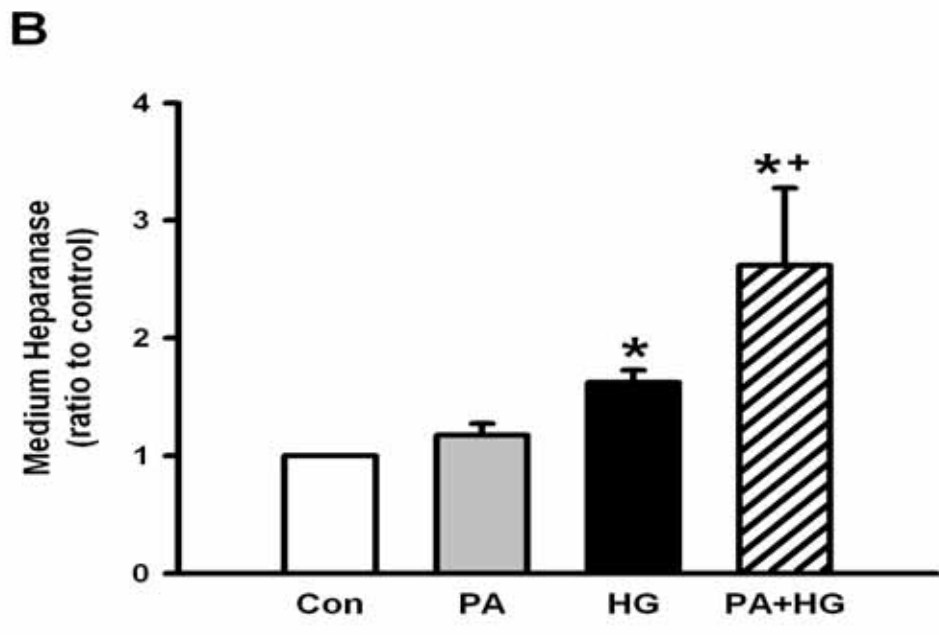
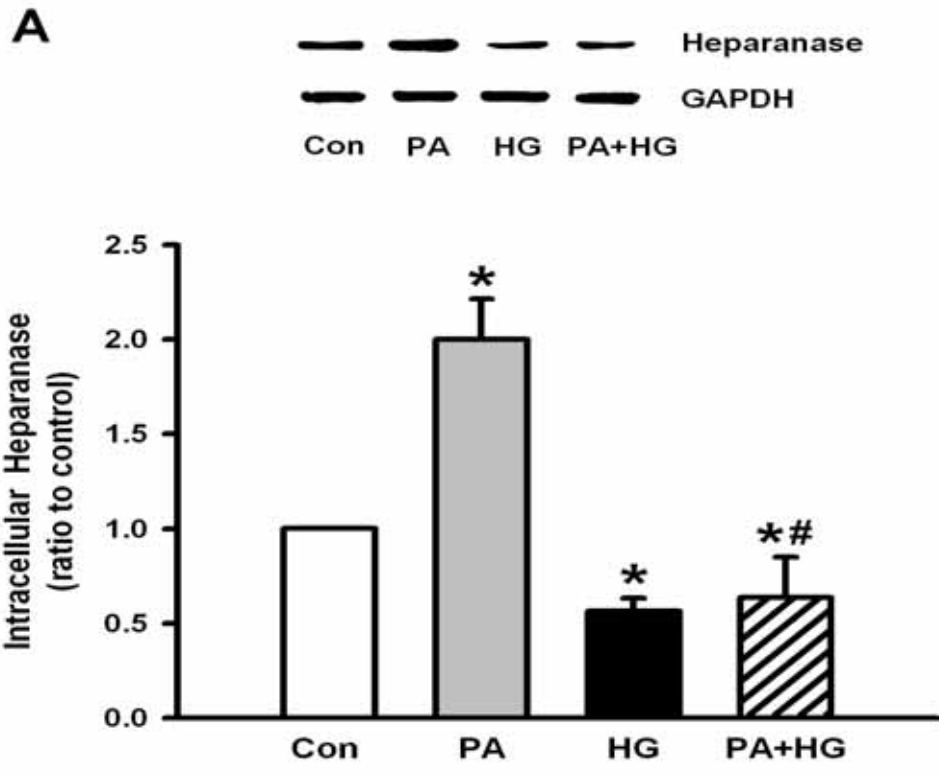


Figure 8 Dual effect of palmitic acid and glucose on endothelial heparanase. bCAECs were incubated, either in the absence or presence of palmitic acid (PA, 1 mM) or glucose (HG, 25 mM) for 30 min. To simulate the substrate change induced by DZ, bCAECs were also incubated for 30 min with palmitic acid prior to exposure to 25 mM glucose for another 30 min (PA+HG). Following separation of medium from the cells, heparanase was determined in both cell lysates (A) and medium (B). Results are mean±SEM of three separate experiments, and are expressed as ratio to control. *Significantly different from control, #Significantly different from PA, †Significantly different from HG, $P<0.05$. (Reprinted with permission of The Am Physiol Soc.)

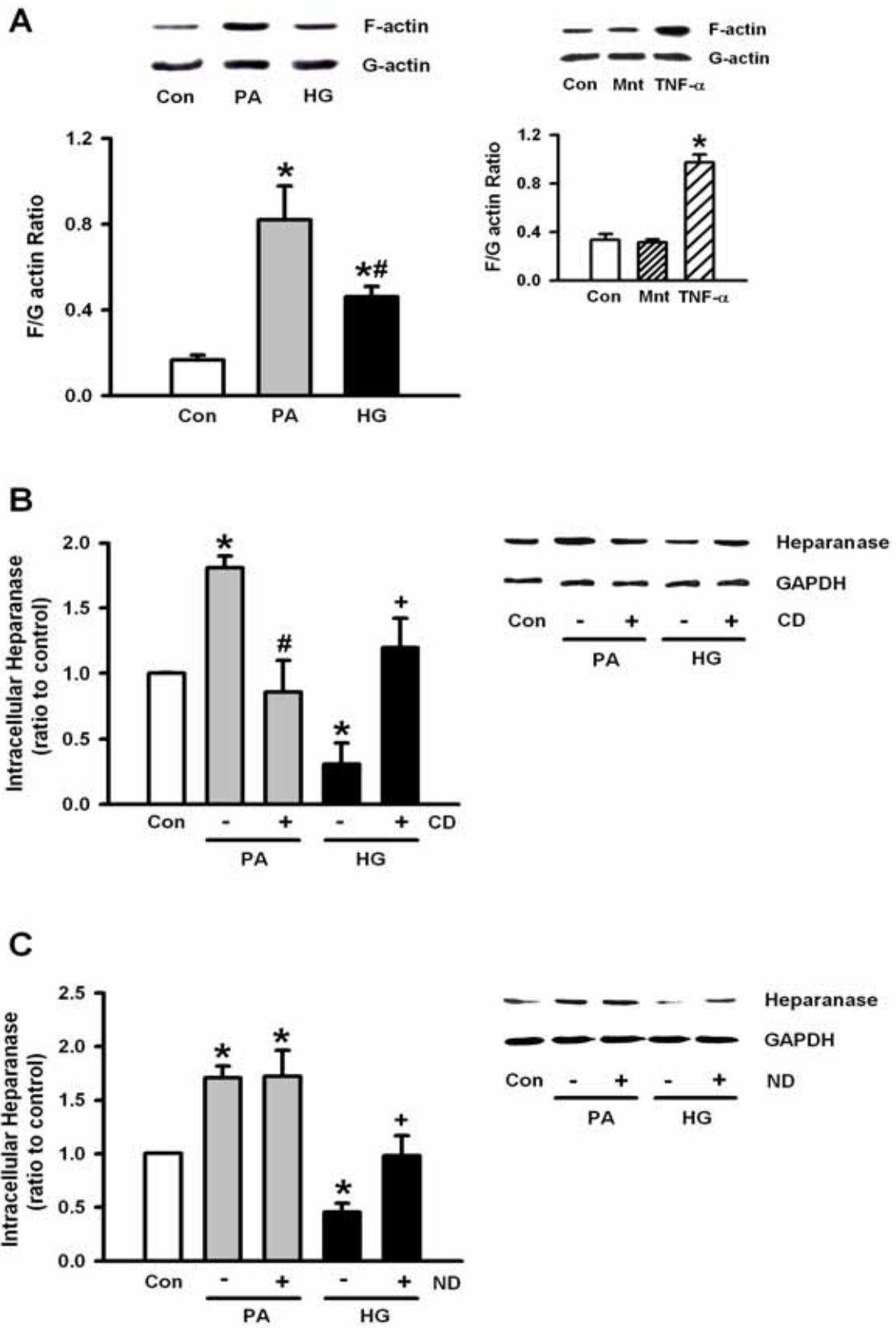


Figure 9 Endothelial cytoskeleton regulates the effects of palmitic acid and glucose on endothelial heparanase. Endothelial actin rearrangement following palmitic acid (PA, 1 mM) or glucose (HG, 25 mM) was determined using an F-actin/G-actin in vivo assay kit (A). The inset depicts the influence of mannitol (Mnt, 20 mM) and TNF- α (5 ng/ml) on the F-actin/G-actin ratio in cell lysates. Intracellular heparanase was also measured after pre-incubations with cytochalasin D (CD, for 10 min) (B) or nocodazole (ND, for 10 min) (C) followed by PA (1 mM, for 30 min) or HG (25 mM, for 30 min). Data is mean \pm SEM of 3 different separate experiments, and are expressed as ratio to control. *Significantly different from control, #Significantly different from PA, +Significantly different from HG, P<0.05. (Reprinted with permission of The Am Physiol Soc.)

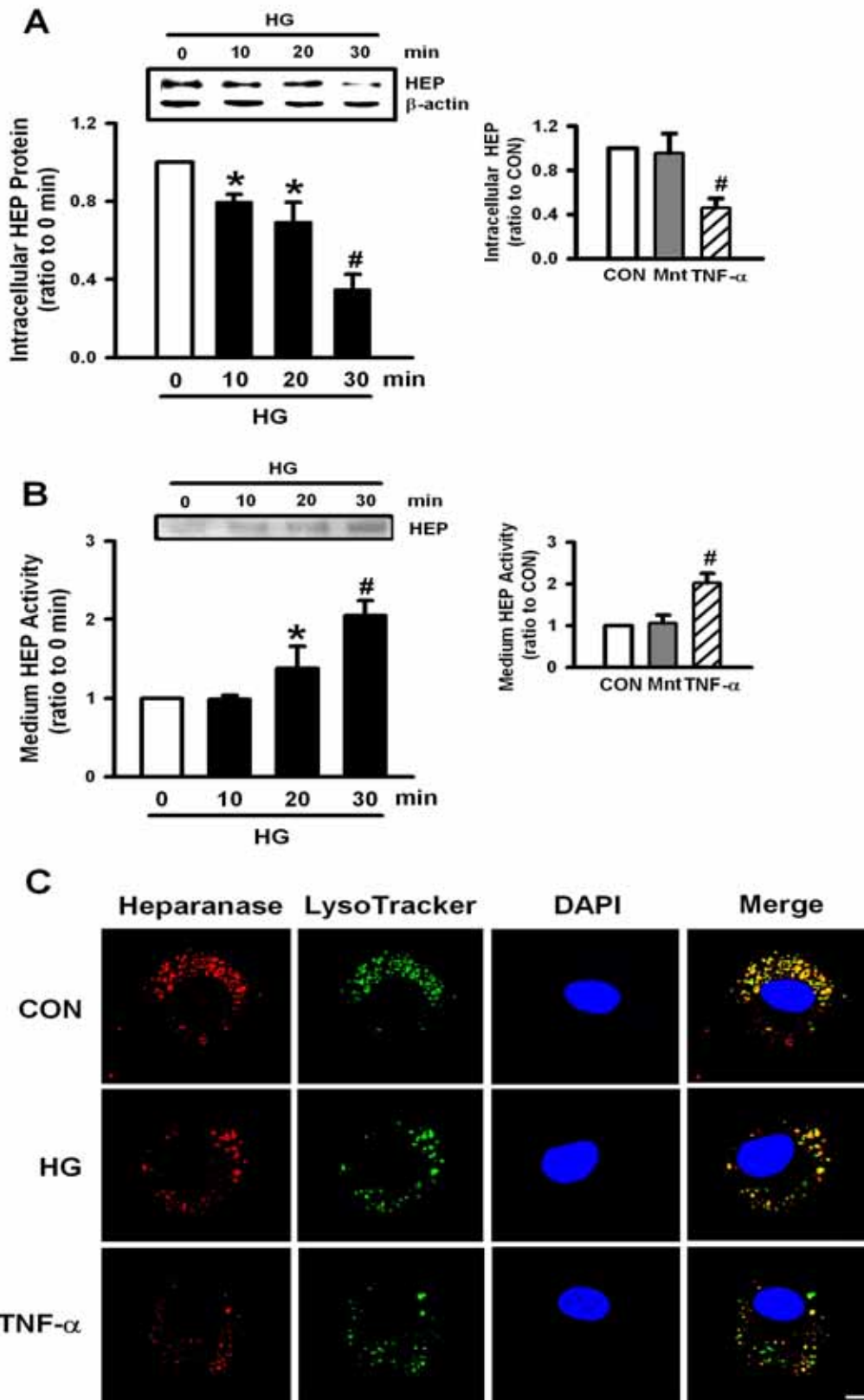


Figure 10 High glucose induces endothelial lysosomal heparanase secretion. bCAECs (0.5×10^6 cells) were grown to 80-90% confluence and incubated with high glucose (HG, 25 mM) over a period of 30 min. Following separation of medium from the cells, heparanase was determined in both cell lysates (A) and medium (B) at the indicated times. The insets depict the influence of mannitol [Mnt (20 mM) in 5 mM glucose] and TNF- α (5 ng/ml) on heparanase in cell lysates (A) and medium (B) after a 30 min incubation. Results are means \pm SEM of three separate experiments, and are expressed as a ratio to 0 min or to control (CON, 5 mM glucose). In a different set of bCAECs, lysosomes were first labeled with LysoTracker (green) for 3 hr, before being treated with glucose (25 mM) or TNF- α (5 ng/ml) for 30 min. Cells were then fixed, permeabilized, and incubated with anti-heparanase mAb 130 (red) and DAPI (blue), and examined under a confocal microscope (C). The merged image of heparanase, lysosomes and nucleus is described in the fourth panel from left (C). Bar = 20 μ m. Data is from a representative experiment done twice. *Significantly different from 0 min or control; #Significantly different from all other groups, $P < 0.05$.

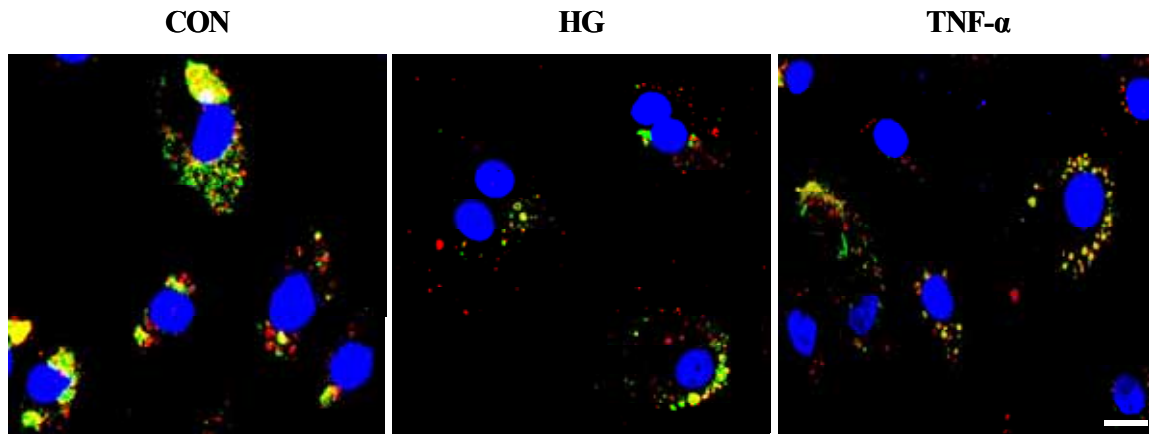


Figure 11 High glucose and TNF- α induces endothelial heparanase secretion shown in multiple cells.

Using bCAECs, lysosomes were first labeled with LysoTracker (green) for 3h, before being treated with glucose (25 mM) or TNF- α (5 ng/ml) for 30 min. Cells were then fixed, permeabilized, and incubated with anti-heparanase mAb 130 (red) and DAPI (blue), and examined under a confocal microscope. The figures represent a merged image of heparanase, lysosomes and nucleus. Bar = 20 μ m.

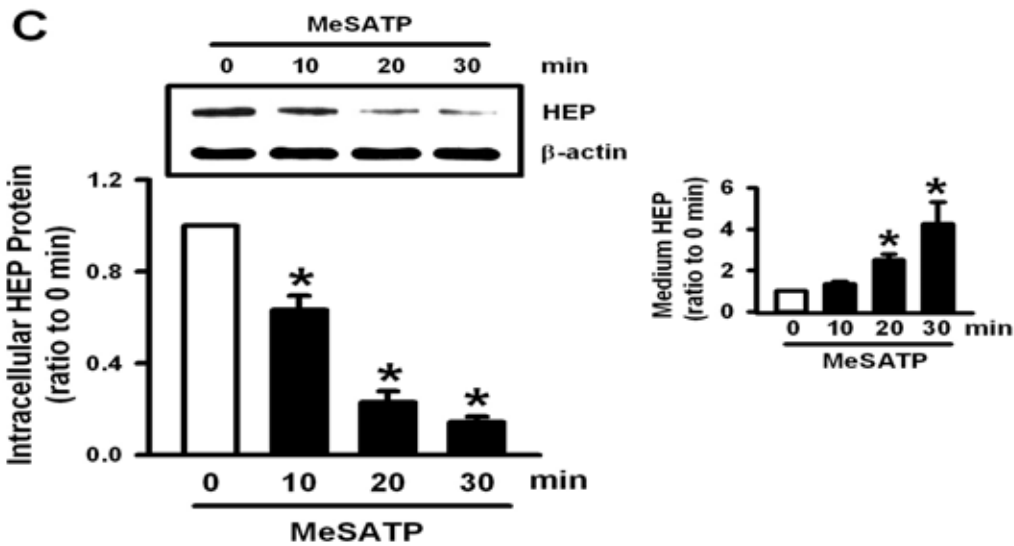
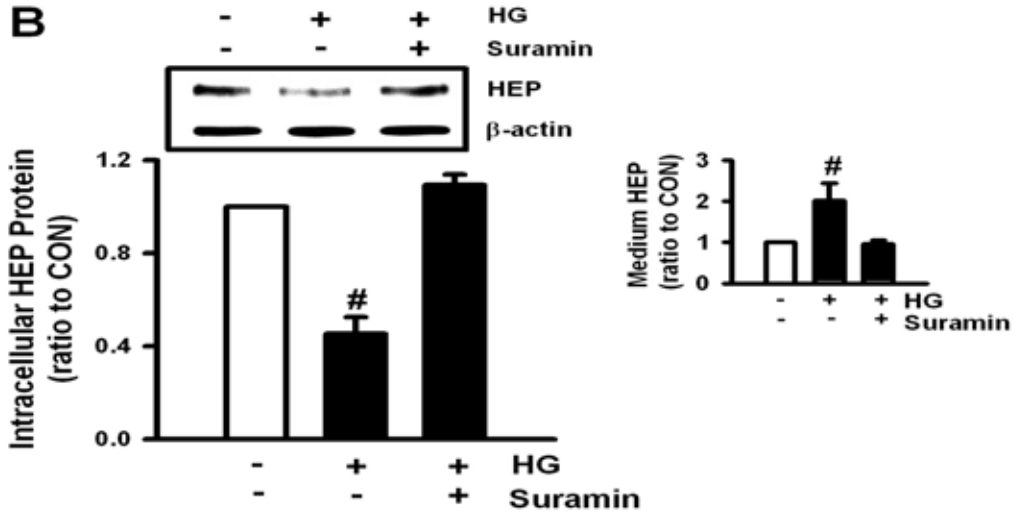
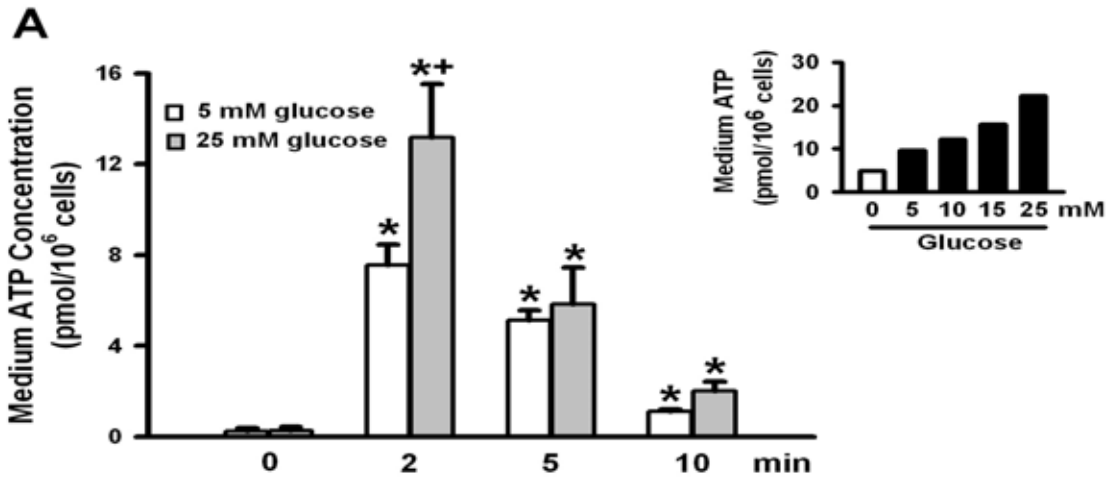


Figure 12 Extracellular ATP mediates the effect of high glucose to induce heparanase secretion.

Endothelial cells were incubated in 5-25 mM glucose for 2 min (A, inset), or 5 and 25 mM glucose over a period of 10 min (A). Following separation of medium from cells, ATP concentration in the media was measured. Cells were also pretreated in the absence or presence of Suramin (100 μ M, P2 receptor antagonist) for 30 min, followed by incubation with glucose (25 mM) for another 30 min. Heparanase protein remaining in the cells (B) or secreted into the incubation medium (B, inset) was then examined. The effects of MeSATP (100 μ M, an ATP analog that acts as a P2Y receptor agonist) on endothelial intracellular (C) and medium heparanase (C, inset) was determined over a period of 30 min. Results are means \pm SEM of three separate experiments, and are expressed as ratio to 0 min or control. *Significantly different from 0 min; ⁺Significantly different from 5 mM glucose; [#]Significantly different from all other groups, $P < 0.05$.

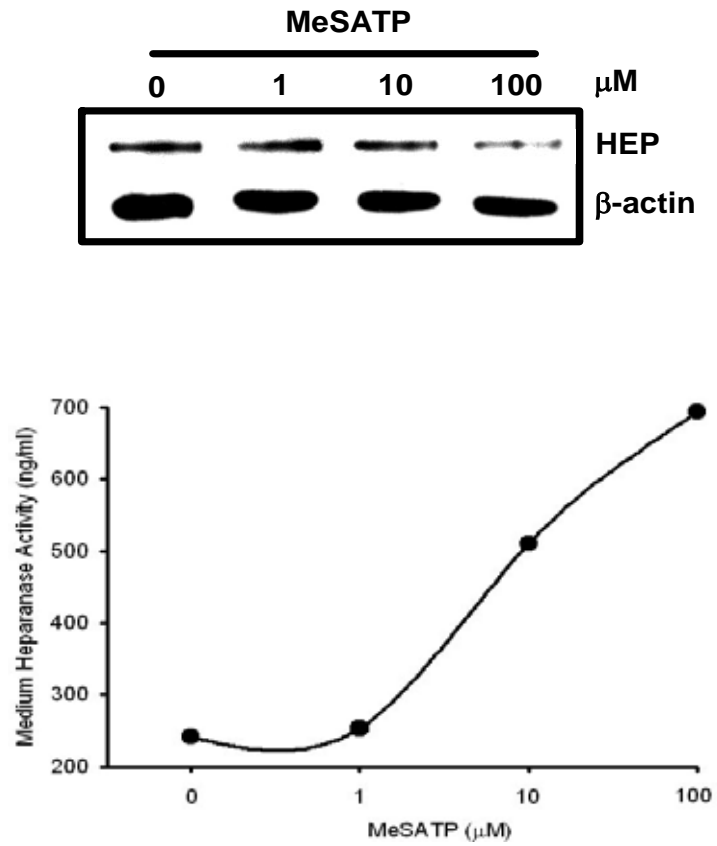


Figure 13 MeSATP duplicates the effect of high glucose to induce endothelial heparanase secretion. Endothelial cells were incubated with various concentrations of MeSATP (0-100 μM) over a period of 30 min. Heparanase protein remaining in the cells or activity appearing in the medium was then examined.

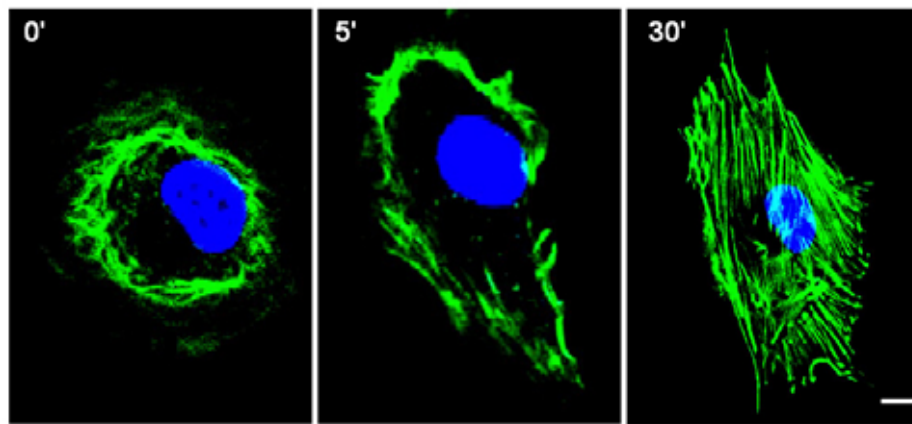
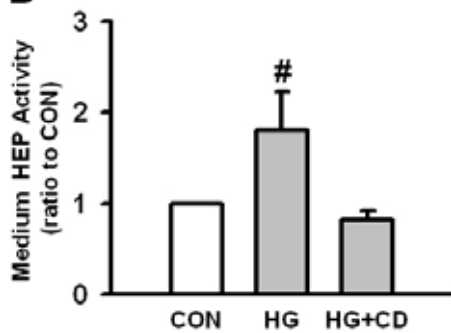
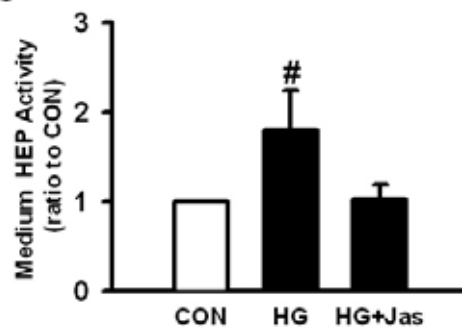
A**B****C**

Figure 14 Glucose-induced endothelial heparanase secretion is dependent on cytoskeleton reorganization.

Following treatment of bCAECs with glucose (25 mM) over a period of 30 min, cells were fixed, permeabilized and double stained with Rhodamine488 Phalloidin for filamentous actin (green) and DAPI for nucleus (blue) at the indicated times (A). In another experiment, after pretreatment with either cytochalasin D (CD; 0.5 μ M for 10 min-left panel) (B) or jasplakinolide (Jas; 1 μ M for 30 min-right panel) (C), cells were then treated with high glucose (HG, 25 mM) for a period of 30 min. Medium collected at this time was used to determine heparanase activity. Bar = 20 μ m. The image is from a representative experiment done three times. Results are means \pm SEM from three separate experiments. [#]Significantly different from all groups; $P < 0.05$.

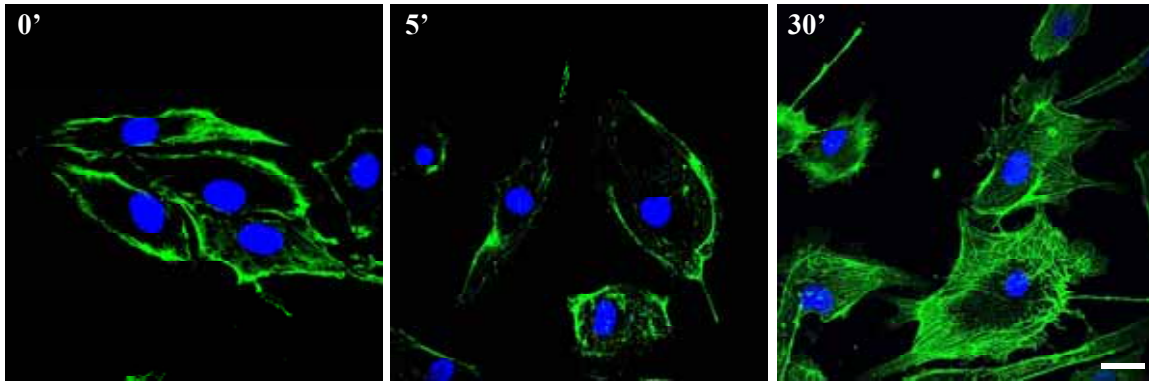


Figure 15 Glucose-induced endothelial heparanase secretion is dependent on cytoskeleton reorganization.

Following treatment of bCAECs with glucose (25 mM) over a period of 30 min, cells were fixed, permeabilized and double stained with Rhodamine488 Phalloidin for filamentous actin (green) and DAPI for nucleus (blue) at the indicated times. Bar = 20 μ m.

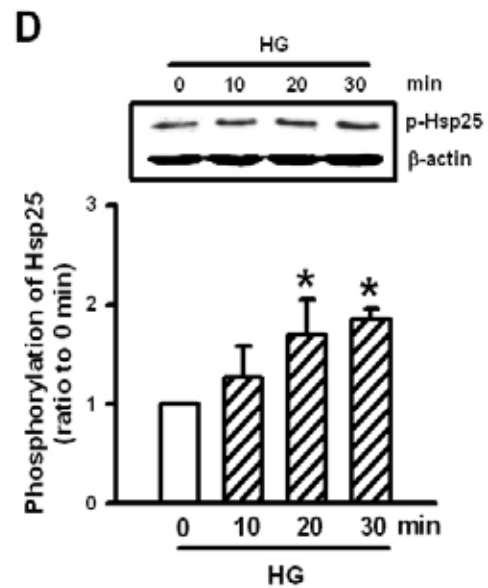
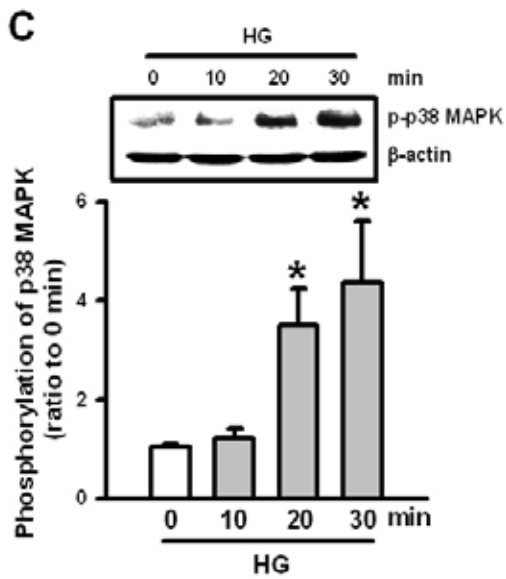
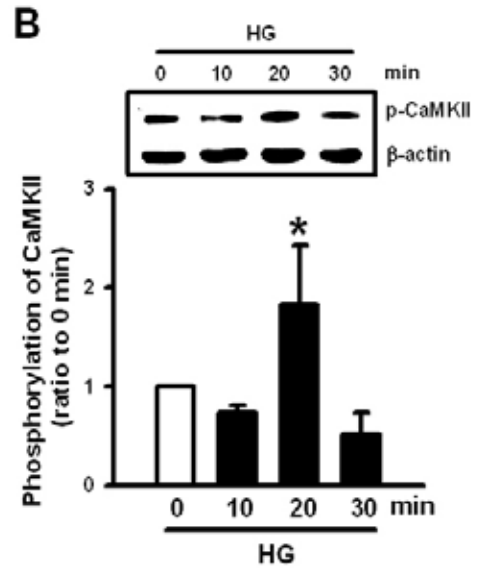
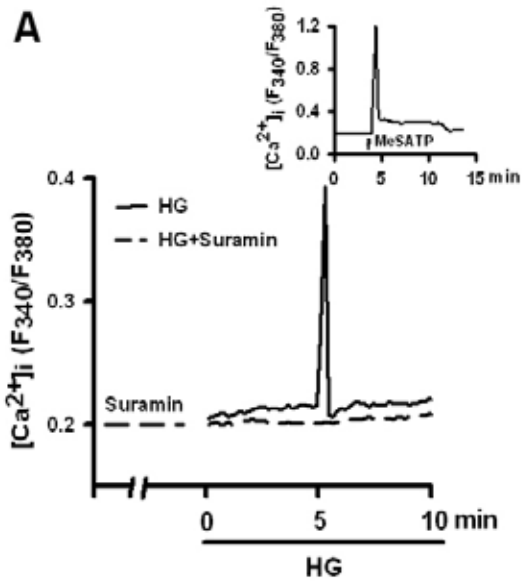


Figure 16 High glucose stimulates Ca²⁺/calmodulin-dependent protein kinase II (CaMKII) and p38 MAPK/Hsp25 phosphorylation. bCAECs were pretreated in the absence or presence of suramin (100 μM) for 30 min, followed by stimulation with 25 mM glucose. The cytosolic Ca²⁺ changes over time were measured as the F₃₄₀/F₃₈₀ ratio using Fura-2 (A). The inset depicts cytosolic Ca²⁺ changes in response to MeSATP (100 μM; A). Results are expressed as an average response of 15-25 endothelial cells from 4 different endothelial cell preparations. In a separate experiment, bCAECs were exposed to 25 mM glucose for a period of 30 min. At the indicated times, protein was extracted to determine phosphorylation of CaMKII (B), p38 MAPK (C) and Hsp25 (D) using Western blot. Results are means ± SEM of three separate experiments, and are expressed as ratio to 0 min. *Significantly different from 0 min; *P*<0.05.

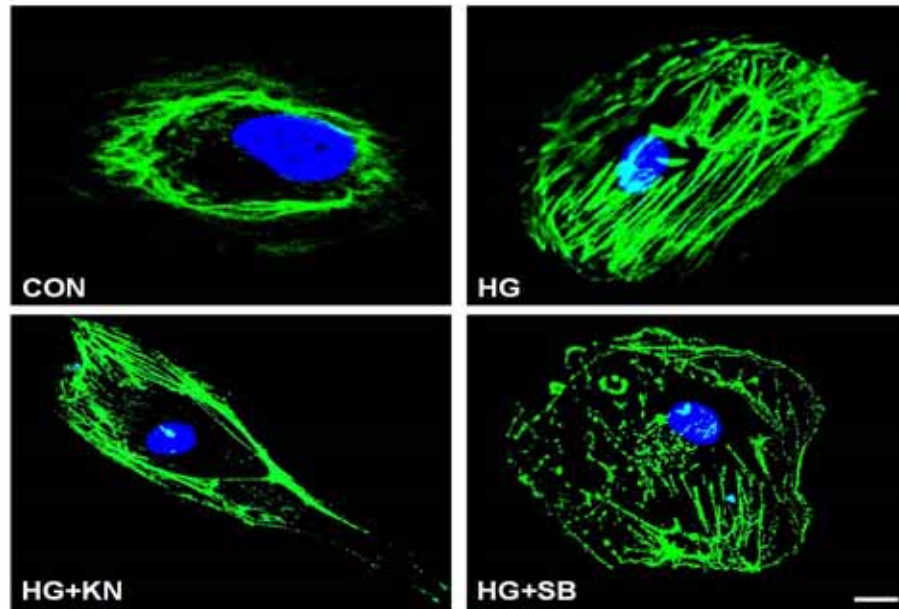
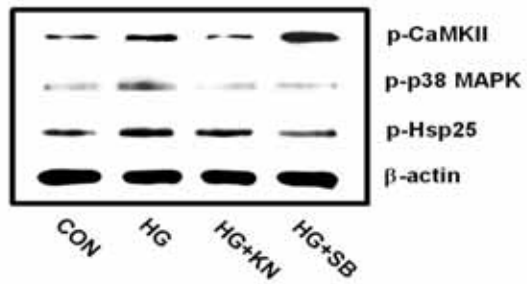
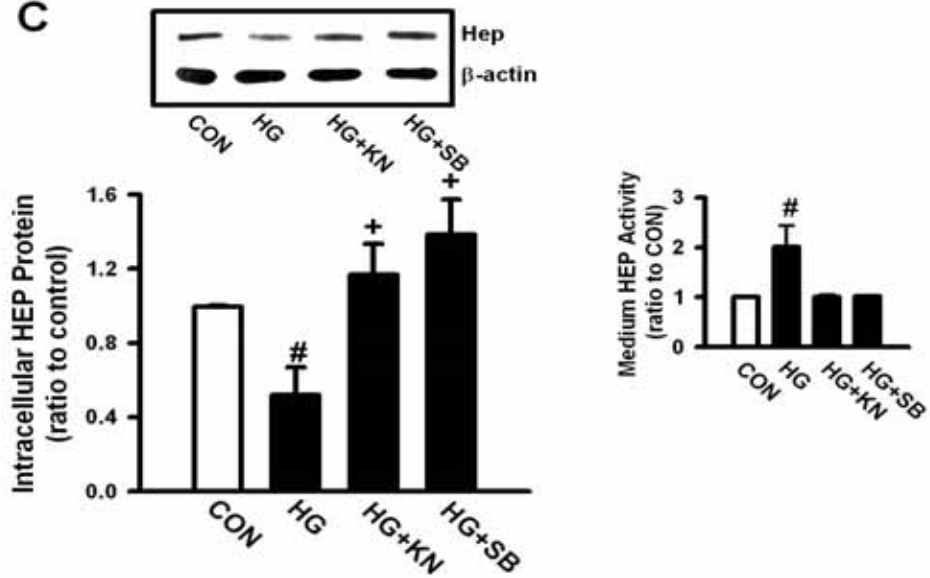
A**B****C**

Figure 17 Inhibiting CaMKII or p38 MAPK regulated stress actin formation prevents glucose-induced endothelial heparanase secretion. Following a 1 hr pretreatment of bCAECs with KN93 (KN;10 μ M) or SB202190 (SB; 20 μ M), specific inhibitors of CaMKII or p38 MAPK respectively, cells were treated with glucose (25 mM) for 30 min. A control and a high glucose group were also included. Cells were fixed, permeabilized and double stained with Rhodamine488 Phalloidin and DAPI (blue) (A). Bar = 20 μ m. The image is from a representative experiment done twice. Cellular proteins were extracted to determine phosphorylation of CaMKII, p38 MAPK and Hsp25 (B) using Western blot. Intracellular heparanase protein (C) and medium heparanase activity (C, inset) were also determined. The representative Western blot and densitometric results illustrated are means \pm SEM from three separate experiments. [#]Significantly different from all groups; ⁺Significantly different from HG group; $P < 0.05$.

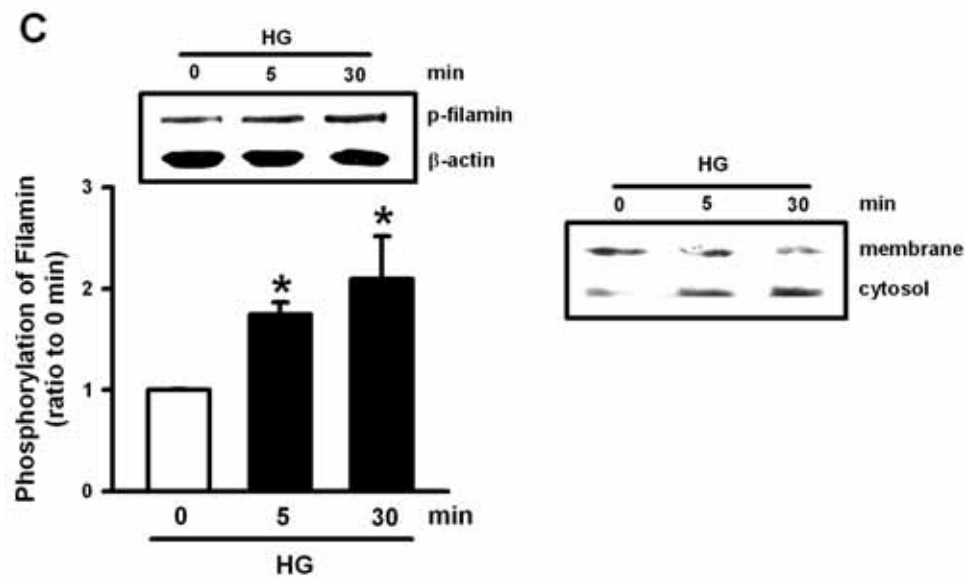
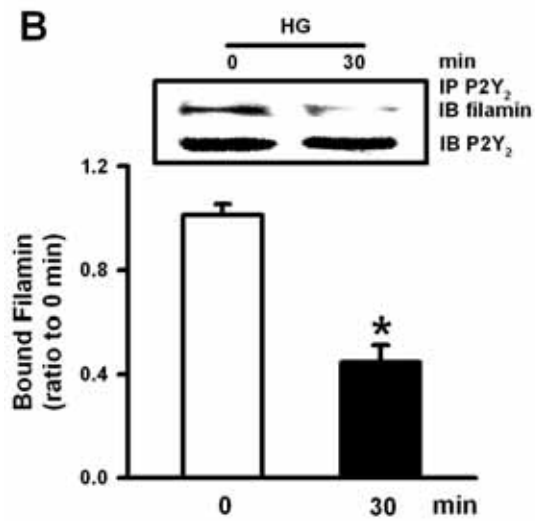
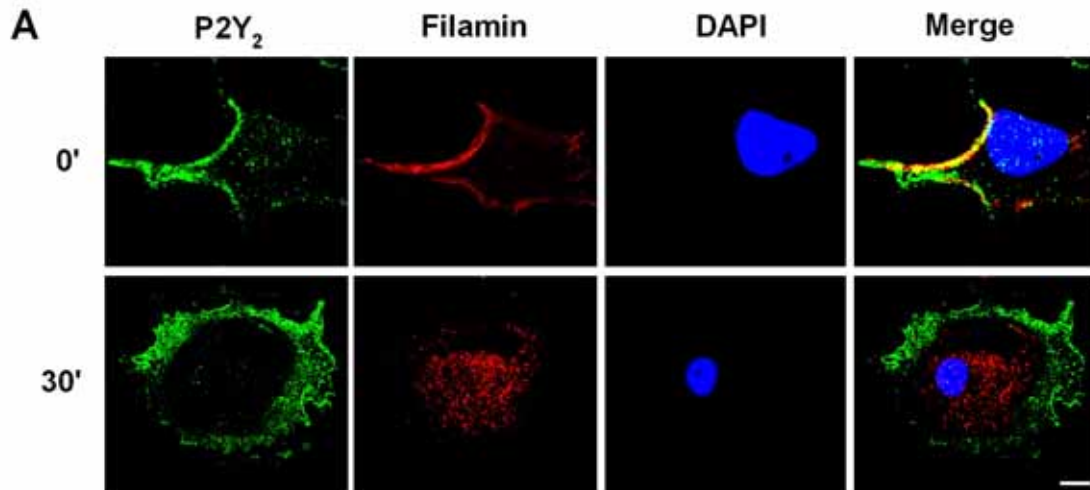


Figure 18 Colocalization of filamin with the P2Y₂ receptor is disrupted by high glucose bringing about filamin redistribution. bCAECs treated with 25 mM glucose (for 0 and 30 min) were fixed, permeabilized, and stained for P2Y₂ receptor (green), filamin (red) and nucleus (blue), and examined under a confocal microscope (A). The merged image of P2Y₂ receptor, filamin and nucleus is described in the fourth panel from left (A). Bar = 20 μm. The image is from a representative experiment done three times. Using a similar protocol in a different set of bCAECs, cells were lysed, and subjected to immunoprecipitation (IP) using anti-P2Y₂ receptor antibody, and immunoblotted with anti-filamin and anti-P2Y₂ receptor antibodies (B). To determine filamin redistribution, endothelial cells were exposed to glucose (25 mM) over a period of 30 min. At the indicated times, total protein was extracted to determine phosphorylation of filamin (C). Membrane and cytosolic fractions were also isolated to examine filamin distribution using Western blot (C, inset). The representative Western blot and densitometric results illustrated are the means ± SEM from three separate experiments. *Significantly different from 0 min; $P < 0.05$.

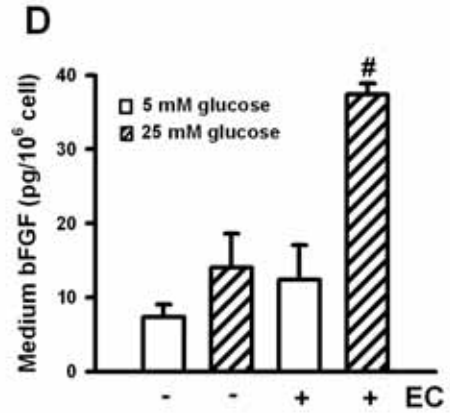
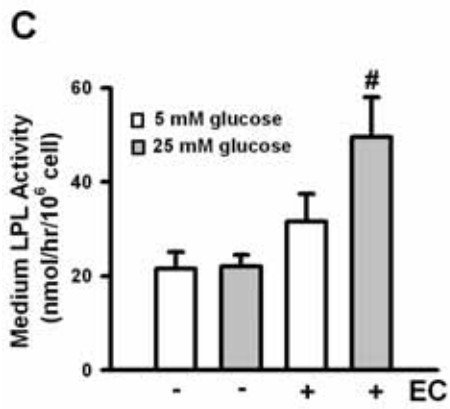
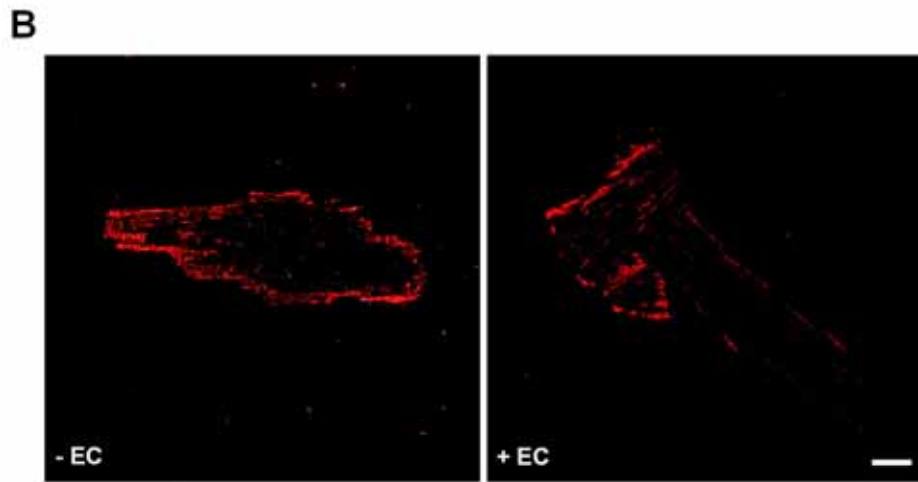
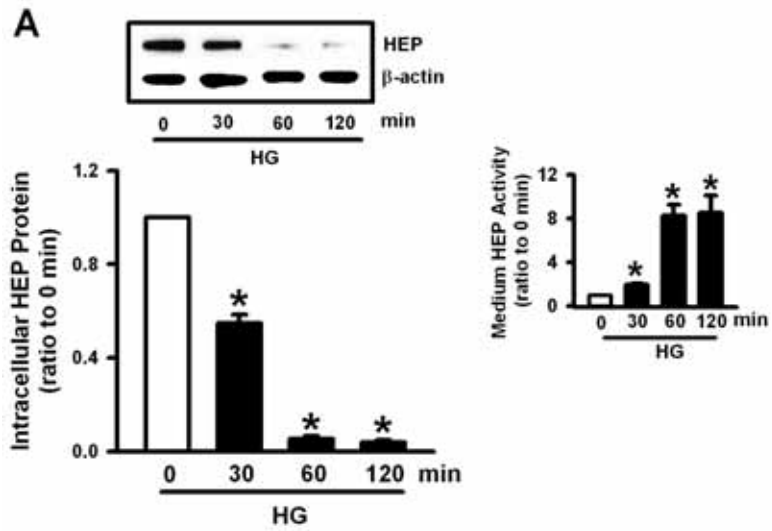


Figure 19 Endothelial secreted heparanase cleaves cardiomyocyte heparan sulfate to release attached proteins. Primary rat cardiomyocytes were plated in a 6-well plate as described. A cell culture insert (Falcon, diameter 23.1 mm) grown with or without confluent endothelial cells was placed above the cardiomyocytes. Cells were incubated in 25 mM glucose over a period of 0-2 hr. At the times indicated, endothelial cells on the insert were lysed and heparanase protein (A) and medium heparanase activity (A, inset) detected. To test the endoglucuronidase activity of endothelial heparanase to specifically cleave the carbohydrate chains of cardiomyocyte heparan sulfate, co-culture (with or without EC) was maintained for 4 hr. Cardiomyocytes were then fixed, and stained for heparan sulfate (red) (B). Bar = 20 μ m. Data is from a representative experiment done twice. Medium was also collected from the lower chambers to measure LPL activity (C) and bFGF (D). Results are means \pm SEM of three separate experiments. *Significantly different from 0 min; #Significantly different from all groups; $P < 0.05$.

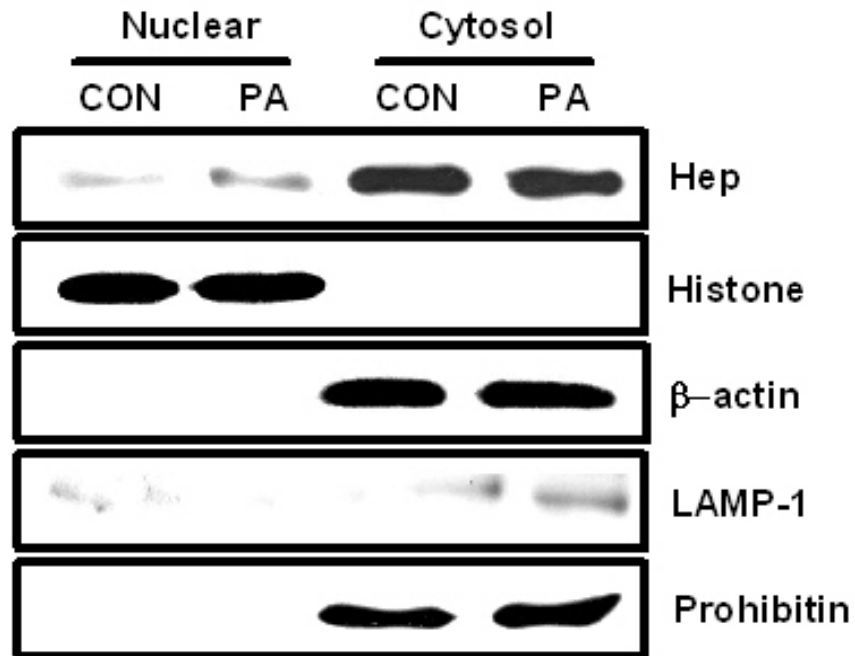


Figure 20 Cellular distribution of endothelial heparanase. bCAECs were incubated in the absence or presence of 1 mM palmitic acid (PA) for a period of 30 min, and heparanase in the nuclear and cytosolic fractions determined. Histone was used as a nuclear marker. The purity of the nuclear fraction was verified by determining its contamination with cytoplasmic proteins like β -actin, LAMP-1 or prohibitin. The immunoblot is a representative figure of three separate experiments.

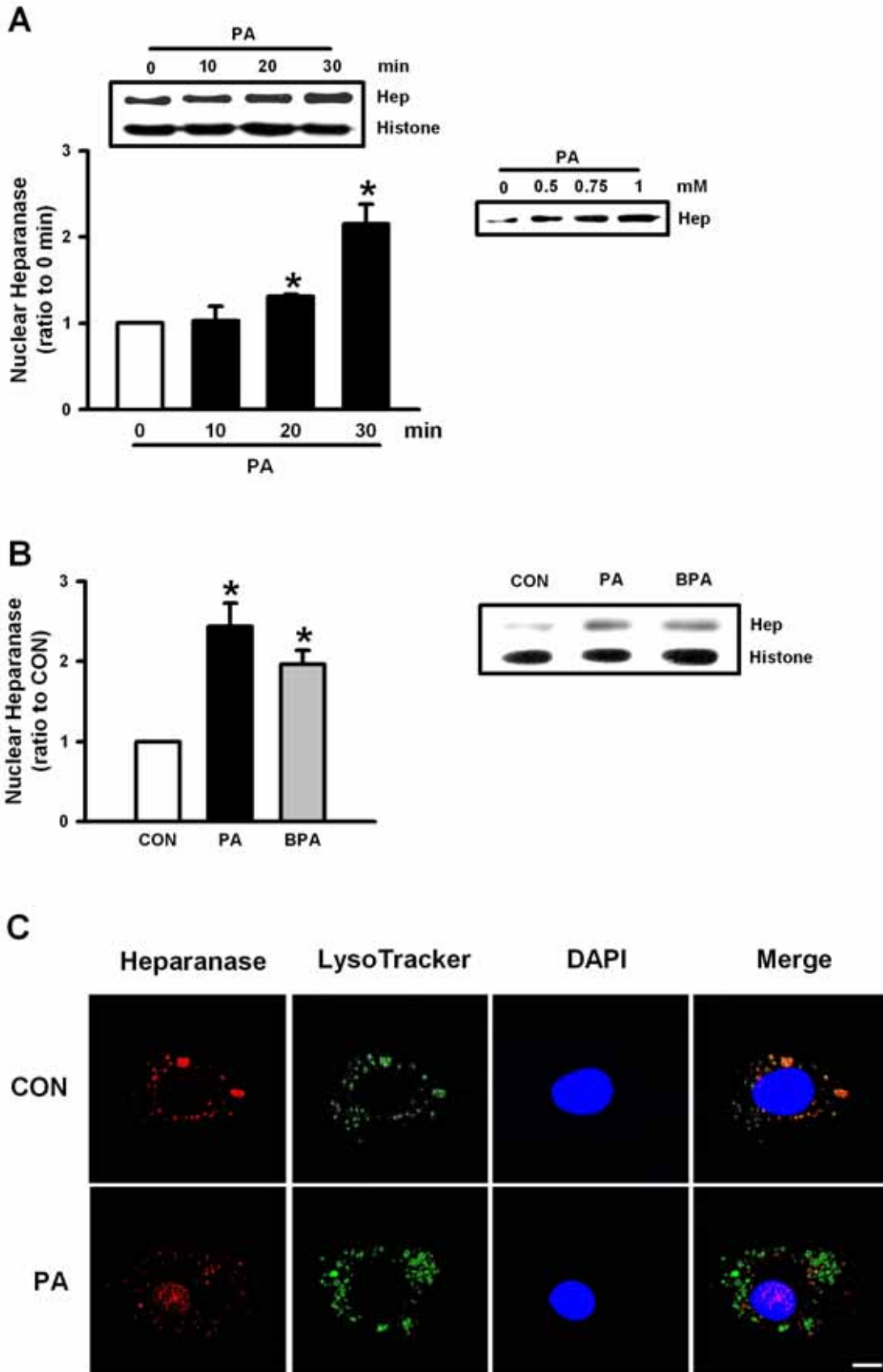


Figure 21 Fatty acid induces a rapid nuclear accumulation of heparanase in endothelial cells. bCAECs were incubated with 0-1 mM albumin bound PA (molar ratio 1:6) for 30 min (A, inset), or 1 mM PA over a period of 30 min (A), and heparanase in the nuclear fractions determined. The influence of BPA (1 mM for 30 min) on nuclear heparanase was compared to PA in B. Results are mean \pm SEM for three experiments expressed as ratio changes. *Significantly different from 0 min/control, #Significantly different from all groups; $P < 0.05$. Cells were stained with LysoTracker (green), anti-heparanase mAb 130 (red) and DAPI (blue). The merged image is described in the fourth panel (C). Bar = 20 μ m. Data is from a representative experiment done three times.

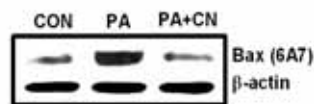
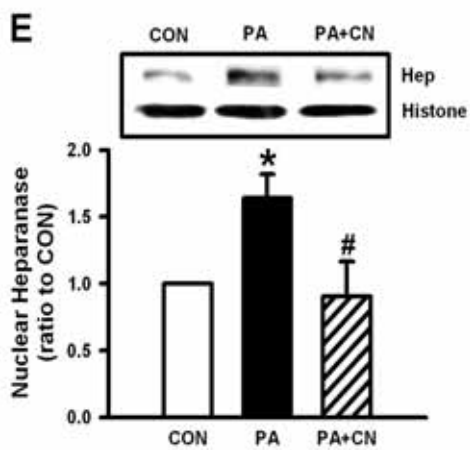
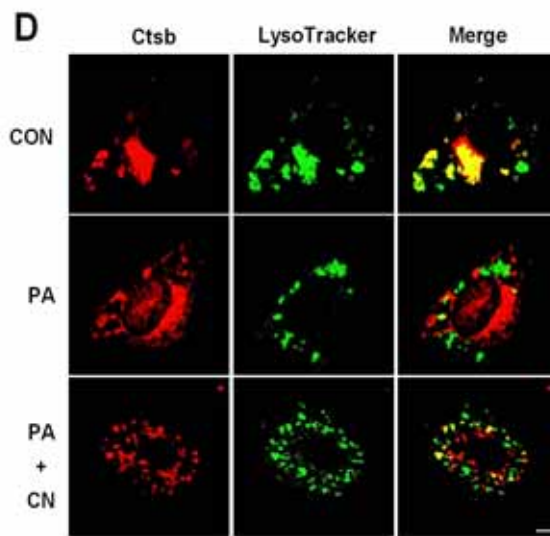
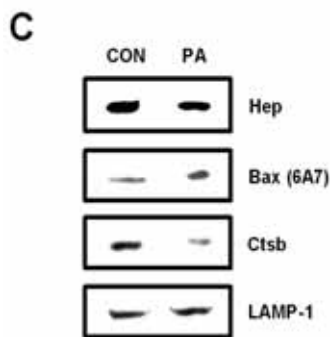
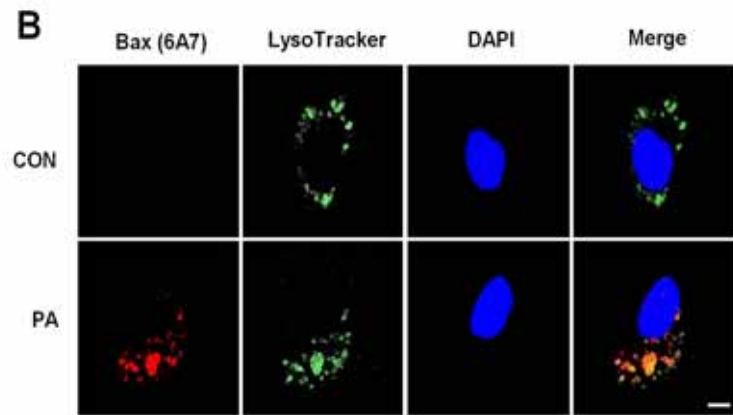
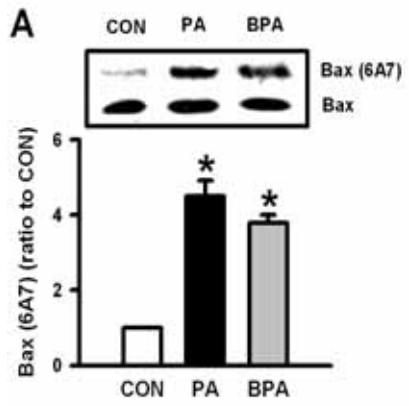


Figure 22 Nuclear translocation of heparanase following PA is dependent on Bax-induced permeabilization of lysosomes. bCAECs were treated with 1 mM albumin bound PA for 30 min, and activated (Bax 6A7) and total Bax determined in whole cell lysates (A). Cells were also stained with LysoTracker (green), anti-Bax mAb 6A7 (red) and anti-Ctsb (red) following 30 min incubation with PA (B and D). Bar = 20 μ m. Data is from a representative experiment done three times. Following isolation of lysosomes, heparanase, activated Bax and Ctsb were also measured (C). LAMP-1 was used as a protein loading control. Following pre-treatment of bCAECs with CN (20 μ M), cells were treated with 1 mM PA for 30 min. Ctsb staining (D), nuclear heparanase (E) and activated Bax (E, inset) were determined. The representative Western blot and densitometric results illustrated are mean \pm SEM for three experiments and are expressed as ratio to control. *Significantly different from control, #Significantly different from PA; $P<0.05$.

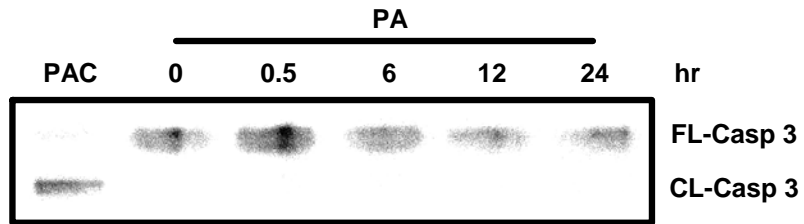


Figure 23 PA for up to 24 hr is unable to induce caspase 3 cleavage. bCAECs were incubated with 1 mM PA over a period of 24 hr. At the indicated times, full-length (FL) and cleaved (CL) caspase (Casp) 3 was determined using Western blot. PAC-1 (PAC, 50 μ M for 2 hr), a procaspase 3 activator was used as a positive control. The immunoblot is a representative figure of three separate experiments.

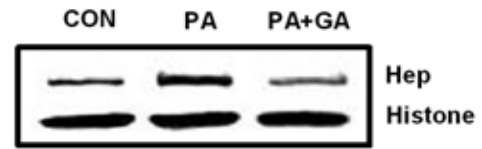
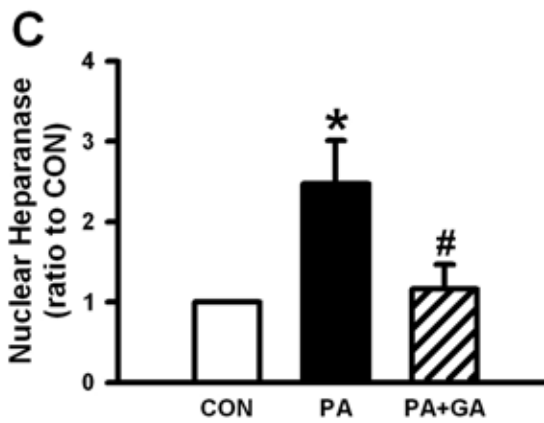
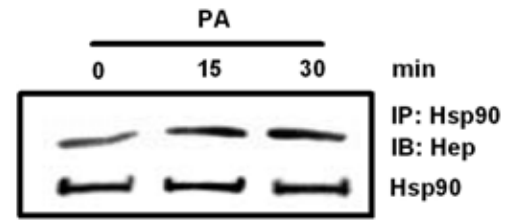
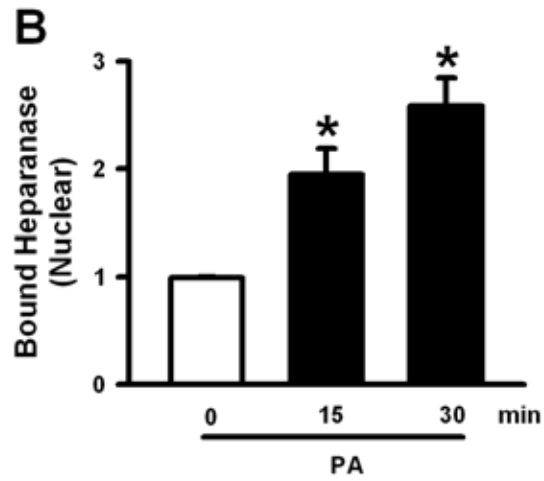
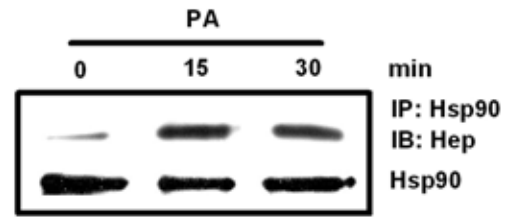
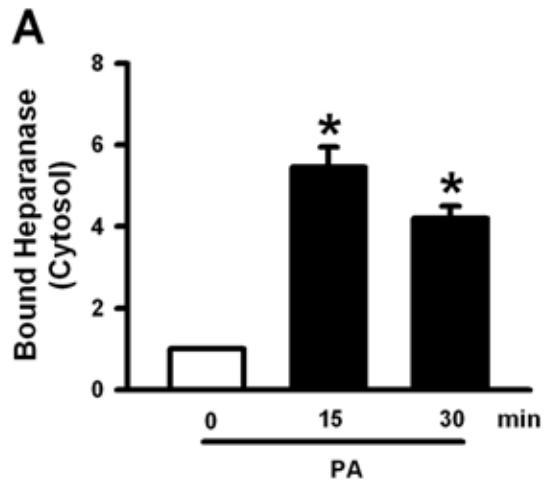


Figure 24 Hsp90 directs the nuclear translocation of heparanase. bCAECs were incubated with 1 mM PA up to 30 min. At the indicated times, cytosolic (A) and nuclear (B) fractions were isolated and immunoprecipitated using anti-Hsp90, and immunoblotted with heparanase mAb 130 and anti-Hsp90 antibody. Cells were also pre-treated with GA (2 μ M for 60 min) and then exposed to 1 mM PA for 30 min. Nuclear heparanase was measured by Western blot (C). Results are mean \pm SEM for three experiments and expressed as ratio changes. *Significantly different from 0 min/control, #Significantly different from PA; $P<0.05$.

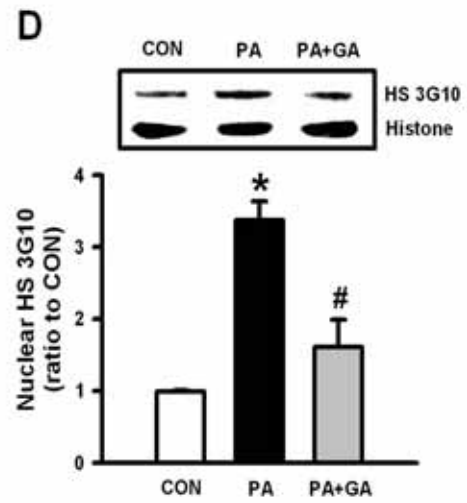
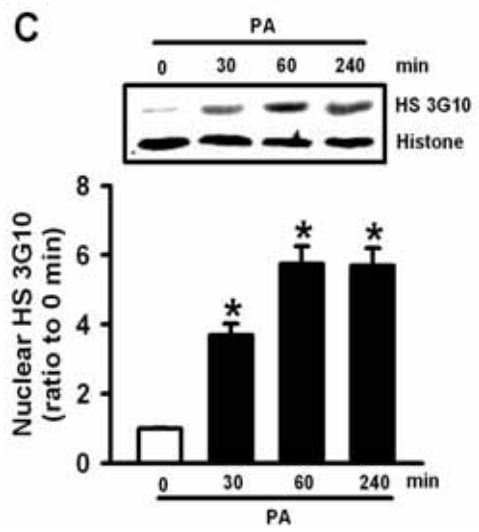
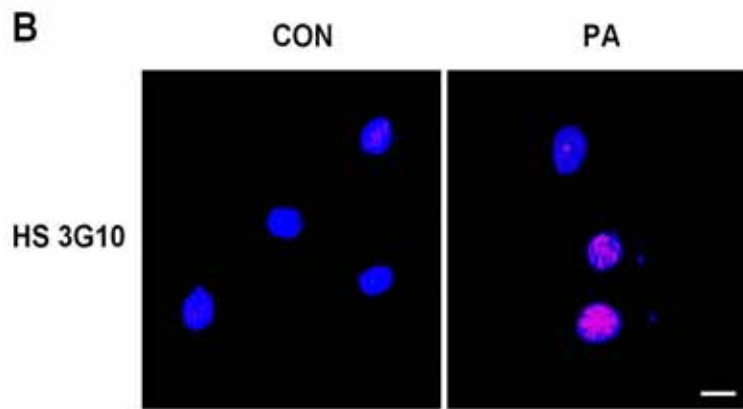
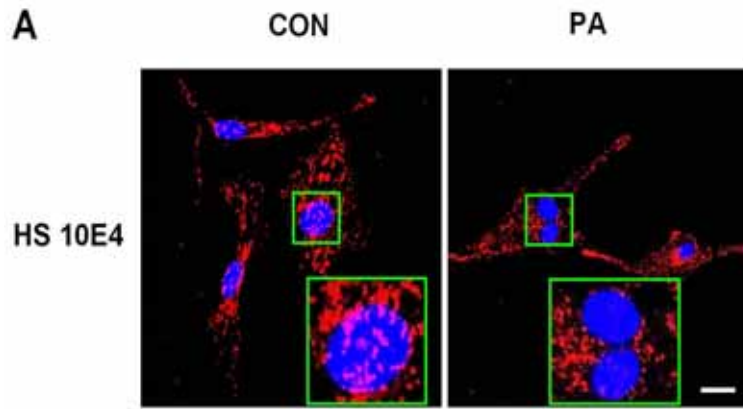


Figure 25 Heparanase cleaves nuclear heparan sulfate (HS). bCAECs treated with 1 mM PA (for 30 min) were immunostained with anti-HS 10E4 (A) and 3G10 (B) antibodies, respectively. A magnified image of nuclear 10E4 staining is depicted in the inset (A). Bar = 20 μ m. Data is from a representative experiment done three times. Western blot and 3G10 antibody was also used to detect cleaved HS in nucleus following exposure to 1 mM PA, in the absence (C, 0-240 min PA) or presence of 60 min pre-treatment with GA (D, 30 min PA). The representative Western blot and densitometric results illustrated are mean \pm SEM for three experiments. *Significantly different from 0 min/control, #Significantly different from PA; $P<0.05$.

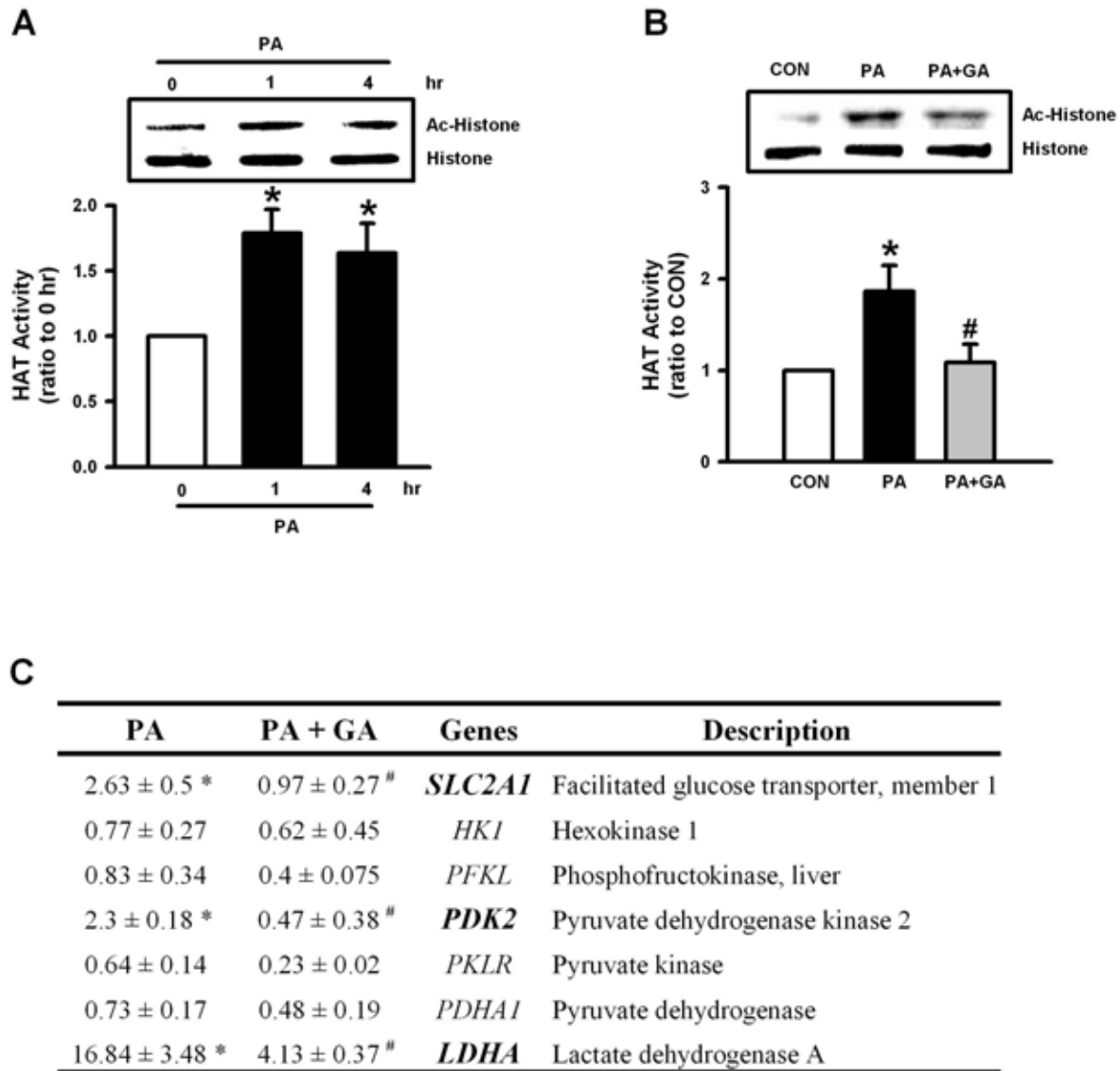


Figure 26 Nuclear heparanase regulates HAT activity and genes involved with glucose metabolism.

bCAECs were treated with 1 mM PA up to 4 hr, and nuclear fractions isolated at the indicated times to measure HAT activity and histone acetylation (A). This experiment was repeated in cells pretreated with 2 μM GA for 60 min, followed by incubation with 1 mM PA for 60 min (B). bCAECs were also incubated with 1 mM PA up to 24 hr in the absence or presence of GA. RNA was isolated to analyze genes involved predominantly with glycolysis using a TaqMan gene expression assay (C). Data shown represents fold change relative to control. The representative Western blot and densitometric results illustrated are mean±SEM for three separate experiments. *Significantly different from control, #Significantly different from PA group; $P < 0.05$.

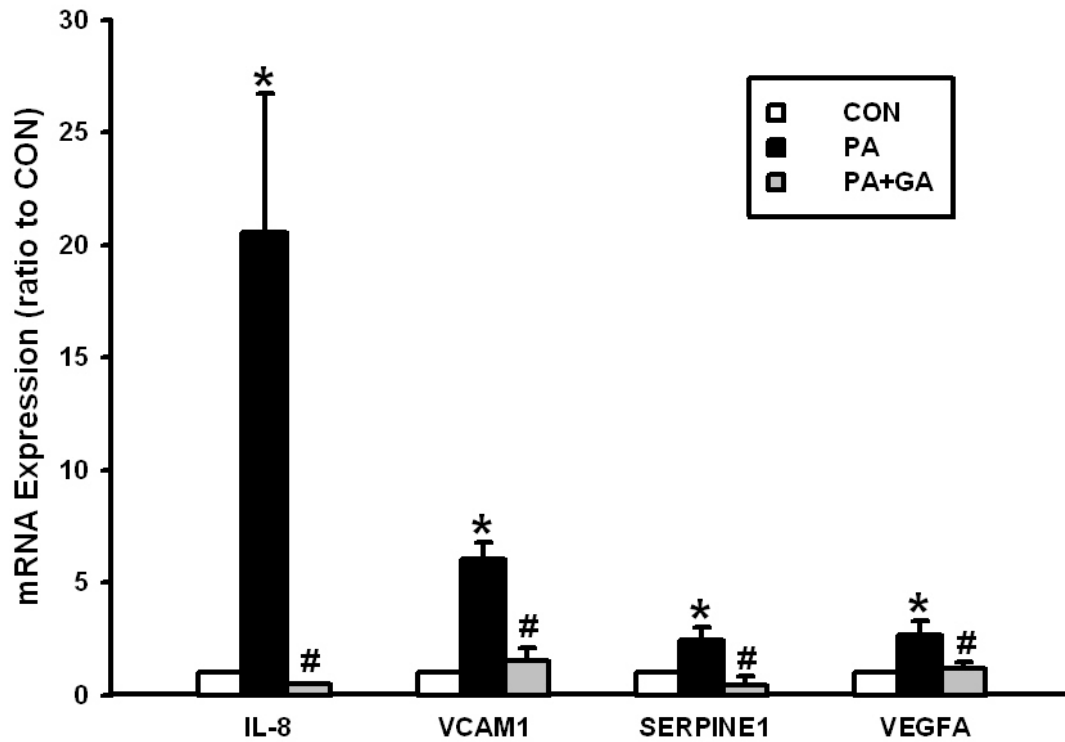


Figure 27 Genes related to inflammation are influenced by PA induced nuclear entry of heparanase. bCAECs were incubated with 1 mM PA up to 24 hr in the absence or presence of 2 μ M geldanamycin (GA). RNA was isolated to analyze genes predominantly involved with inflammation using a TaqMan gene expression assay. IL-8, interleukin-8; VCAM1, vascular cell adhesion molecule 1; SERPINE1, plasminogen activator inhibitor type 1; VEGFA, vascular endothelial growth factor A. Data represents fold change relative to control and is illustrated as mean \pm SEM for three separate experiments. *Significantly different from CON, #Significantly different from PA; $P < 0.05$.

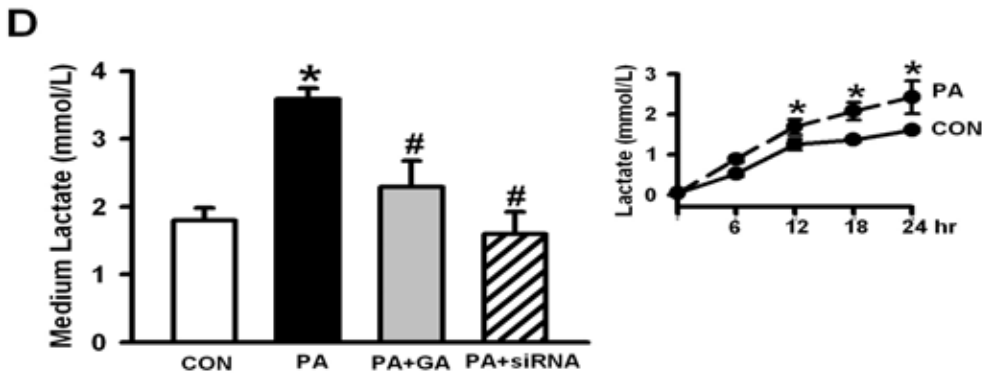
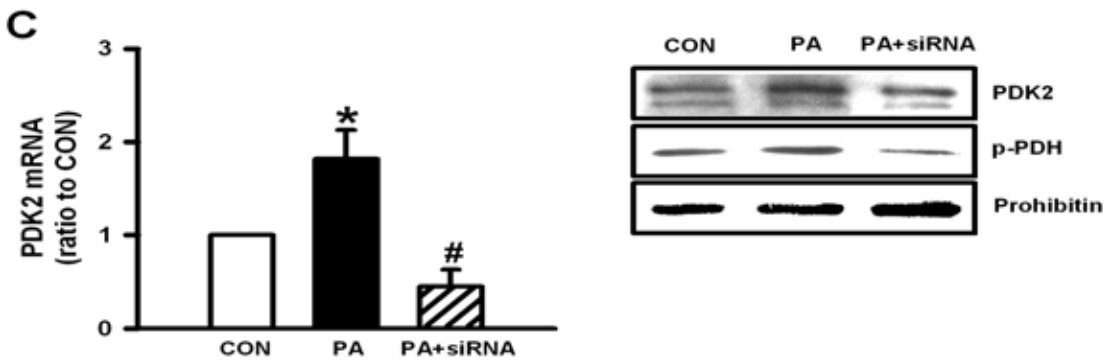
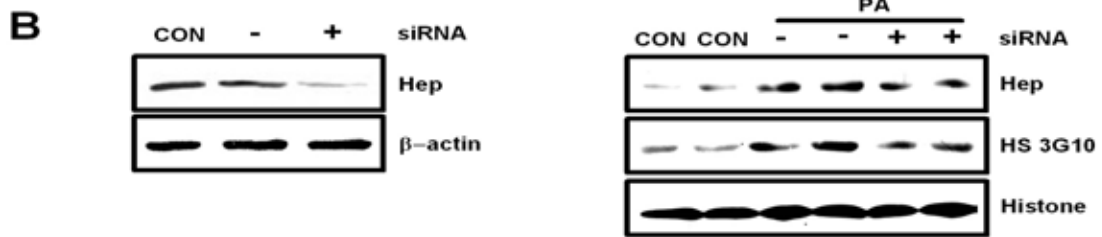
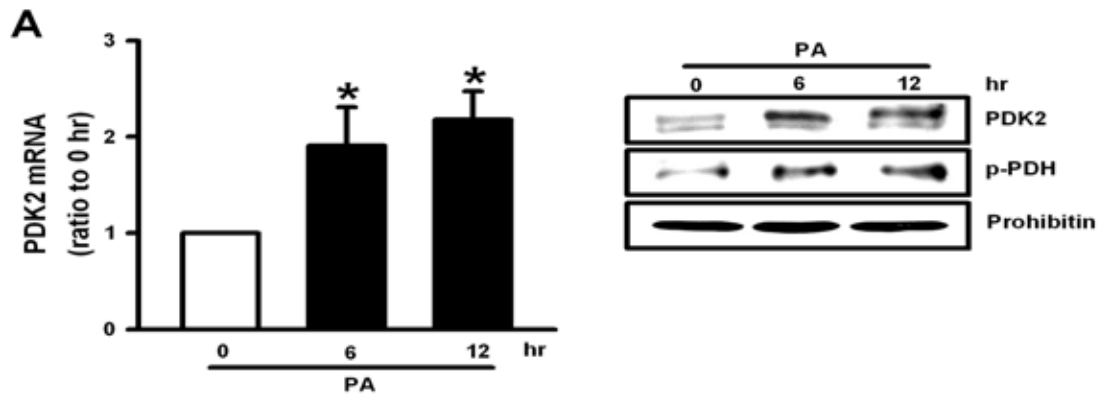


Figure 28 Nuclear heparanase increases PDK2 expression and extracellular lactate accumulation. Cells were treated with 1 mM PA up to 12 hr. At the indicated times, mitochondrial fractions were isolated to detect PDK2 protein and phosphorylation of PDH (p-PDH) (A, inset). RNA was also isolated to identify PDK2 gene expression (A). bCAECs were transfected with heparanase siRNA (B, left). These cells were exposed to 1 mM PA for 30 min and nuclear heparanase and cleaved HS were detected (B, right). The effect of heparanase siRNA on PA-induced PDK2 expression and p-PDH is illustrated in C. In a separate experiment, cells were treated with 1 mM PA in the presence or absence of GA or heparanase siRNA for 24 hr, and medium collected to measure lactate (D and inset). Results are mean±SEM for three separate experiments. *Significantly different from control, #Significantly different from PA group; $P<0.05$.

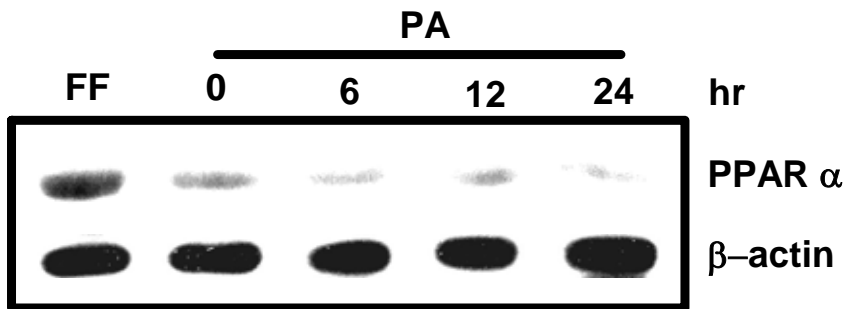


Figure 29 PA has no influence on the expression of endothelial PPAR α . bCAECs were incubated with 1 mM PA over a period of 24 hr. At the indicated times, PPAR α protein was measured using Western blot. Fenofibrate (50 μ M for 24 hr), a PPAR α agonist, was used as a positive control. The immunoblot is a representative figure of three separate experiments.

Chapter 4: Discussion

The earliest change that occurs in the diabetic heart is altered energy metabolism where in the presence of lower glucose utilization, the heart switches to predominantly using fatty acids (FA) for energy supply.¹⁸ One means by which this is achieved is through rapid augmentation of lipoprotein lipase activity (LPL-a key enzyme, which hydrolyzes lipoproteins to release FA) at the coronary lumen.^{126, 127, 130} Given that vascular endothelial LPL is acquired from the cardiomyocyte, previous studies from our lab have examined the mechanisms by which DZ-induced hypoinsulinemia increases cardiomyocyte cell surface LPL, a reservoir that can rapidly augment coronary luminal LPL when the need for FA is intensified. In the myocyte, the recruitment of LPL to the cell surface was controlled by protein kinase D (which regulated LPL vesicle fission),¹²⁹ whereas stress kinases like AMP-activated protein kinase (AMPK) and p38 MAPK allowed for actin cytoskeleton polymerization, providing the cardiomyocyte with an infrastructure to facilitate LPL movement.¹²⁸ My studies reveal that high glucose is a potent stimulator of endothelial heparanase secretion, which helps in the transfer of lipoprotein lipase from the cardiomyocyte to the vascular lumen, permitting augmented fatty acid provision to cardiomyocytes. Unlike high glucose, augmented concentrations of FA, by inducing lysosome permeabilization, initiates endothelial heparanase nuclear translocation, and induction of gene transcription that affects glucose metabolism and inflammation.

4.1 Endothelial heparanase secretion in diabetes is regulated by glucose and FA

In co-culture experiments using bovine endothelial cells and adipocytes, endothelial cells secreted compounds with heparanase-like activity that released adipocyte LPL, promoting its transfer to the luminal endothelial surface.⁵⁹ Interestingly, this heparanase secretion

following lysophosphatidylcholine was polarized, with preferential secretion towards the basolateral rather than the apical side of endothelial cells.⁵⁹ If this mechanism was also to occur in the heart, we hypothesized that hyperglycemia would increase the amount of heparanase in the interstitial space. Using a modified Langendorff heart perfusion that separates coronary from interstitial fluid, we established for the first time that following DZ, heparanase indeed increased rapidly (within 30 min of DZ) in the interstitial compartment, an effect that was lost by 2 hr (Figure 5A). This secretion of active heparanase into the interstitial space paralleled the observations that with increased duration of hyperglycemia (2 hr), the residual content of heparanase in the whole heart, endothelial cells, and interstitial fluid decreased (Figure 5B and C). In HEK-293 cells, the time required for the conversion of latent to active heparanase requires at least 4 hr.⁸⁸ Hence, following secretion, 2 hr of hyperglycemia may be insufficient for either latent heparanase to be synthesized or active heparanase to be regenerated, and could explain this reduction in activity over time. Interestingly, the peak increase in interstitial heparanase closely mirrored the amplification in interstitial LPL (Figure 5D), suggesting that following DZ, it is possible that this rapid secretion of endothelial heparanase initiates the release of subendothelial myocyte cell surface LPL. Once released, this bolus amount of interstitial LPL has to traverse the endothelial cell to reach HSPG binding sites at the coronary lumen. As this process is unlikely to occur rapidly, it could explain the discrepancy between interstitial heparanase and LPL after 2 hr of DZ. Our results imply that following hyperglycemia, secretion of endothelial heparanase is an important element in facilitating LPL translocation from its site of synthesis (cardiomyocyte) to its site of action (endothelial lumen). It should be noted that other methods have also been proposed to explain the transfer of LPL from the

cardiomyocyte to the endothelial cell and include vectorial movement of enzyme along a continuous network of HSPG that extends from myocyte to endothelial cells.¹⁴⁶

As immunohistochemical localization of heparanase in the heart revealed a predominant expression in endothelial cells and depletion with progression of hyperglycemia, we attempted to examine the mechanism of endothelial heparanase secretion. bCAECs were incubated with concentrations of palmitic acid (PA) or glucose that duplicated the plasma concentrations of these substrates observed after DZ. Unexpectedly, with increasing concentrations of PA, intracellular heparanase increased within 30 min, with no release into the medium observed even at the highest concentration of PA used (1 mM). This effect was not exclusive to PA as the unsaturated oleic acid also had a similar outcome (Figure 6A). Visualization of the enzyme after treatment with 1 mM PA illustrated a predominant perinuclear and nuclear localization, an observation confirmed by nuclear isolation followed by Western blot (Figure 6B). This acute effect of FA is likely through an increased reuptake of the latent 65 kDa enzyme followed by lysosomal activation and nuclear translocation,⁸⁸ heparanase has been reported to have two potential nuclear localization sequences.¹⁴⁷ At present, the motive behind this FA-induced nuclear compartmentalization of heparanase is unclear. In hepatocytes, approximately 12% of the total heparan sulfate pool is located within the nucleus.¹⁴⁸ It is possible that within the endothelial nucleus, heparanase can facilitate heparan sulfate degradation, a feedback safety mechanism to limit expression of endothelial HSPG and eventually LPL-derived FA. Alternatively, the nucleus can serve as a storage reservoir for heparanase. Overall, our data suggests that high FA, by increasing perinuclear and nuclear heparanase, may limit the hydrolysis of circulating TG by LPL to avoid excess FA delivery to cardiomyocytes.

In human microvascular endothelial cells, the inflammatory cytokine TNF- α has been shown to facilitate heparanase secretion.¹⁰¹ In the absence of an effect of FA on endothelial heparanase secretion, we tested the influence of glucose in mediating heparanase release. Both TNF- α and glucose lowered endothelial intracellular heparanase (there was a robust dispersion of perinuclear heparanase towards the plasma membrane), with a related increase in heparanase activity in the incubation medium (Figure 7). At present, it is unclear whether this glucose-induced secretion of heparanase is through the apical or basolateral (or both) side of endothelial cells. To more closely mimic the temporal changes in substrates observed with DZ, bCAECs were first incubated with PA prior to addition of high glucose. Addition of high glucose to cells pretreated with PA prevented intracellular accumulation of heparanase (Figure 8). More importantly, under these conditions, the amount of heparanase released into medium was higher than that observed with glucose alone, suggesting that FA can increase the amount of intracellular heparanase available for subsequent release by glucose. Taken together with the observation that DZ increases heparanase release into the cardiac interstitial space, our data suggests that high glucose is likely the predominant reason for endothelial heparanase secretion. At present, the mechanism by which high glucose initiates heparanase release is unclear. At least in HEK 293 cells, nucleotides mediate heparanase secretion by stimulation of P2Y receptors and activation of protein kinase C signaling, mechanisms that are currently being tested in our system. Irrespective of the mechanism, high glucose-dependent secretion of heparanase could facilitate a) cardiomyocyte HSPG cleavage and LPL release, b) translocation of LPL to the vascular lumen, and c) increased provision of TG-derived FA when cardiac utilization of glucose is compromised.

Cellular heparanase is present predominantly in lysosomes,¹³³ whose exocytosis is highly regulated and dependent on both microtubules and the actin cytoskeleton.¹⁴⁹ In cardiomyocytes, the G-actin to F-actin ratio is approximately 10:90, whereas non-activated platelets may have an 80:20 G-actin to F-actin ratio. We have previously reported that following acute hyperglycemia, the increase in the F/G actin ratio is a function of a reduction in G-actin;¹²⁸ we could not detect any increase in F-actin as this was the overwhelming form of actin in the cardiomyocytes. bCAECs treated with high glucose demonstrated an increase in the F-to-G actin ratio, indicating actin polymerization (Figure 9A). Interestingly, HG had little influence on G-actin with F-actin being the key element in cytoskeleton rearrangement. Other studies also reported that postconfluency has little influence on G-actin in bovine aortic endothelial cells.¹⁵⁰ As the actin polymerization inhibitor, cytochalasin D, prevented the high glucose-induced depletion of intracellular heparanase, an effect similar to that observed using nocodazole to disrupt microtubules, our data suggests that both microtubules and actin cytoskeleton are important means by which high glucose enables heparanase secretion (Figure 9B and C). It should be noted that the actin cytoskeleton also plays a key role in promoting insulin-induced glucose transporter 4 translocation¹⁵¹ and in managing myocyte LPL secretion.^{128, 129} PA also increased actin polymerization, which has previously been shown to facilitate the uptake of latent heparanase that is processed into an active form and stored in the lysosomal compartment.¹³⁵ As pretreatment with cytochalasin D prevented the intracellular accumulation of heparanase, whereas nocodazole had no influence on this PA-induced buildup of heparanase (Figure 9B and C), our data suggests that the actin cytoskeleton, but not the microtubules, is responsible for this effect of PA on intracellular heparanase.

In summary, our data demonstrates that following DZ induced hypoinsulinemia, hyperglycemia is likely the major instigator for releasing heparanase into the interstitial compartment and cleaving cardiomyocyte surface LPL. This process is dependent on the ability of FA to increase endothelial intracellular heparanase followed by the rapid secretion of this endothelial enzyme by glucose (Figure 30).

4.2 Glucose-induced endothelial heparanase secretion requires cortical and stress actin reorganization

Cellular heparanase is stored in lysosomes with predominant perinuclear localization. Exposure of bCAECs to HG time-dependently (within 30 min) released heparanase.¹³⁷ Thus, for heparanase to undergo secretion, movement of lysosomes to the cell surface would be a prerequisite. Indeed, immunofluorescent images of endothelial cells revealed that heparanase colocalized with lysosomes, in close proximity to the nucleus (Figure 10C). More importantly, for the first time, we demonstrate that in response to HG, there is a repositioning of lysosomal heparanase away from the nucleus and loss of total staining for endothelial heparanase and lysosomes. It should be noted that although heparanase gene expression is augmented in HEK 293 cells exposed to HG for 24 hr,¹⁰⁰ we were unable to detect any change in gene expression up to 2 hr with HG. Overall, our data suggests that in response to stimulation by HG, mechanisms that regulate lysosomal exocytosis are also likely to control endothelial heparanase secretion.

In various cell types including endothelial cells, cytoplasmic ATP can be released by shear stress, hypoxia or agents like thrombin.¹⁵²⁻¹⁵⁴ When released, ATP is an important mediator of vascular tone and blood coagulation by regulating endothelial nitric oxide and von Willebrand factor secretion respectively.^{155, 156} We observed that bCAECs exposed to 5

or 25 mM glucose rapidly released ATP into the medium, with 25 mM glucose having a more robust effect (Figure 12A). Extracellular ATP, through a P2Y G-protein coupled receptor signal cascade, is known to initiate intracellular heparanase secretion.¹³⁷ P2Y is the predominant purinergic receptor subtype in endothelial cells.^{157, 158} Using the P2 receptor antagonist suramin, we prevented the effect of HG to bring about heparanase secretion (Figure 12B). As MeSATP, a more potent P2Y agonist than ATP, also had a profound effect in releasing endothelial heparanase (Figure 12C), our data provide strong evidence that ATP release and subsequent purinergic receptor activation are essential for mediating HG effect on endothelial heparanase release.

Actin cytoskeleton is a dynamic network, and its reorganization from a distribution predominantly in the outer portion of the cells (cortical actin) into fibers that stretch across the cell body (stress actin), is a characteristic change of endothelial cells in response to inflammatory agents.^{159, 160} For example, a 30 min exposure to thrombin significantly increases calf pulmonary artery endothelial cell permeability to albumin, which was associated with loss of cortical and increases in stress actin.¹⁵⁹ Recent studies have also specified a dual role of actin cytoskeleton in controlling vesicle transport and exocytosis.¹⁶⁰ It was suggested that cortical actin serves as a barrier, and its transient depolymerization is necessary for vesicle secretion.¹⁶¹ Related to stress actin, its formation as a track for vesicle translocation towards the plasma membrane would also be essential for vesicular secretion. In this study, immunofluorescent images of endothelial cells demonstrated cortical actin disassembly on exposure to HG, with subsequent stress actin formation (Figure 14A). As agents that disrupted actin dynamics prevented the HG-induced depletion of intracellular

heparanase (Figure 14B and C), our data suggest that both cortical actin disassembly and stress actin formation are indispensable for HG-induced heparanase secretion.

In pancreatic beta cells, CaMKII contributes towards calcium-regulated exocytosis of insulin secretory granules.¹⁶² In our study, albeit with different kinetics, HG and MeSATP provoked an increase in $[Ca^{2+}]_i$. As suramin impeded this effect of HG on $[Ca^{2+}]_i$, our data suggests that ATP is a key element that facilitates HG-induced increases in endothelial $[Ca^{2+}]_i$ (Figure 16A). Related to this increase in $[Ca^{2+}]_i$, there was an associated augmentation in phosphorylation of CaMKII, that was not sustainable and declined to control levels at 30 min even though heparanase was continuously being secreted (Figure 16B). We considered the possibility that the early activation of CaMKII may have turned on other downstream signals. Downstream targets of CaMKII include p38 MAPK/Hsp25, and there was coincident activation of this pathway following HG (Figure 16C and D). Hsp25 is known to inhibit actin polymerization, and its phosphorylation results in a decline of this inhibitory function.¹⁶³ In this setting, actin monomers are released from the phosphorylated Hsp25 to self-associate to form actin filaments. Interestingly, CaMKII inhibition with KN93 or blocking of p38 MAPK with SB202190 prevented stress actin formation, and abolished HG-induced endothelial heparanase secretion (Figure 17). These data suggest that in response to HG, CaMKII and p38 MAPK, through their control of Hsp25 and stress actin, act in unison to facilitate heparanase secretion from endothelial cells.

Filamin is a 280 kDa protein that contains an N-terminal actin-binding domain (that assists in actin filament cross linking), and a C-terminal protein binding end (that connects the actin network to plasma membrane bound proteins like the insulin and P2Y₂ receptors).^{141, 164-166} In this way, filamin plays a critical role in cortical actin organization.

We established a strong association between filamin and P2Y₂ receptors in endothelial cells. More importantly, incubation with HG reduced this association, facilitating filamin translocation to the cytosol (Figure 18). In endothelial cells exposed to thrombin, filamin phosphorylation is required for its translocation from the cell periphery to cytosol.¹⁶⁵ Our data also indicates that HG induces a robust phosphorylation of filamin with subsequent membrane to cytosol relocation, and is associated with disassembly of the endothelial cortical actin network and endothelial heparanase secretion.

Co-culturing of endothelial cells and cardiomyocytes is an appropriate means by which the endoglucuronidase activity of endothelial heparanase can be tested. This is because in endothelial cells, heparanase exocytosis is polarized, with preferential secretion towards the basolateral rather than the apical side.^{59, 164} Using this co-culture preparation, we were successful in depleting endothelial intracellular heparanase (Figure 19A). More importantly, we observed that in response to HG and heparanase secretion, cardiomyocyte surface heparan sulfate was cleaved, with an associated increase in LPL activity and bFGF protein in the lower chamber (Figure 19).

In summary, our results suggest that HG stimulates ATP release and purinergic receptor activation. One downstream cascade of this event is increase in $[Ca^{2+}]_i$, stimulation of CaMKII, phosphorylation of p38 MAPK/Hsp25, and eventual formation of stress actin. Another outcome is detachment of filamin from the P2Y receptor, resulting in cortical actin disassembly. Together, these processes might contribute towards robust stimulation of endothelial heparanase secretion (Figure 31).

4.3 Fatty acid-induced nuclear translocation of heparanase uncouples glucose metabolism in endothelial cells

In endothelial cells exposed to PA, a rapid nuclear accumulation of heparanase was observed (Figure 21A). This nuclear presence of heparanase is not uncommon, and several groups have detected this enzyme in the nucleus of MDA-435 human breast carcinoma cells and U87 glioma cells that were stable transfected with heparanase.¹⁴⁷ As the non-metabolizable palmitate analog BPA had similar effects in mediating nuclear translocation of heparanase (Figure 21B), it is unlikely that this nuclear shuttling requires prior oxidation of fatty acids. Given the immediate effect of fatty acids in translocating heparanase, we determined the cellular location of heparanase. Immunofluorescent images showed that heparanase was colocalized within lysosomes, in close proximity to the nucleus (Figure 21C). This perinuclear position of heparanase precludes protracted transit time, and could explain the quick nuclear entry of heparanase in response to fatty acids.

Given the predominant lysosome localization of heparanase, its prior release from lysosomes would be anticipated before its nuclear entry. In HepG2 cells, high fatty acid-induced lysosome permeabilization is preceded by activation of the pro-apoptotic protein Bax.¹⁶⁷ A Bax-dependent lysosome disruption is also involved in the alpha-lactalbumin and oleic acid-induced early leakage of lysosomes in tumor cells.¹⁶⁸ Results from this study also implicate Bax in the PA-induced nuclear entry of heparanase in endothelial cells. Thus, fatty acids induced Bax activation, which colocalized with lysosomes and was associated with release of lysosome contents including heparanase and Ctsb (Figure 22). At present, the mechanism by which fatty acid induces lysosomal permeabilization through Bax is unclear. In mitochondria from human cancer cells, activated Bax undergoes a conformational change,

binds to the mitochondrial outer membrane to form complex oligomer pores, and induces membrane potential loss and permeabilization.¹⁶⁹ Interestingly, overexpression of Bcl-X_L, which antagonizes Bax pore formation activity, prevented PA-induced lysosomal permeabilization in HepG2 cells.¹⁷⁰ As the Bax channel blocker CN also inhibited lysosomal leakiness in this study, our data provide strong evidence that PA-induced lysosomal permeabilization and release of heparanase is related to Bax induced pore formation.

Although different pathways exist for nuclear import of proteins, common shared features include a nuclear localization sequence, carrier molecules and translocation through nuclear pore complexes.¹⁷¹ Human heparanase contains two potential nuclear localization sequences (residues 271-277 and 427-430).¹⁴⁷ Regarding carriers, at least with the glucocorticoid receptor, a ubiquitous chaperone protein Hsp90, binds with the GR and together with the immunophilin assembly system, forms a transportosome to help GR shift from cytoplasm to nucleus.¹⁷² Recently, a role for Hsp90 as a chaperone for nuclear translocation of heparanase has also been reported in HL-60 cells.¹⁴⁴ Consistent with this report, our immunoprecipitation experiments revealed a robust cytoplasmic association between Hsp90 and heparanase, and their time-dependent shuttling into the nucleus (Figure 24A and B). As the Hsp90 inhibitor GA effectively abolished the nuclear presence of heparanase in response to PA (Figure 24C), our study suggests that Hsp90 is the likely carrier in nuclear shuttling of heparanase in endothelial cells.

HS are linear polysaccharide chains that require vesicle transport to be transferred onto the cell surface.⁵³ However, the presence of HS in the nucleus has been reported in various cell types.^{148, 173} For example, in primary hepatocytes, 18% of the total intracellular HS pool is located in the nucleus.¹⁴⁸ Our immunofluorescent images also demonstrated staining for

intact HS in the nucleus of endothelial cells. With PA, staining for intact nuclear HS was lost, and this coincided with appearance of cleaved HS in the nucleus (Figure 25A and B). It should be noted that although intact HS displayed whole cell distribution, cleaved HS following PA was only evident in the nucleus. One explanation for this observation is the possibility that released heparanase from lysosomes has limited access to intact HS that are transported in vesicles. As GA, which prevented the nuclear entry of heparanase, effectively attenuated the cleavage of nuclear HS (Figure 25D), our data suggest that it is the PA-induced nuclear entry of heparanase that facilitates HS cleavage. The unique location of cleaved HS stimulated us to examine nuclear functions of HS. Recently, HS has been reported to be a potent repressor of gene transcription through its inhibitory effect on HAT, the enzyme that acetylates the lysine side chain of histone, allowing access of transcription factors to bind DNA and initiate transcription.^{145, 174} Indeed, augmented HAT activity and histone acetylation were observed when nuclear HS was cleaved, effects that were prevented by GA (Figure 26 A and B). A broad range of genes are regulated by HAT, including genes related to cell metabolism, inflammation and proliferation.¹⁷⁵ As our special interest was glucose metabolism that is a major provider of ATP to endothelial cells, we carried out a gene expression assay for key enzymes in this pathway. Interestingly, activation of gene expression was limited to genes encoding glucose transport (SLC2A1), glucose oxidation (PDK2), and lactate formation (LDHA) (Figure 26C). As these effects were attenuated by GA, our data suggest that PA could possibly influence gene transcription through nuclear entry of heparanase.

Phosphorylation of the PDH complex at its E1 site by PDK has been recognized to inactivate PDH and lower glucose oxidation.¹⁷⁶ In response to starvation and diabetes, PDK

expression is adjusted in a tissue-dependent manner; PDK expression increases in heart and skeletal muscle, but not in brain.¹⁷⁷⁻¹⁷⁹ Of the different isoforms of PDK, PDK2 is a ubiquitously and abundantly present isoenzyme.¹⁸⁰ As PDK2 responds rapidly to control the PDH complex,¹⁸⁰ we examined its endothelial expression following PA treatment. PA for 6 hr was sufficient to induce PDK2 mRNA and protein, with a corresponding increase in the phosphorylation of PDH (Figure 30A). In skeletal muscle and heart, fatty acid is a well-known stimulator of PDK through activation of PPAR α .¹⁸¹ As PPAR α was unaffected by PA up to 24 hr (Figure 29), and as silencing of heparanase prevented these effects of PA on PDK2 and PDH (Figure 30C), our study provides evidence for another potential regulator of PDK in endothelial cells. Inactivation of PDH uncouples glucose oxidation from glycolysis, resulting in increased pyruvate conversion to lactate, as observed in this study (Figure 30D). As this lactate accumulation was prevented by GA or heparanase siRNA, our present data also suggest an important role for nuclear heparanase in regulation of endothelial glucose metabolism.

Overall, the results presented in this study demonstrate that fatty acid can provoke lysosomal release of heparanase, its nuclear translocation, and activation of genes controlling glucose metabolism and inflammation (Figure 32). The ensuing uncoupling between glucose oxidation and glycolysis leads to accumulation of lactate. Given that lactate and its lowering of pH has been implicated in the progression of atherosclerosis through its promotion of lipoprotein binding to proteoglycans,¹⁸² angiogenesis and plaque rupture,^{23, 183} and the critical role of IL-8, VCAM and VEGF in the development of atherosclerosis,¹⁸⁴⁻¹⁸⁶ these data detailing the novel mechanism by which FA shuttles endothelial heparanase into the nucleus may serve to reduce the associated cardiovascular complications seen during diabetes.

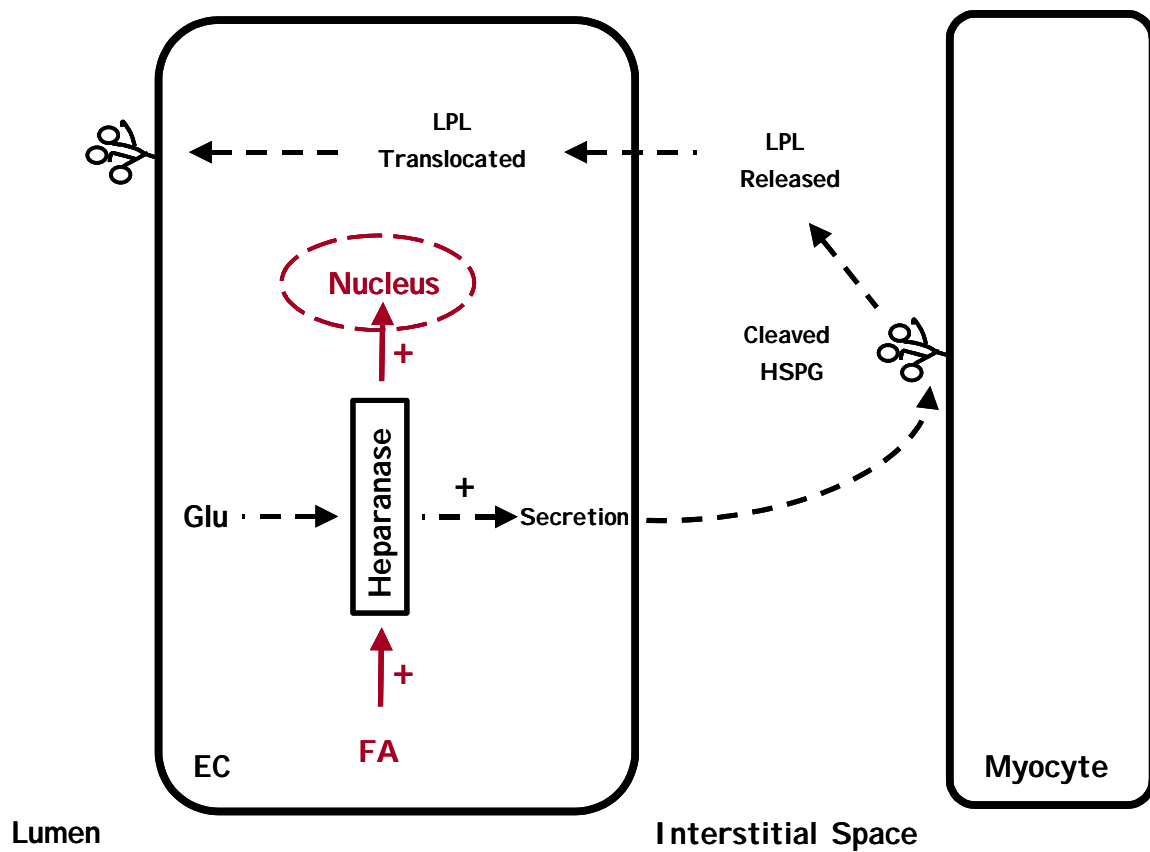


Figure 30 A summary diagram describe the mechanism of endothelial heparanase regulation of cardiac **LPL**. Following diabetes and the development of hyperglycemia and hyperlipidemia, there is increased translocation of LPL from the cardiomyocyte cell surface to the apical side of endothelial cells. This process is dependent on the ability of FA to increase endothelial intracellular heparanase, followed by the rapid secretion of this endothelial enzyme by high glucose.

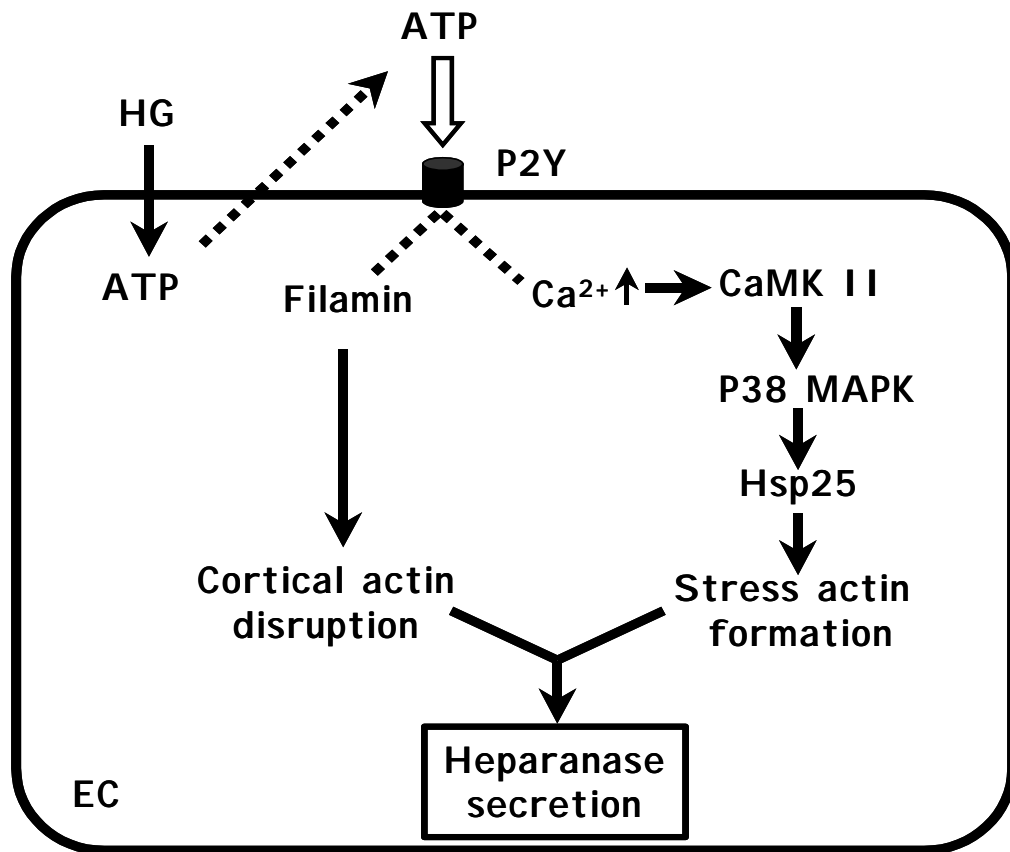


Figure 31 Schematic mechanism of how high glucose stimulates endothelial heparanase secretion. HG stimulates ATP release and purinergic receptor (P2Y) activation. One downstream cascade of this event is increase in $[Ca^{2+}]_i$, stimulation of CaMKII, phosphorylation of p38 MAPK/Hsp25, and eventual formation of stress actin. Another outcome is detachment of filamin from the P2Y receptor, resulting in cortical actin disassembly. Together, these processes contribute towards robust stimulation of endothelial heparanase secretion.

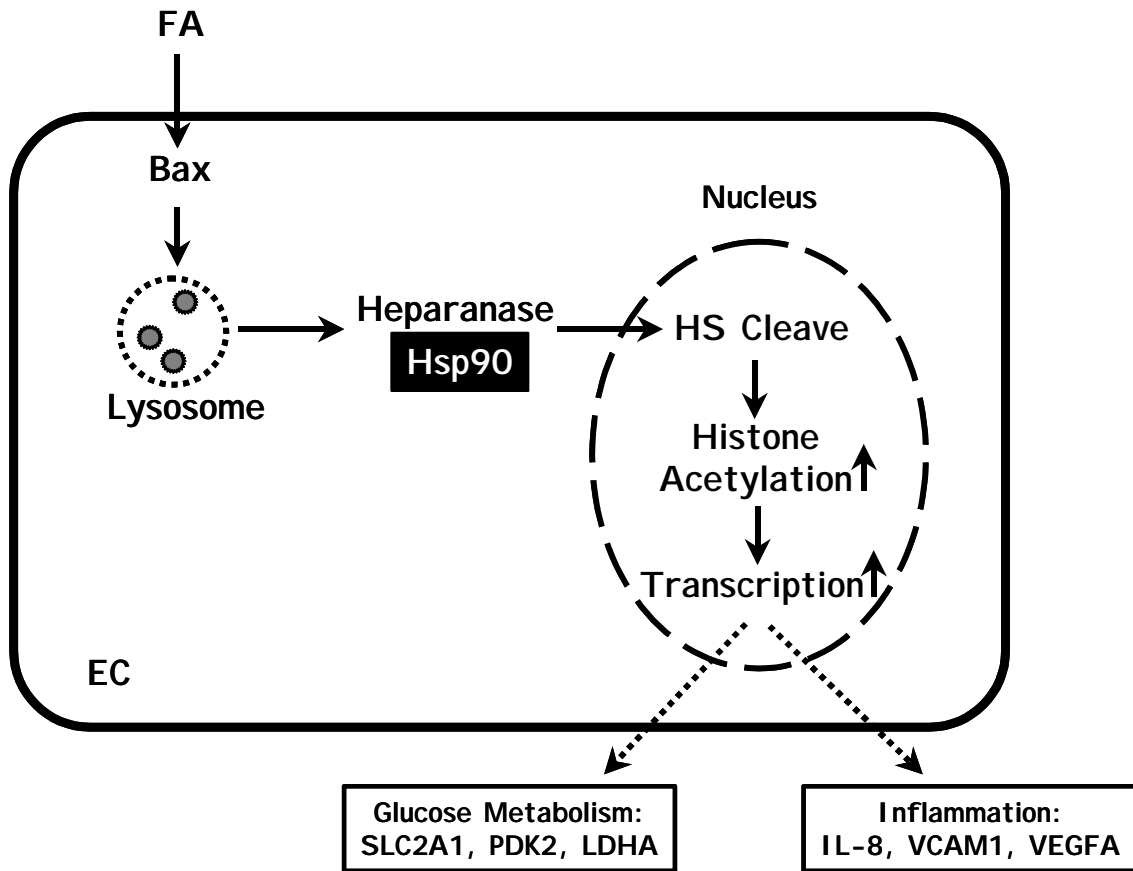


Figure 32 Scheme of probable mechanisms of how high FA stimulates nuclear translocation of endothelial heparanase. In response to high FA, endothelial Bax is activated which can provoke lysosome permeabilization and release of heparanase. Using Hsp90 as a chaperone, this endoglycosidase undergo nuclear translocation and cleaves nuclear HS, which increases histone acetylation and activation of genes controlling glucose metabolism and inflammation.

Chapter 5: Conclusions and Future Directions

5.1 Conclusions

Following acute hypoinsulinemia, in the presence of lower glucose utilization in cardiomyocytes, the heart switches to predominantly using FA for energy supply.¹⁸ As lipoprotein lipase (LPL) is the key enzyme that hydrolyzes circulating TG-rich lipoproteins to release free FA, multiple mechanisms are turned on in the heart to increase vascular lumen LPL, thereby providing sufficient fatty acid (FA) to meet the high energy consumption of the diabetic heart. These include an increased transfer of LPL to the cardiomyocyte cell surface and subsequent translocation to the apical side of ECs.^{126, 127, 130} Previous investigations from our lab indicated that within the cardiomyocyte, recruitment of LPL to the cardiomyocyte cell surface was controlled by stress kinases like AMPK and p38 MAPK that allowed for actin cytoskeleton polymerization,¹²⁸ whereas LPL vesicle formation and movement was controlled by activation of protein kinase D.¹²⁹ Together, they provided the cell with an infrastructure to facilitate the movement of LPL to the cardiomyocyte cell surface, followed by its sequestration to cell surface HSPG. Studies from my projects revealed that translocation of LPL from cardiomyocyte cell surface to the apical side of ECs is dependent on the secretion of endothelial heparanase into the interstitial compartment, where the enzyme is capable of degrading HSPG and instigating LPL detachment from cardiomyocyte cell surface. This mechanism could be a lead up to the eventual transfer of LPL to the vascular endothelial lumen.

Heparanase secretion is a tightly regulated process. We observed opposing effects of high glucose and FA on the processing and secretion of endothelial heparanase during diabetes. HG was a potent stimulator of endothelial heparanase secretion. Unlike HG, FA

had no effect on secretion of endothelial heparanase. However, it had a novel function in increasing intracellular heparanase content, and more specifically, inducing the nuclear translocation of heparanase to affect endothelial gene transcription. We also studied the mechanisms behind the regulation of endothelial heparanase by HG and FA respectively. bCAECs exposed to 25 mM glucose induced a rapid ATP release into the extracellular space, with a maximum effect observed at 2 min. Extracellular ATP interacted and activated endothelial purinergic receptors (such as P2Y receptor) and triggered cortical actin disassembly and stress actin formation within 30 min. Since cortical actin was suggested to serve as a barrier, and stress actin to provide a track for vesicle secretion,^{160, 161} depolymerization of cortical actin and formation of stress actin is likely involved in endothelial heparanase secretion. Phosphorylation of filamin following P2Y receptor activation contributed towards the cortical actin disassembly, as filamin is the actin binding protein that attaches actin filaments to the P2Y receptor on plasma membrane.^{140, 141} Increased extracellular ATP also provoked a rapid elevation of endothelial $[Ca^{2+}]_i$, which stimulated CaMK II and p38 MAPK/Hsp25 phosphorylation-mediated stress actin formation. Through these mechanisms, HG turns out to be a potent stimulator of endothelial heparanase secretion. The endothelial-secreted heparanase in response to HG demonstrated endoglycosidase activity, cleaved HSPG on the surface of cardiomyocytes, and released attached proteins like LPL and bFGF.

Compared to HG, ECs incubated with 1 mM FA significantly increased Bax activation, which exhibited a colocalization with lysosomes and provoked lysosome permeabilization. As cellular heparanase is stored in lysosomes with predominant perinuclear localization,^{133,}¹³⁷ it can leak out when the integrity of lysosome is disrupted. The released heparanase,

using Hsp90 as a chaperone, underwent nuclear translocation, cleaved nuclear HS, and increased histone acetylation and activation of genes controlling glucose metabolism (SLC2A1, PDK2 and LDHA) and inflammation (IL-8, VCAM1 and VEGFA). In addition, endothelial glycolysis was uncoupled from glucose oxidation, resulting in accumulation of lactate.

These data are especially important given the pivotal role of heparanase in diabetes-associated complications. For example, heparanase increases the permeability of the glomerular basement membrane through loss of negatively charged heparan sulfate, leading to urinary protein excretion.¹⁰⁰ In vascular tissue, endothelial heparanase has been implicated in regulating arterial structure, mechanics, and repair,¹²⁴ which could explain the increased incidence of atherosclerosis in diabetes. In addition, FA-induced nuclear translocation of heparanase activated genes controlling endothelial glucose metabolism and inflammation, which also contribute to the development of atherosclerosis. More importantly, following diabetes, heparanase has been implicated in transferring LPL from the cardiomyocyte cell surface to the apical side of endothelial cells, leading to augmented fatty acid uptake and eventually diabetic cardiomyopathy. By gaining more insight into regulation of endothelial heparanase, we can attempt to piece together a part of the cascade of events leading to complications associated with diabetes.

5.2 Future directions

To further investigate the contribution of endothelial heparanase towards cardiovascular diseases seen during diabetes, future studies should focus on the following areas:

1. We demonstrated that following reduced insulin level, high glucose induces endothelial heparanase secretion into the interstitial space and cleaving of cardiomyocyte surface HS

to release LPL. This mechanism could be a lead up to eventual transfer of LPL to the vascular endothelial lumen. However, we haven't proved directly that this released interstitial heparanase actually caused the observed translocation of LPL from cardiomyocyte surface to vascular lumen. Therefore, future experimentation using coculture of endothelial cells and cardiomyocytes will need to determine this heparanase release, HS cleavage and LPL translocation to the endothelium lumen.

2. In my thesis, we used diazoxide (DZ), a selective K^+_{ATP} channel opener, to examine cardiac metabolism under conditions where insulin secretion are rapidly decreased from pancreatic β -cells. Besides its significant and rapid increase in plasma parameters of glucose, FA and TG, another advantage of using DZ is achievement of reversible hyperglycemia in the absence of any pancreatic β -cell death. However, this model is not representative for other scenarios observed in diabetes, such as insulin resistance in T2D. The regulation of endothelial heparanase towards cardiac LPL during diabetes should be also investigated in some other diabetes models.
3. In our study, we focused on the acute changes during hypoinsulinemia. Both high glucose-stimulated endothelial heparanase secretion, and fatty acid-induced nuclear translocation of heparanase were observed within 30 min in bCAECs. However, diabetes is a chronic disease. It will be interesting to study the long-term regulation of endothelial heparanase by high glucose or fatty acid, and more importantly, how it affects the pathogenesis of diabetes.
4. Since fatty acid-induced nuclear translocation of heparanase activated genes related to inflammation, such as IL-8, VCAM1 and VEGFA, experiments should be carried to

investigate how heparanase correlates to pathological processes regulated by these bioactive molecules.

References

1. Ogasawara, K., et al., *NKG2D blockade prevents autoimmune diabetes in NOD mice*. Immunity, 2004. **20**(6): p. 757-67.
2. Das, S.K. and R. Chakrabarti, *Non-insulin dependent diabetes mellitus: present therapies and new drug targets*. Mini Rev Med Chem, 2005. **5**(11): p. 1019-34.
3. Voulgari, C., D. Papadogiannis, and N. Tentolouris, *Diabetic cardiomyopathy: from the pathophysiology of the cardiac myocytes to current diagnosis and management strategies*. Vasc Health Risk Manag. **6**: p. 883-903.
4. Bertoni, A.G., et al., *Diabetes and idiopathic cardiomyopathy: a nationwide case-control study*. Diabetes Care, 2003. **26**(10): p. 2791-5.
5. Severson, D.L., *Diabetic cardiomyopathy: recent evidence from mouse models of type 1 and type 2 diabetes*. Can J Physiol Pharmacol, 2004. **82**(10): p. 813-23.
6. Anguera, I., et al., *[Anatomopathological bases of latent ventricular dysfunction in insulin-dependent diabetics]*. Rev Esp Cardiol, 1998. **51**(1): p. 43-50.
7. Saito, F., et al., *Alteration in haemodynamics and pathological changes in the cardiovascular system during the development of Type 2 diabetes mellitus in OLETF rats*. Diabetologia, 2003. **46**(8): p. 1161-9.
8. Fang, Z.Y., J.B. Prins, and T.H. Marwick, *Diabetic cardiomyopathy: evidence, mechanisms, and therapeutic implications*. Endocr Rev, 2004. **25**(4): p. 543-67.
9. Rodrigues, B., M.C. Cam, and J.H. McNeill, *Metabolic disturbances in diabetic cardiomyopathy*. Mol Cell Biochem, 1998. **180**(1-2): p. 53-7.
10. Avogaro, A., et al., *Myocardial metabolism in insulin-deficient diabetic humans without coronary artery disease*. Am J Physiol, 1990. **258**(4 Pt 1): p. E606-18.

11. Saddik, M. and G.D. Lopaschuk, *Myocardial triglyceride turnover and contribution to energy substrate utilization in isolated working rat hearts*. J Biol Chem, 1991. **266**(13): p. 8162-70.
12. Lopaschuk, G.D., et al., *Regulation of fatty acid oxidation in the mammalian heart in health and disease*. Biochim Biophys Acta, 1994. **1213**(3): p. 263-76.
13. Paulson, D.J. and M.F. Crass, 3rd, *Endogenous triacylglycerol metabolism in diabetic heart*. Am J Physiol, 1982. **242**(6): p. H1084-94.
14. Haffner, S.M., *Lipoprotein disorders associated with type 2 diabetes mellitus and insulin resistance*. Am J Cardiol, 2002. **90**(8A): p. 55i-61i.
15. Blanchette-Mackie, E.J., et al., *Lipoprotein lipase in myocytes and capillary endothelium of heart: immunocytochemical study*. Am J Physiol, 1989. **256**(6 Pt 1): p. E818-28.
16. Augustus, A.S., et al., *Routes of FA delivery to cardiac muscle: modulation of lipoprotein lipolysis alters uptake of TG-derived FA*. Am J Physiol Endocrinol Metab, 2003. **284**(2): p. E331-9.
17. Randle, P.J., et al., *Mechanisms modifying glucose oxidation in diabetes mellitus*. Diabetologia, 1994. **37 Suppl 2**: p. S155-61.
18. An, D. and B. Rodrigues, *Role of changes in cardiac metabolism in development of diabetic cardiomyopathy*. Am J Physiol Heart Circ Physiol, 2006. **291**(4): p. H1489-506.
19. Sambandam, N., et al., *Metabolism of VLDL is increased in streptozotocin-induced diabetic rat hearts*. Am J Physiol Heart Circ Physiol, 2000. **278**(6): p. H1874-82.

20. Mazumder, P.K., et al., *Impaired cardiac efficiency and increased fatty acid oxidation in insulin-resistant ob/ob mouse hearts*. Diabetes, 2004. **53**(9): p. 2366-74.
21. How, O.J., et al., *Increased myocardial oxygen consumption reduces cardiac efficiency in diabetic mice*. Diabetes, 2006. **55**(2): p. 466-73.
22. van Hinsbergh, V.W., *Regulatory functions of the coronary endothelium*. Mol Cell Biochem, 1992. **116**(1-2): p. 163-9.
23. Parra-Bonilla, G., et al., *Critical role for lactate dehydrogenase A in aerobic glycolysis that sustains pulmonary microvascular endothelial cell proliferation*. Am J Physiol Lung Cell Mol Physiol. **299**(4): p. L513-22.
24. Krutzfeldt, A., et al., *Metabolism of exogenous substrates by coronary endothelial cells in culture*. J Mol Cell Cardiol, 1990. **22**(12): p. 1393-404.
25. Crabtree, H.G., *Observations on the carbohydrate metabolism of tumours*. Biochem J, 1929. **23**(3): p. 536-45.
26. Mann, G.E., D.L. Yudilevich, and L. Sobrevia, *Regulation of amino acid and glucose transporters in endothelial and smooth muscle cells*. Physiol Rev, 2003. **83**(1): p. 183-252.
27. Fernandes, R., et al., *Downregulation of retinal GLUT1 in diabetes by ubiquitinylation*. Mol Vis, 2004. **10**: p. 618-28.
28. Bassingthwaite, J.B., et al., *Modeling of palmitate transport in the heart*. Mol Cell Biochem, 1989. **88**(1-2): p. 51-8.
29. van der Vusse, G.J., et al., *Critical steps in cellular fatty acid uptake and utilization*. Mol Cell Biochem, 2002. **239**(1-2): p. 9-15.

30. Spahr, R., et al., *Fatty acids are not an important fuel for coronary microvascular endothelial cells*. Mol Cell Biochem, 1989. **88**(1-2): p. 59-64.
31. Leighton, B., et al., *Maximum activities of some key enzymes of glycolysis, glutaminolysis, Krebs cycle and fatty acid utilization in bovine pulmonary endothelial cells*. FEBS Lett, 1987. **225**(1-2): p. 93-6.
32. Dagher, Z., et al., *The effect of AMP-activated protein kinase and its activator AICAR on the metabolism of human umbilical vein endothelial cells*. Biochem Biophys Res Commun, 1999. **265**(1): p. 112-5.
33. Merkel, M., R.H. Eckel, and I.J. Goldberg, *Lipoprotein lipase: genetics, lipid uptake, and regulation*. J Lipid Res, 2002. **43**(12): p. 1997-2006.
34. Pulinilkunnil, T. and B. Rodrigues, *Cardiac lipoprotein lipase: metabolic basis for diabetic heart disease*. Cardiovasc Res, 2006. **69**(2): p. 329-40.
35. Camps, L., et al., *Lipoprotein lipase: cellular origin and functional distribution*. Am J Physiol, 1990. **258**(4 Pt 1): p. C673-81.
36. Eckel, R.H., *Lipoprotein lipase. A multifunctional enzyme relevant to common metabolic diseases*. N Engl J Med, 1989. **320**(16): p. 1060-8.
37. Blanchette-Mackie, E.J., N.K. Dwyer, and L.A. Amende, *Cytochemical studies of lipid metabolism: immunogold probes for lipoprotein lipase and cholesterol*. Am J Anat, 1989. **185**(2-3): p. 255-63.
38. Otarod, J.K. and I.J. Goldberg, *Lipoprotein lipase and its role in regulation of plasma lipoproteins and cardiac risk*. Curr Atheroscler Rep, 2004. **6**(5): p. 335-42.

39. Takahashi, S., et al., *Enhancement of the binding of triglyceride-rich lipoproteins to the very low density lipoprotein receptor by apolipoprotein E and lipoprotein lipase.* J Biol Chem, 1995. **270**(26): p. 15747-54.
40. Rutledge, J.C. and I.J. Goldberg, *Lipoprotein lipase (LpL) affects low density lipoprotein (LDL) flux through vascular tissue: evidence that LpL increases LDL accumulation in vascular tissue.* J Lipid Res, 1994. **35**(7): p. 1152-60.
41. Deshaies, Y., D. Richard, and J. Arnold, *Lipoprotein lipase in adipose tissues of exercise-trained, cold-acclimated rats.* Am J Physiol, 1986. **251**(3 Pt 1): p. E251-7.
42. Rogers, M.P. and X. Zhao, *Effect of insulin and serum on lipoprotein lipase in lactation.* Biochem Soc Trans, 1998. **26**(2): p. S145.
43. Wu, G., G. Olivecrona, and T. Olivecrona, *The distribution of lipoprotein lipase in rat adipose tissue. Changes with nutritional state engage the extracellular enzyme.* J Biol Chem, 2003. **278**(14): p. 11925-30.
44. Doolittle, M.H., et al., *The response of lipoprotein lipase to feeding and fasting. Evidence for posttranslational regulation.* J Biol Chem, 1990. **265**(8): p. 4570-7.
45. Ruge, T., et al., *Nutritional regulation of binding sites for lipoprotein lipase in rat heart.* Am J Physiol Endocrinol Metab, 2000. **278**(2): p. E211-8.
46. Kitajima, S., et al., *Overexpression of lipoprotein lipase improves insulin resistance induced by a high-fat diet in transgenic rabbits.* Diabetologia, 2004. **47**(7): p. 1202-9.
47. Levak-Frank, S., et al., *Muscle-specific overexpression of lipoprotein lipase causes a severe myopathy characterized by proliferation of mitochondria and peroxisomes in transgenic mice.* J Clin Invest, 1995. **96**(2): p. 976-86.

48. Kim, J.K., et al., *Tissue-specific overexpression of lipoprotein lipase causes tissue-specific insulin resistance*. Proc Natl Acad Sci U S A, 2001. **98**(13): p. 7522-7.
49. Noh, H.L., H. Yamashita, and I.J. Goldberg, *Cardiac metabolism and mechanics are altered by genetic loss of lipoprotein triglyceride lipolysis*. Cardiovasc Drugs Ther, 2006. **20**(6): p. 441-4.
50. Yagyu, H., et al., *Lipoprotein lipase (LpL) on the surface of cardiomyocytes increases lipid uptake and produces a cardiomyopathy*. J Clin Invest, 2003. **111**(3): p. 419-26.
51. Braun, J.E. and D.L. Severson, *Tissue-specific regulation of lipoprotein lipase*. Cmaj, 1992. **147**(8): p. 1192.
52. Braun, J.E. and D.L. Severson, *Regulation of the synthesis, processing and translocation of lipoprotein lipase*. Biochem J, 1992. **287** (Pt 2): p. 337-47.
53. Yanagishita, M. and V.C. Hascall, *Cell surface heparan sulfate proteoglycans*. J Biol Chem, 1992. **267**(14): p. 9451-4.
54. Kjellen, L. and U. Lindahl, *Proteoglycans: structures and interactions*. Annu Rev Biochem, 1991. **60**: p. 443-75.
55. Lindahl, U., et al., *More to "heparin" than anticoagulation*. Thromb Res, 1994. **75**(1): p. 1-32.
56. Kusche, M., et al., *Biosynthesis of heparin. Availability of glucosaminyl 3-O-sulfation sites*. J Biol Chem, 1990. **265**(13): p. 7292-300.
57. Salmivirta, M. and M. Jalkanen, *Syndecan family of cell surface proteoglycans: developmentally regulated receptors for extracellular effector molecules*. Experientia, 1995. **51**(9-10): p. 863-72.

58. Gallagher, J.T. and J.E. Turnbull, *Heparan sulphate in the binding and activation of basic fibroblast growth factor*. *Glycobiology*, 1992. **2**(6): p. 523-8.
59. Pillarisetti, S., et al., *Endothelial cell heparanase modulation of lipoprotein lipase activity. Evidence that heparan sulfate oligosaccharide is an extracellular chaperone*. *J Biol Chem*, 1997. **272**(25): p. 15753-9.
60. Bernfield, M., et al., *Functions of cell surface heparan sulfate proteoglycans*. *Annu Rev Biochem*, 1999. **68**: p. 729-77.
61. Pillarisetti, S., *Lipoprotein modulation of subendothelial heparan sulfate proteoglycans (perlecan) and atherogenicity*. *Trends Cardiovasc Med*, 2000. **10**(2): p. 60-5.
62. van der Hoek, Y.Y., et al., *Binding of recombinant apolipoprotein(a) to extracellular matrix proteins*. *Arterioscler Thromb*, 1994. **14**(11): p. 1792-8.
63. Beauvais, D.M., B.J. Burbach, and A.C. Rapraeger, *The syndecan-1 ectodomain regulates alphavbeta3 integrin activity in human mammary carcinoma cells*. *J Cell Biol*, 2004. **167**(1): p. 171-81.
64. Iozzo, R.V., et al., *Structural and functional characterization of the human perlecan gene promoter. Transcriptional activation by transforming growth factor-beta via a nuclear factor I-binding element*. *J Biol Chem*, 1997. **272**(8): p. 5219-28.
65. Stringer, S.E. and J.T. Gallagher, *Heparan sulphate*. *Int J Biochem Cell Biol*, 1997. **29**(5): p. 709-14.
66. Hollmann, J., et al., *Relationship of sulfated glycosaminoglycans and cholesterol content in normal and arteriosclerotic human aorta*. *Arteriosclerosis*, 1989. **9**(2): p. 154-8.

67. Sanderson, R.D., et al., *Enzymatic remodeling of heparan sulfate proteoglycans within the tumor microenvironment: growth regulation and the prospect of new cancer therapies*. J Cell Biochem, 2005. **96**(5): p. 897-905.
68. Jensen, T., *Pathogenesis of diabetic vascular disease: evidence for the role of reduced heparan sulfate proteoglycan*. Diabetes, 1997. **46 Suppl 2**: p. S98-100.
69. Hoogewerf, A.J., et al., *Glycosaminoglycans mediate cell surface oligomerization of chemokines*. Biochemistry, 1997. **36**(44): p. 13570-8.
70. Sivaram, P., J.C. Obunike, and I.J. Goldberg, *Lysolecithin-induced alteration of subendothelial heparan sulfate proteoglycans increases monocyte binding to matrix*. J Biol Chem, 1995. **270**(50): p. 29760-5.
71. Koyama, N., et al., *Heparan sulfate proteoglycans mediate a potent inhibitory signal for migration of vascular smooth muscle cells*. Circ Res, 1998. **83**(3): p. 305-13.
72. Pillarisetti, S., et al., *Subendothelial retention of lipoprotein (a). Evidence that reduced heparan sulfate promotes lipoprotein binding to subendothelial matrix*. J Clin Invest, 1997. **100**(4): p. 867-74.
73. Bullock, S.L., et al., *Renal agenesis in mice homozygous for a gene trap mutation in the gene encoding heparan sulfate 2-sulfotransferase*. Genes Dev, 1998. **12**(12): p. 1894-906.
74. Kanwar, Y.S., A. Linker, and M.G. Farquhar, *Increased permeability of the glomerular basement membrane to ferritin after removal of glycosaminoglycans (heparan sulfate) by enzyme digestion*. J Cell Biol, 1980. **86**(2): p. 688-93.

75. Woodrow, D., et al., *Diabetic glomerulosclerosis--immunogold ultrastructural studies on the glomerular distribution of type IV collagen and heparan sulphate proteoglycan*. J Pathol, 1992. **167**(1): p. 49-58.
76. van den Hoven, M.J., et al., *Heparanase in glomerular diseases*. Kidney Int, 2007. **72**(5): p. 543-8.
77. Eccles, S.A., *Heparanase: breaking down barriers in tumors*. Nat Med, 1999. **5**(7): p. 735-6.
78. Elkin, M., et al., *Heparanase as mediator of angiogenesis: mode of action*. Faseb J, 2001. **15**(9): p. 1661-3.
79. Pikas, D.S., et al., *Substrate specificity of heparanases from human hepatoma and platelets*. J Biol Chem, 1998. **273**(30): p. 18770-7.
80. Hulett, M.D., et al., *Cloning of mammalian heparanase, an important enzyme in tumor invasion and metastasis*. Nat Med, 1999. **5**(7): p. 803-9.
81. Baker, E., et al., *Human HPA endoglycosidase heparanase. Map position 4q21.3*. Chromosome Res, 1999. **7**(4): p. 319.
82. Vreys, V. and G. David, *Mammalian heparanase: what is the message?* J Cell Mol Med, 2007. **11**(3): p. 427-52.
83. Vreys, V., et al., *Cellular uptake of mammalian heparanase precursor involves low density lipoprotein receptor-related proteins, mannose 6-phosphate receptors, and heparan sulfate proteoglycans*. J Biol Chem, 2005. **280**(39): p. 33141-8.
84. Abboud-Jarrous, G., et al., *Site-directed mutagenesis, proteolytic cleavage, and activation of human proheparanase*. J Biol Chem, 2005. **280**(14): p. 13568-75.

85. Nardella, C., et al., *Mechanism of activation of human heparanase investigated by protein engineering*. *Biochemistry*, 2004. **43**(7): p. 1862-73.
86. Fairbanks, M.B., et al., *Processing of the human heparanase precursor and evidence that the active enzyme is a heterodimer*. *J Biol Chem*, 1999. **274**(42): p. 29587-90.
87. Vlodavsky, I., et al., *Mammalian heparanase: gene cloning, expression and function in tumor progression and metastasis*. *Nat Med*, 1999. **5**(7): p. 793-802.
88. Gingis-Velitski, S., et al., *Heparanase uptake is mediated by cell membrane heparan sulfate proteoglycans*. *J Biol Chem*, 2004. **279**(42): p. 44084-92.
89. McKenzie, E.A., *Heparanase: a target for drug discovery in cancer and inflammation*. *Br J Pharmacol*, 2007. **151**(1): p. 1-14.
90. Fux, L., et al., *Heparanase: busy at the cell surface*. *Trends Biochem Sci*, 2009. **34**(10): p. 511-9.
91. Hulett, M.D., et al., *Identification of active-site residues of the pro-metastatic endoglycosidase heparanase*. *Biochemistry*, 2000. **39**(51): p. 15659-67.
92. Henrissat, B. and G. Davies, *Structural and sequence-based classification of glycoside hydrolases*. *Curr Opin Struct Biol*, 1997. **7**(5): p. 637-44.
93. Levy-Adam, F., et al., *Identification and characterization of heparin/heparan sulfate binding domains of the endoglycosidase heparanase*. *J Biol Chem*, 2005. **280**(21): p. 20457-66.
94. Kelly, T., et al., *High heparanase activity in multiple myeloma is associated with elevated microvessel density*. *Cancer Res*, 2003. **63**(24): p. 8749-56.

95. Jiang, P., et al., *Cloning and characterization of the human heparanase-1 (HPR1) gene promoter: role of GA-binding protein and Sp1 in regulating HPR1 basal promoter activity.* J Biol Chem, 2002. **277**(11): p. 8989-98.
96. Lu, W.C., et al., *Trans-activation of heparanase promoter by ETS transcription factors.* Oncogene, 2003. **22**(6): p. 919-23.
97. Ogishima, T., et al., *Promoter CpG hypomethylation and transcription factor EGR1 hyperactivate heparanase expression in bladder cancer.* Oncogene, 2005. **24**(45): p. 6765-72.
98. Ogishima, T., et al., *Increased heparanase expression is caused by promoter hypomethylation and up-regulation of transcriptional factor early growth response-1 in human prostate cancer.* Clin Cancer Res, 2005. **11**(3): p. 1028-36.
99. de Mestre, A.M., et al., *Regulation of inducible heparanase gene transcription in activated T cells by early growth response 1.* J Biol Chem, 2003. **278**(50): p. 50377-85.
100. Maxhimer, J.B., et al., *Heparanase-1 gene expression and regulation by high glucose in renal epithelial cells: a potential role in the pathogenesis of proteinuria in diabetic patients.* Diabetes, 2005. **54**(7): p. 2172-8.
101. Chen, G., et al., *Inflammatory cytokines and fatty acids regulate endothelial cell heparanase expression.* Biochemistry, 2004. **43**(17): p. 4971-7.
102. Edovitsky, E., et al., *Role of endothelial heparanase in delayed-type hypersensitivity.* Blood, 2006. **107**(9): p. 3609-16.
103. Baraz, L., et al., *Tumor suppressor p53 regulates heparanase gene expression.* Oncogene, 2006. **25**(28): p. 3939-47.

104. Shteper, P.J., et al., *Role of promoter methylation in regulation of the mammalian heparanase gene*. *Oncogene*, 2003. **22**(49): p. 7737-49.
105. Koliopanos, A., et al., *Heparanase expression in primary and metastatic pancreatic cancer*. *Cancer Res*, 2001. **61**(12): p. 4655-9.
106. Bitan, M., et al., *Heparanase expression in human leukemias is restricted to acute myeloid leukemias*. *Exp Hematol*, 2002. **30**(1): p. 34-41.
107. Yang, Y., et al., *Heparanase promotes the spontaneous metastasis of myeloma cells to bone*. *Blood*, 2005. **105**(3): p. 1303-9.
108. Cohen, I., et al., *Heparanase promotes growth, angiogenesis and survival of primary breast tumors*. *Int J Cancer*, 2006. **118**(7): p. 1609-17.
109. Edovitsky, E., et al., *Heparanase gene silencing, tumor invasiveness, angiogenesis, and metastasis*. *J Natl Cancer Inst*, 2004. **96**(16): p. 1219-30.
110. Parish, C.R., et al., *Identification of sulfated oligosaccharide-based inhibitors of tumor growth and metastasis using novel in vitro assays for angiogenesis and heparanase activity*. *Cancer Res*, 1999. **59**(14): p. 3433-41.
111. Reiland, J., et al., *FGF2 binding, signaling, and angiogenesis are modulated by heparanase in metastatic melanoma cells*. *Neoplasia*, 2006. **8**(7): p. 596-606.
112. Zhao, H., et al., *Oligomannururate sulfate, a novel heparanase inhibitor simultaneously targeting basic fibroblast growth factor, combats tumor angiogenesis and metastasis*. *Cancer Res*, 2006. **66**(17): p. 8779-87.
113. Zetser, A., et al., *Heparanase affects adhesive and tumorigenic potential of human glioma cells*. *Cancer Res*, 2003. **63**(22): p. 7733-41.

114. Goldshmidt, O., et al., *Heparanase mediates cell adhesion independent of its enzymatic activity*. *Faseb J*, 2003. **17**(9): p. 1015-25.
115. Levy-Adam, F., et al., *Heparanase facilitates cell adhesion and spreading by clustering of cell surface heparan sulfate proteoglycans*. *PLoS One*, 2008. **3**(6): p. e2319.
116. Gingis-Velitski, S., et al., *Heparanase induces endothelial cell migration via protein kinase B/Akt activation*. *J Biol Chem*, 2004. **279**(22): p. 23536-41.
117. Zetser, A., et al., *Heparanase induces vascular endothelial growth factor expression: correlation with p38 phosphorylation levels and Src activation*. *Cancer Res*, 2006. **66**(3): p. 1455-63.
118. Reynolds, A.B., *p120-catenin: Past and present*. *Biochim Biophys Acta*, 2007. **1773**(1): p. 2-7.
119. Nadir, Y., et al., *Heparanase induces tissue factor expression in vascular endothelial and cancer cells*. *J Thromb Haemost*, 2006. **4**(11): p. 2443-51.
120. Fux, L., et al., *Structure-function approach identifies a COOH-terminal domain that mediates heparanase signaling*. *Cancer Res*, 2009. **69**(5): p. 1758-67.
121. Levidiotis, V., et al., *A synthetic heparanase inhibitor reduces proteinuria in passive Heymann nephritis*. *J Am Soc Nephrol*, 2004. **15**(11): p. 2882-92.
122. Levidiotis, V., et al., *Increased expression of heparanase in puromycin aminonucleoside nephrosis*. *Kidney Int*, 2001. **60**(4): p. 1287-96.
123. An, X.F., et al., *Advanced glycation end-products induce heparanase expression in endothelial cells by the receptor for advanced glycation end products and through activation of the FOXO4 transcription factor*. *Mol Cell Biochem*.

124. Baker, A.B., et al., *Heparanase alters arterial structure, mechanics, and repair following endovascular stenting in mice*. *Circ Res*, 2009. **104**(3): p. 380-7.
125. Sambandam, N., et al., *Localization of lipoprotein lipase in the diabetic heart: regulation by acute changes in insulin*. *Arterioscler Thromb Vasc Biol*, 1999. **19**(6): p. 1526-34.
126. Pulinilkunnil, T., et al., *Evidence for rapid "metabolic switching" through lipoprotein lipase occupation of endothelial-binding sites*. *J Mol Cell Cardiol*, 2003. **35**(9): p. 1093-103.
127. Pulinilkunnil, T., et al., *Circulating triglyceride lipolysis facilitates lipoprotein lipase translocation from cardiomyocyte to myocardial endothelial lining*. *Cardiovasc Res*, 2003. **59**(3): p. 788-97.
128. Kim, M.S., et al., *Acute diabetes moderates trafficking of cardiac lipoprotein lipase through p38 mitogen-activated protein kinase-dependent actin cytoskeleton organization*. *Diabetes*, 2008. **57**(1): p. 64-76.
129. Kim, M.S., et al., *Protein kinase D is a key regulator of cardiomyocyte lipoprotein lipase secretion after diabetes*. *Circ Res*, 2008. **103**(3): p. 252-60.
130. Rodrigues, B., et al., *Differential effects of streptozotocin-induced diabetes on cardiac lipoprotein lipase activity*. *Diabetes*, 1997. **46**(8): p. 1346-53.
131. De Deckere, E.A. and P. Ten Hoor, *A modified Langendorff technique for metabolic investigations*. *Pflugers Arch*, 1977. **370**(1): p. 103-5.
132. Jansen, H., et al., *On the dual localization of lipoprotein lipase in rat heart. Studies with a modified perfusion technique*. *Biochem Biophys Res Commun*, 1980. **92**(2): p. 411-6.

133. Zetser, A., et al., *Processing and activation of latent heparanase occurs in lysosomes.* J Cell Sci, 2004. **117**(Pt 11): p. 2249-58.
134. Pulinilkunnil, T., et al., *Palmitoyl lysophosphatidylcholine mediated mobilization of LPL to the coronary luminal surface requires PKC activation.* J Mol Cell Cardiol, 2004. **37**(5): p. 931-8.
135. Nadav, L., et al., *Activation, processing and trafficking of extracellular heparanase by primary human fibroblasts.* J Cell Sci, 2002. **115**(Pt 10): p. 2179-87.
136. Pearson, J.D. and J.L. Gordon, *Vascular endothelial and smooth muscle cells in culture selectively release adenine nucleotides.* Nature, 1979. **281**(5730): p. 384-6.
137. Shafat, I., I. Vlodaysky, and N. Ilan, *Characterization of mechanisms involved in secretion of active heparanase.* J Biol Chem, 2006. **281**(33): p. 23804-11.
138. Wang, F., et al., *Endothelial heparanase secretion after acute hypoinsulinemia is regulated by glucose and fatty acid.* Am J Physiol Heart Circ Physiol, 2009. **296**(4): p. H1108-16.
139. Nguyen, A., P. Chen, and H. Cai, *Role of CaMKII in hydrogen peroxide activation of ERK1/2, p38 MAPK, HSP27 and actin reorganization in endothelial cells.* FEBS Lett, 2004. **572**(1-3): p. 307-13.
140. Fox, J.E., *Identification of actin-binding protein as the protein linking the membrane skeleton to glycoproteins on platelet plasma membranes.* J Biol Chem, 1985. **260**(22): p. 11970-7.
141. Yu, N., et al., *Binding of the P2Y2 nucleotide receptor to filamin A regulates migration of vascular smooth muscle cells.* Circ Res, 2008. **102**(5): p. 581-8.

142. Liu, L., et al., *Adult cardiomyocytes express functional high-affinity receptors for basic fibroblast growth factor*. Am J Physiol, 1995. **268**(5 Pt 2): p. H1927-38.
143. Kagedal, K., et al., *Lysosomal membrane permeabilization during apoptosis--involvement of Bax?* Int J Exp Pathol, 2005. **86**(5): p. 309-21.
144. Nobuhisa, T., et al., *Translocation of heparanase into nucleus results in cell differentiation*. Cancer Sci, 2007. **98**(4): p. 535-40.
145. Buczek-Thomas, J.A., et al., *Inhibition of histone acetyltransferase by glycosaminoglycans*. J Cell Biochem, 2008. **105**(1): p. 108-20.
146. Scow, R.O. and E.J. Blanchette-Mackie, *Endothelium, the dynamic interface in cardiac lipid transport*. Mol Cell Biochem, 1992. **116**(1-2): p. 181-91.
147. Schubert, S.Y., et al., *Human heparanase nuclear localization and enzymatic activity*. Lab Invest, 2004. **84**(5): p. 535-44.
148. Fedarko, N.S. and H.E. Conrad, *A unique heparan sulfate in the nuclei of hepatocytes: structural changes with the growth state of the cells*. J Cell Biol, 1986. **102**(2): p. 587-99.
149. Blott, E.J. and G.M. Griffiths, *Secretory lysosomes*. Nat Rev Mol Cell Biol, 2002. **3**(2): p. 122-31.
150. DuBose, D.A. and R. Haugland, *Comparisons of endothelial cell G- and F-actin distribution in situ and in vitro*. Biotech Histochem, 1993. **68**(1): p. 8-16.
151. Tong, P., et al., *Insulin-induced cortical actin remodeling promotes GLUT4 insertion at muscle cell membrane ruffles*. J Clin Invest, 2001. **108**(3): p. 371-81.

152. Bodin, P., D. Bailey, and G. Burnstock, *Increased flow-induced ATP release from isolated vascular endothelial cells but not smooth muscle cells*. Br J Pharmacol, 1991. **103**(1): p. 1203-5.
153. Burnstock, G., *Unresolved issues and controversies in purinergic signalling*. J Physiol, 2008. **586**(14): p. 3307-12.
154. Ahmad, S., et al., *Extracellular ATP-mediated signaling for survival in hyperoxia-induced oxidative stress*. J Biol Chem, 2004. **279**(16): p. 16317-25.
155. Kimura, C., et al., *Hypotonic stress-induced NO production in endothelium depends on endogenous ATP*. Biochem Biophys Res Commun, 2000. **274**(3): p. 736-40.
156. Vischer, U.M. and C.B. Wollheim, *Purine nucleotides induce regulated secretion of von Willebrand factor: involvement of cytosolic Ca²⁺ and cyclic adenosine monophosphate-dependent signaling in endothelial exocytosis*. Blood, 1998. **91**(1): p. 118-27.
157. Allsup, D.J. and M.R. Boarder, *Comparison of P₂ purinergic receptors of aortic endothelial cells with those of adrenal medulla: evidence for heterogeneity of receptor subtype and of inositol phosphate response*. Mol Pharmacol, 1990. **38**(1): p. 84-91.
158. Shen, J. and P.E. DiCorleto, *ADP stimulates human endothelial cell migration via P₂Y₁ nucleotide receptor-mediated mitogen-activated protein kinase pathways*. Circ Res, 2008. **102**(4): p. 448-56.
159. Phillips, P.G., et al., *Phalloidin prevents thrombin-induced increases in endothelial permeability to albumin*. Am J Physiol, 1989. **257**(3 Pt 1): p. C562-7.

160. Malacombe, M., M.F. Bader, and S. Gasman, *Exocytosis in neuroendocrine cells: new tasks for actin*. *Biochim Biophys Acta*, 2006. **1763**(11): p. 1175-83.
161. Rose, S.D., et al., *Chromaffin cell F-actin disassembly and potentiation of catecholamine release in response to protein kinase C activation by phorbol esters is mediated through myristoylated alanine-rich C kinase substrate phosphorylation*. *J Biol Chem*, 2001. **276**(39): p. 36757-63.
162. Easom, R.A., *CaM kinase II: a protein kinase with extraordinary talents germane to insulin exocytosis*. *Diabetes*, 1999. **48**(4): p. 675-84.
163. Dai, T., et al., *Glucose and diabetes: effects on podocyte and glomerular p38MAPK, heat shock protein 25, and actin cytoskeleton*. *Kidney Int*, 2006. **69**(5): p. 806-14.
164. Stossel, T.P., et al., *Filamins as integrators of cell mechanics and signalling*. *Nat Rev Mol Cell Biol*, 2001. **2**(2): p. 138-45.
165. Borbiev, T., et al., *Regulation of endothelial cell barrier function by calcium/calmodulin-dependent protein kinase II*. *Am J Physiol Lung Cell Mol Physiol*, 2001. **280**(5): p. L983-90.
166. He, H.J., et al., *Interaction of filamin A with the insulin receptor alters insulin-dependent activation of the mitogen-activated protein kinase pathway*. *J Biol Chem*, 2003. **278**(29): p. 27096-104.
167. Feldstein, A.E., et al., *Free fatty acids promote hepatic lipotoxicity by stimulating TNF-alpha expression via a lysosomal pathway*. *Hepatology*, 2004. **40**(1): p. 185-94.
168. Rammer, P., et al., *BAMLET activates a lysosomal cell death program in cancer cells*. *Mol Cancer Ther*. **9**(1): p. 24-32.

169. Valero, J.G., et al., *Bax-derived membrane-active peptides act as potent and direct inducers of apoptosis in cancer cells*. J Cell Sci. **124**(Pt 4): p. 556-64.
170. Feldstein, A.E., et al., *Bax inhibition protects against free fatty acid-induced lysosomal permeabilization*. Am J Physiol Gastrointest Liver Physiol, 2006. **290**(6): p. G1339-46.
171. Bayliss, R., A.H. Corbett, and M. Stewart, *The molecular mechanism of transport of macromolecules through nuclear pore complexes*. Traffic, 2000. **1**(6): p. 448-56.
172. Pratt, W.B., A.M. Silverstein, and M.D. Galigniana, *A model for the cytoplasmic trafficking of signalling proteins involving the hsp90-binding immunophilins and p50cdc37*. Cell Signal, 1999. **11**(12): p. 839-51.
173. Kobayashi, M., et al., *Heparanase regulates esophageal keratinocyte differentiation through nuclear translocation and heparan sulfate cleavage*. Differentiation, 2006. **74**(5): p. 235-43.
174. Chen, L. and R.D. Sanderson, *Heparanase regulates levels of syndecan-1 in the nucleus*. PLoS One, 2009. **4**(3): p. e4947.
175. Rekowski, M.W. and A. Giannis, *Histone acetylation modulation by small molecules: a chemical approach*. Biochim Biophys Acta. **1799**(10-12): p. 760-7.
176. Sugden, M.C. and M.J. Holness, *Mechanisms underlying regulation of the expression and activities of the mammalian pyruvate dehydrogenase kinases*. Arch Physiol Biochem, 2006. **112**(3): p. 139-49.
177. Wu, P., et al., *Starvation and diabetes increase the amount of pyruvate dehydrogenase kinase isoenzyme 4 in rat heart*. Biochem J, 1998. **329** (Pt 1): p. 197-201.

178. Wu, P., et al., *Starvation increases the amount of pyruvate dehydrogenase kinase in several mammalian tissues*. Arch Biochem Biophys, 2000. **381**(1): p. 1-7.
179. Harris, R.A., B. Huang, and P. Wu, *Control of pyruvate dehydrogenase kinase gene expression*. Adv Enzyme Regul, 2001. **41**: p. 269-88.
180. Bowker-Kinley, M.M., et al., *Evidence for existence of tissue-specific regulation of the mammalian pyruvate dehydrogenase complex*. Biochem J, 1998. **329 (Pt 1)**: p. 191-6.
181. Keller, H., et al., *Fatty acids and retinoids control lipid metabolism through activation of peroxisome proliferator-activated receptor-retinoid X receptor heterodimers*. Proc Natl Acad Sci U S A, 1993. **90**(6): p. 2160-4.
182. Sneek, M., P.T. Kovanen, and K. Oorni, *Decrease in pH strongly enhances binding of native, proteolyzed, lipolyzed, and oxidized low density lipoprotein particles to human aortic proteoglycans*. J Biol Chem, 2005. **280**(45): p. 37449-54.
183. Naghavi, M., et al., *pH Heterogeneity of human and rabbit atherosclerotic plaques; a new insight into detection of vulnerable plaque*. Atherosclerosis, 2002. **164**(1): p. 27-35.
184. Riederer, M., et al., *Endothelial lipase (EL) and EL-generated lysophosphatidylcholines promote IL-8 expression in endothelial cells*. Atherosclerosis. **214**(2): p. 338-44.
185. Ley, K. and Y. Huo, *VCAM-1 is critical in atherosclerosis*. J Clin Invest, 2001. **107**(10): p. 1209-10.
186. Kimura, K., et al., *Serum VEGF--as a prognostic factor of atherosclerosis*. Atherosclerosis, 2007. **194**(1): p. 182-8.